SYNAPTIC AND DENDRITIC MECHANISMS MEDIATING DIRECTION-SELECTIVE SIGNALING IN THE RETINA

By

Nicholas W. Oesch

A THESIS

Presented to the Neuroscience Graduate Program

and the Oregon Health & Science University

School of Medicine

in partial fulfillment of

the requirements for the degree of

Doctor of Philosophy

July 2008

School of Medicine

Oregon Health & Science University

CERTIFICATE OF APPROVAL

This is to certify that the Ph.D. dissertation of

Nicholas W. Oesch

Has been approved

Member

Member

Member

Member

Member

ACKNOWLEDGEMENTS

I would like to take this opportunity to thank all those who have been involved in my life as graduate student and contributed to my passage through graduate school, both academically and otherwise.

First and foremost, I will thank my advisor Dr. W. Rowland Taylor. Rowland has not only been a great acedemic mentor, but a fun scientist and friend to work with. I can only hope that I can become the scientist and mentor that he has been to me. I would also like to thank my committee for helping guide my development as a young scientist. The committee consists of Peter Larsson, Craig Jahr, and Pat Roberts, and John Williams. Other faculty members at the NSI have also been invaluable in my time as a graduate studend. Robert Duvoisin, Catherine Morgans, Matt Frerking, and David Rossi are only a few of the many.

In addition to the many who have lent support and advice are the many individuals who gave support my making life as a graduate student not only tolerable, but enjoyable. This includes my friends and aqaintances. Whether skiing, climbing or just enjoying a meal, these people made the past six years a great experience.

Finally and most importantly I want to thank the behavioral neuroscientist, runner and skier who as become my partner in life and love. Christina Gremel has shaped my life it ways too numerable to list, but without her I would undoubtedly not be the person I am today. I cannot express my gratitude enough to her.

This work was supported by NIH grant EY014888 to WRT, NHMRC (Australia) grant 179837 to D.I. Vaney and WRT, and the Max-Panck Society.

Abstract

Understanding how information is integrated and processed in single neurons and small circuits is crucial for comprehending information processing in neural circuits, and will help elucidate the biophysical basis of cognition and cognitive dysfunction. The direction selective circuit of the retina has been an archetypical model for understanding how neural circuits process information in the brain since the direction selective ganglion cell (DSGC) was first discovered more than 40 years ago. Much progress has been made towards understanding how the direction selective circuits extracts information from moving stimuli on the retina and computes the direction of motion; however, several key questions have remained unanswered. While it had been shown that directional inhibitory inputs to the DSGC are crucial to forming directional responses, the mechanisms underlying the integration of synaptic inputs to produce directional spiking in the DSGC are unknown. Furthermore, the cell that mediates the crucial directional inhibition, the starburst amacrine cell (SBAC) has been identified, yet we do not have a complete understand how the SBAC generates this directional inhibitory signal.

Using *In-vitro* patch-clamp recordings and two-photon calcium imaging, we show that DSGCs employ orthograde spikes originating in the dendrites to locally integrate excitatory and inhibitory synaptic inputs and signal the direction of motion, which enhances the directional selectivity of the circuit. This represents the first demonstration of how dendritic action potentials contribute to direction selectivity and more generally it is one of the first demonstrations of a

physiological role for orthograde dendritic spiking in a clearly defined neural computation.

By making patch-clamp electrical recordings from the SBAC, we demonstrate that the SBACs receive directional inputs and that this directional difference is boosted by tetrodotoxin-resistant voltage gated sodium channels. From these data we conclude that direction selectivity first arises presynaptically to the SBAC, and that tetrodotoxin-resistant sodium channels boost the directional signal in the SBAC. This work suggests a previously unconsidered role for the mechanism that generates directional signals in the SBAC and more generally demonstrates the physiological role of the non-typical tetrodotoxin-resistant sodium channels in a clearly defined neural computation

CHAPTER 1: NEURAL MECHANISMS OF DIRECTION DETECTION IN THE RETINA

Neural computation of spatio-temporal patterns, and direction selectivity

Comprehending how neurons encode and compute information is a major goal of neuroscience. Motion detection is an important computational task to understand, not only because it has significant behavioral relevance, but also because the computation of direction can act as a model problem for understanding mechanisms of neural computation as well as neural computation itself. It is obvious that motion detection is required for the prediction and tracking of object paths through our immediate world, and that it provides important feedback about our relative position to objects in our world allowing us to meaningfully interact with them. This is evident by the observation that the ability to detect motion is wide spread among nearly all types of organisms.

Less obvious is the observation that motion detection can represent a broad range of spatio-temporal processing tasks that must be performed continuously by the nervous system. One key aspect that makes motion detection a useful tool for understanding neural computation is that the locus of computation first occurs relatively early in the flow of information through the nervous system. For most animals visual motion detection occurs in the retina, placing it a maximum of two to three synapses from the photodetectors in all species that have been examined so far (Barlow and Hill, 1963; Euler et al., 2002a; Maturana and Frenk, 1963; Stone and Fabian, 1966; Werblin, 1970). This proximity to the sen-

sory input allows the researcher greater experimental access to the neural system as well as greater access to input information and its relation to the real world.

Motion detection is a computational task which can be well described by mathematical means, and this makes it an attractive system for study. Exxner (1894) made the first recorded attempt to provide a theoretical description of the neural requirements for motion detection. Nearly 60 years later Hassentein and Reichardt (Hassenstein and Reichardt, 1951), came up with the first computationally based description, which was further extended by Reichardt (1961). The model proposed from this work initial work has come to be known as the Hassenstein-Reichardt detector, Figure 1a. From this first model and subsequent work by Reichardt and others (Buchner, 1984; Poggio and Reichardt, 1973; Reichardt, 1987) a minimum set of requirements for a directionally selective motion detection can be defined. First, the system must have a minimum of two inputs, second, there must be a asymmetry somewhere between the inputs and the outputs, and finally, these two inputs must be interact in a non-linear way.

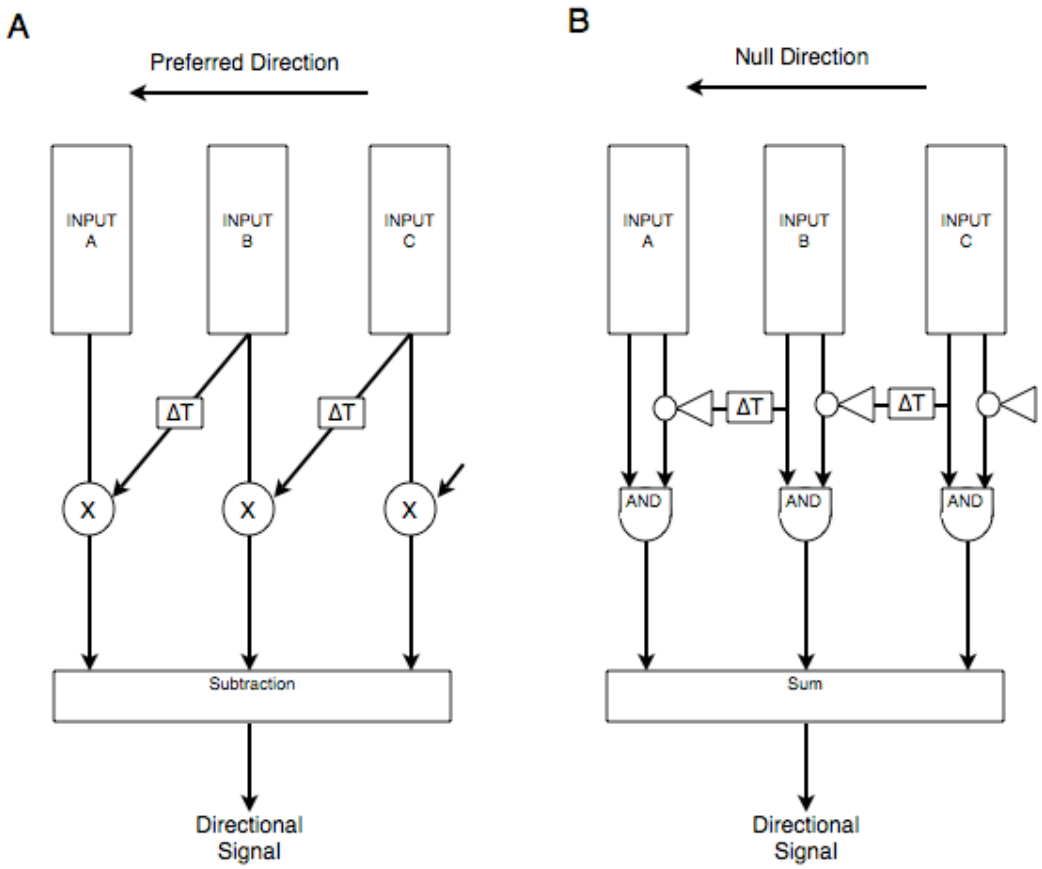

Figure 1.1:

Two correlation schemes for discriminating motion direction. A. Model schematic after the correlation portion of the Hassenstein-Reichardt detector (Reichardt, 1961). Where inputs are delayed by ΔT, so that inputs from detector C reach the multiplication operation B at the same time as direct input from input B. When the outputs of the multiplication operations during different sequences are subtracted from each other a directional signal is obtained. B.

A variety of models for motion detectors have been proposed that meet these requirements and they can all be characterized as one of two basic types

of detectors, the gradient type detector or the correlation type detector (for review see (Borst and Egelhaaf, 1989; Ullman, 1983)). In a gradient type detector the system measures intensity gradients, as related to an object in the cells receptive field and motion is detected by measuring the rate of change of intensity at particular point on the intensity curve. The direction is indicated by the sign of the rate of change and speed is encoded in the magnitude. Obviously this system is most sensitive for points on the intensity curve where the spatio-intensity slope is the steepest, such as edges of objects (Marr and Ullman, 1981).

In contrast to coding rates of change in the gradient model, the basic premise of the second scheme for a motion detector is to calculate the cross-correlation between two points, hence the name, correlation detector. The fundamental component of this model is a delay-and-compare mechanism where the instantaneous signal from one input is compared to the delayed signal from a neighboring input. In its simplest form it is comprised of two detectors at different spatial locations. Motion is detected by comparing the output of a detector at spatial point 1, at time t with the output of a detector at spatial point 2 at t plus a temporal delay, Figure 1a. The average of an array of this type of detector would be the equivalent of a cross-correlation of the inputs. Importantly, by taking the response from stimulation in two opposite directions and subtracting the input signals, a directional signal is obtained. This basic scheme has proven to be a reliable description of mechanisms employed by insect opto-motor systems (Reichardt, 1961; Reichardt, 1987), as well has vertebrate visual systems

(Barlow and Levick, 1965a), including humans, (van Doorn and Koenderink, 1982).

In the vertebrate retina, shortly after Barlow and Hill discovered the existence of directional units in the rabbit retina (Barlow and Hill, 1963b), (Barlow and Levick, 1965b) proposed a variation on the Hassenstein-Reichardt detector, to explain the mechanism of the motion detector in the vertebrate retina. This proposition was stimulated by the observation that directional selectivity in the retina was dependent on inhibition. The variation of the Hassenstein-Reichardt detector that Barlow and Levick proposed was later referred to as the “Barlow-Levick” model, or more generally the “AND-NOT” or “veto” model. They proposed that instead of the offset delayed signal adding positively to the non-linear integrator, the sign was inverted resulting in a logical NOT operation at the integrator, now conceptualized as an AND logic gate. Therefore, motion activating the inputs on the delayed line first resultes in a veto of the signal from the other detector. Motion in the opposite direction resulted in an input passing through the integrator before the NOT signal reaches the AND logic gate, Figure 1b.

These early theoretical ideas about the mechanism for generating direction selectivity in the retina, as well as many following theoretical investigations has directed experimentation into the biophysical mechanism of DS in the retina and given us a useful context to evaluate the contribution of various observations. Investigation into retinal direction selectivity began with a preconception of these minimum requirements for a directional mechanism.

Direction selectivity in the retina

A brief introduction to the retina

A systematic description of the retina was first begun over 100 years ago by Ramon y Cajal, and today the circuitry of the retina is relatively well described compared to many nervous system areas. The retina is a part of the central nervous system located at the back surface of the eye, consisting of 6 major classes of neurons organized into a laminar structure (Figure, 2). In the outer portion of the retina, closest to the surface of the eye, photoreceptors and their outer segments form the outer segment and outer nuclear layer. The role of the photoreceptors is to transduce energy from photons into electrical signals. Photoreceptors can be further divided into two classes, rods and cones. In rods, the phototransduction cascade is tuned for high sensitivity vision at low light levels, while in the cones are sensitive to different wavelengths of light and underly the basis of color detection in the visual system. The absorption of photons by the retinal-opsin complex in the outer segments of photoreceptors ultimately leads to a hyper-polarization of the photoreceptor and a reduction in the release of glutamate from its synaptic terminal. Thus in the dark, transmitter release is high and the absorption of light causes a reduction in transmitter release from the photoreceptor.

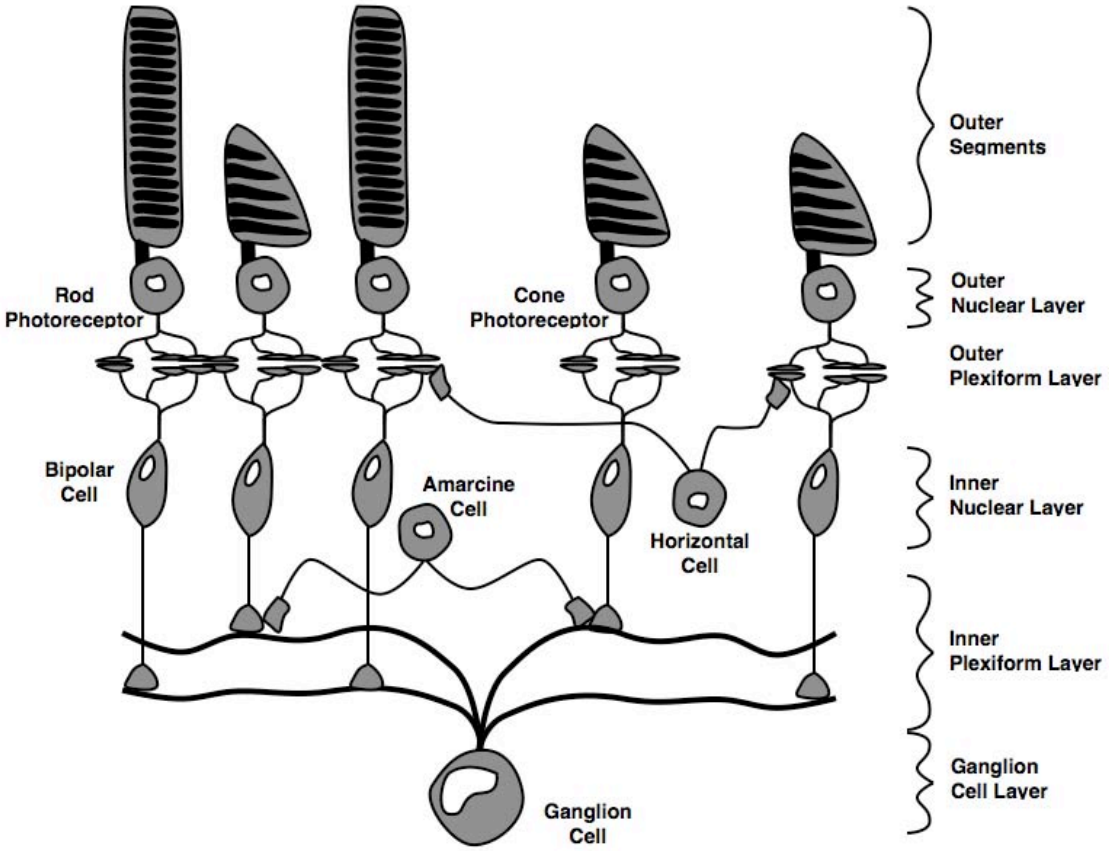

Figure 1.2:

The retina.

Light-induced electrical signals in photoreceptors are transmitted to bipolar cells via synaptic terminals called cone pedicles, which form the outer plexiform layer (OPL) of the retina. Photoreceptors make synapses onto three major classes of bipolar cells, the ON and OFF cone bipolar cell and the rod bipolar cell. The cell bodies of bipolar cells, along with the inhibitory amacrine interneurons comprise the inner nuclear layer (INL) of the retina. Rod and cone bipolar cells receive input from rod and cone photoreceptors, respectively. Cone bipolar cells are classified into ON and OFF type depending on the sign of the light-

induced voltage response. For ON bipolar cells the light induced reduction in transmitter it receives is transduced into a depolarizing voltage response by the metabotoropic glutamate receptor mGluR6. At the OFF bipolar cell AMPA receptors mediate a hyperpolarizing response to light and a subsequent decrease in neurotransmitter. The rod bipolar cell utilizes the mGluR6 receptor giving it an ON type response.

Bipolar cells next pass the light signal to ganglion cells located in the ganglion cell layer, through synaptic connections that make up the inner plexiform layer (IPL) of the retina. Ganglion cells function as the output neurons of the brain by collecting synaptic inputs from the retina circuitry and generating action potentials which travel down their axon to the brain. The division of the ON and OFF information pathways in the retina is maintained in the IPL layer where ON and OFF bipolar cell terminals form synaptic connections to ganglion cell dendrites that stratify in different sublamina of the IPL. OFF bipolar cells terminate in the outer portion of the IPL in sublamina a, and ON bipolar cells terminate in inner portion of the IPL in sublamina b. By making selective contact with the ON and OFF layers of the IPL ganglion cells receive input from either one or the other pathway giving rise to ON and OFF ganglion cells, or they can contact both layers for an ON-OFF response.

In addition to the direct pathway through the retina, there are extensive lateral connections in the retina mediated by horizontal and amacrine cells. Horizontal cells make lateral connections with photoreceptor terminals in the OPL and are thought to give bipolar cells a center surround organization. In the IPL

the inhibitory amacrine cells make extensive connections with bipolar cell terminals as well as ganglion cell dendrites. This extensive lateral processing gives rise to the many complex receptive field properties of the ganglion cells.

One special pathway in the retina is the rod bipolar, to AII amacrine cell, to cone bipolar cell pathway. This circuit is special, because it is the primary pathway for low-light level information in the rods to travel through the retina to the brain. Through this circuit rod output is separated into ON and OFF signals by the AII amacrine cell and fed into the ON and OFF cone bipolar cell system. This eliminates the need for redundant inner processing mechanisms in the retina for low light level signals.

The retina performs an extensive coding process of visual information as evidenced by the 20 different types of ganglion cells each representing a different type of visual information being sent in parallel to the brain. A majority of these pathways convey spatio-temporal information about the pattern of light on the retina making them particularly useful for extracting information about the constantly moving visual scene that an animal experiences. One type of motion sensitive cell responds differentially to the direction of image motion across the retina. Since the time that direction selective cells in the retina were first described, the retina direction selective circuit has been the subject of a considerable amount of study, as it is viewed as being both an experimentally and theoretically tractable example of neural computation in the nervous system.

Early descriptions of direction selectivity in the retina

Motion sensitive cells in the vertebrate retina were first described in the frog in 1953 by Horace Barlow (BARLOW, 1953). The first *direction-selective* cells in the vertebrate retina were first described by Maturana et al in 1960. In the mammalian retina direction-selective ganglion cells (DSGCs) were first described by Barlow and HIll in 1963. This early description was quickly extended to characterize the fundamental aspects of much that is known about retinal direction selectivity, including directional and velocity tuning and contrast sensitivity (Barlow et al., 1964; Barlow and Levick, 1965b). These early recordings were done in intact anesthetized or de-cerebrated animals with single unit recordings from the retina. Later advances in in-vivo preparations, electrical recording techniques, and visual stimulation have refined and extended these initial findings, yet the fundamental observations remain unchanged over the years.

The direction selective ganglion cell circuit

Two types of DSGCs have been identified in the retina, the ON-OFF and ON type DSGC (Barlow and Levick, 1965b); (Oyster, 1968). While there are key differences between in the response properties of the two cells, there are also many similarities, and it appears that both may share a similar mechanism for generating the directional signal. Because the majority of studies, as well as the research presented in this dissertation, have been conducted on the ON-OFF subtype, the majority of the discussion will refer to the ON-OFF type DSGC and we will simply refer to this type as the DSGCs, unless otherwise specified.

Direction-selective ganglion cells are found in all vertebrate retinas and make up about 10% to 20% of the ganglion cells in the rabbit (Oyster et al., 1972 Vaney, 1994). The characteristic response of the DSGC is robust firing of action potentials in response to an object moving in one direction across its receptive field, called the preferred direction of the cell, and little or no response to movement in the opposite direction, called the null direction. This behavior was found to be surprisingly robust over a wide range of stimulus conditions independent contrast sign, shape, direction and velocity of the stimulus (Barlow et al., 1964). Both the ON and the ON-OFF direction selective ganglion cell contribute to the vestibulo-ocular reflex (Yoshida et al., 2001). The ON type is thought to subserve the detection of global motion and the ON-OFF type is thought to contribute to local motion detection; however, the role ON DSGCs role is more securely defined by both theoretical and experimental evidence (Oyster et al., 1972; Soodak and Simpson, 1988); for further discussion see (Vaney et al., 2001).

Receptive field properties of the DSGC. DSGCs give both an ON and OFF response to stationary and moving stimuli. In response to stationary stimuli the DSGCs response transiently with a short latency (Barlow et al., 1964), often with only a few spikes. Experiments mapping the extent of the receptive field by flashing small spots or bars at locations across the receptive field have demonstrated that the receptive field appears to be fairly uniform, although more detailed studies have revealed a limited amount variation within the receptive field (He et al., 1999a). This type of study has also revealed that the spatial extent of the cells

receptive field corresponds well with its dendritic field for both static and moving stimuli (Yang and Masland, 1994b).

For moving stimuli, the direction selective firing pattern of the DSGC defines the cell type. For preferred direction motion DSGCs respond transiently and robustly, with firing rates approaching 250 Hz, near the limit set by the time course of the action potential after-hyperpolarization. Responses remain equally directionally selective for ON and OFF responses and over a range of stimulus contrasts, luminance and velocities, and the directional tuning of ON and OFF responses perfectly overlap (Yang and Masland, 1994b). The DSGC responds well to velocities ranging from 0.1 degrees per second, to greater than 10 degrees per second, In contrast, the ON type DSGC responds with much greater sensitivity to slow velocities, but overall has a narrower velocity tuning. DSGC responses are robust over a wide range of luminance values and can operate throughout the scotopic and photopic ranges.

Oyster and Barlow found that the preferred directions of DSGCs could be grouped into one of four directions, roughly corresponding to the four cardinal axis of the eye (Oyster and BARLOW, 1967), thus delineating four subpopulations of DSGCs with a different preferred direction. Later work demonstrated that each of these four subtypes independently tiles the retina, so that every point in visual space is represented by each of the four directions of DSGC (Vaney, 1994b). The previously mentioned ON type DSGC has only 3 different preferred directions, though only the up direction subpopulation shares a preferred direction with the ON-OFF DSGCs, with the other two directions being dis-

tributed so that each of the three directions is equidistant from each other over 360 degrees.

Barlow and Levick were the first to postulate the idea of a directional subunit when they observed that the DSGC was able discriminate the direction of motion for stimuli that traversed 0.25 to 0.5 degrees of the cells receptive field, corresponding to only 5 to 10% of their receptive field (Barlow and Levick, 1965a). A more recent study suggests that the spatial resolution is at least 10-fold finer, providing evidence that DSGCs can compute the direction of motion for stimuli that traverse only 1.1 microns of the retina, a surprising accomplishment given that the minimal spacing between photoreceptors is 1.9 microns (Grzywacz et al., 1994). Theoretical modeling of the passive electrotonic properties of the DSGC dendrites lent support to the hypothesis of multiple computational subunits by suggesting that DSGC dendrites were electrically isolated enough that interactions between excitation and shunting inhibition could occur independently at multiple locations in the dendritic arbor (Koch et al., 1982; Koch et al., 1986). The idea of local computational subunits were originally evoked to explain hyperacuity in the DSGC; however, most of these early modeling studies on computational subunits focused on post-synaptic models of directional, which has now been shown to be incomplete in the face of evidence, that inputs to the DSGC are themselves directional (Borg-Graham, 2001a; Taylor and Vaney, 2002). Work presented in this thesis, lends further experimental evidence for the directionally selective subunit within the DSGC receptive field, and demonstrates that

a local dendritic action potentials are a substrate for directional subunits that is compatible with both pre and post synaptic mechanisms of directional selectivity.

The DSGC receptive field for static stimuli appears to be homogeneous, but direction selective subunits do not appear to be evenly distributed throughout the cell's receptive field. On the side of the DSGC receptive field that a preferred direction stimuli would encounter first, termed the preferred side, is a region that does not show directional selectivity (Barlow and Levick, 1965a) giving an equal response for preferred and null direction motion. He and Masland (1999) later physiologically probed the non-DS zone with finer resolution and paired their observations with morphological data. They described a non-DS zone that comprised between 20 and 25% of the receptive field on the preferred side of the cell and were unable to find any morphological feature or heterogeneity that correlated or explained the non-DS zone.

The existence of a non-DS zone is consistent with the hypothesis that the mechanism of direction selectivity utilizes spatially offset feed forward inhibition and that the locus of directional computation occurs locally and at multiple locations within the receptive field. However, work early in this decade demonstrated that both excitatory and inhibitory synaptic inputs are directionally selective, indicating that the directional computation occurs presynaptic to the DSGC (Borg-Graham, 2001a; Taylor and Vaney, 2002). This work provides a mechanism to account for local computational subunits in the DSGC, while still allowing for a presynaptic mechanism of direction selectivity. In addition, it provided a cohered explanation of the non-DS zone.

Morphology of the DSGC. The physiological description of the DSGC (Barlow and Hill, 1963a) preceded the morphological description by 20 years. Amthor et al was the first to inject intracellular dyes into physiologically identified DSGCs and recover their morphology (Amthor et al., 1984). Many other morphological descriptions of the DSGC followed (Amthor and Oyster, 1995; Amthor et al., 1989; Oyster et al., 1993; Yang and Masland, 1992). These studies revealed that the DSGC was a bistratified ganglion cell with a particularly unique morphology that has been described in other morphological classification schemes as type-1 bistratified (Amthor et al., 1984). DSGCs can easily be discerned from other ganglion cell by their large round soma and characteristic crescent shaped nucleus (Vaney, 1994c), allowing morphological descriptions without the limitations of needing to physiologically identify the cell (Famiglietti, 1987; Famiglietti, 1992; Vaney et al., 1989), which is particularly useful for ultra-structural (Famiglietti, 2005b). DSGC dendrites project to the ON and OFF sublamina of the IPL, sublamina b and a respectively, consistant their ON and OFF responses. Choline acetyl transferase immuno staining reacts with two well-defined plexi delineating sublamina b and a and is often used as a morphological guidepost of IPL position. When the level of stratification of the DSGC was investigated using the cholinergic maker to delineate the IPL sublamina, it was observed that the DSGC dendrites co-stratified with the ON and OFF dendrites of the cholinergic SBAC (Famiglietti, 1987; Famiglietti, 1992; Vaney et al., 1989).

The structure of the DSGC dendrites consists of an extensive branched network consisting largely of thin terminal dendrites (Figure 3a). These dendrites have been described as having a mesh-like appearance that regularly cover the extent of the retina. The fine terminal branches are often several branching orders away from the three to four primary dendrites that give rise to them. Except for the primary dendrites, it is rare to find dendrites crossing between sublamina (Amthor et al., 1984; Kier et al., 1995; Oyster et al., 1993; Panico and Sterling, 1995; Yang and Masland, 1994a).

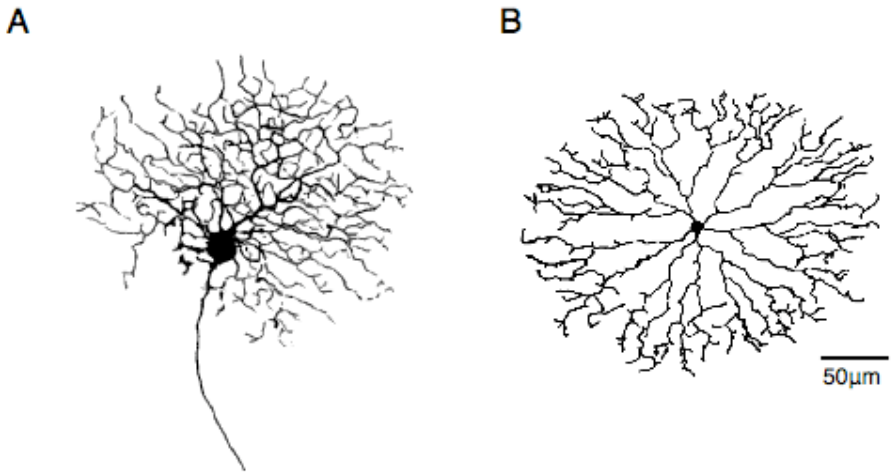

Figure 1.3:

Neurons of retinal direction selectivity. A. Direction selective ganglion cells. Maximum projection image of a multi-photon stack from a Alexa-488 filled DSGC, after offline thesholding and filtering. B Starburst Amacrine cell. Drawing of a SBAC, after Taylor and Wassle, (1995). Note: dendrite thickness is not to scale, A and B.

An obvious place to look for the asymmetry needed to generate directional selectivity is in the morphology of the DSGC. Despite an extensive search no asymmetry has been found in the dendritic architecture, the pattern of association with SBACs or bipolar cells, or in the distribution of various receptor proteins (Amthor et al., 1984 Vaney, 2000; Brown and Masland, 1999b; Chen and Chiao, 2008; Dong and Hare, 2002; Famiglietti, 1992; Famiglietti, 2002; Jeon et al., 2002b; Jeong et al., 2006; Kwon et al., 2007; Yang and Masland, 1994a). As previously noted, there are four subtypes of DSGCs. Though they are physiologically distinct based on their preferred direction, there are no morphological cues that can be used to distinguish cells with different preferred directions from each other, nor that can predict their preferred direction (Vaney, 1994b). The dendrites of the four of DSGC subtypes are not independent of each other, but loosely follow the same path across their respective receptive fields (Vaney, 1994b). Furthermore, these bundles of dendrites closely follow the dendrites of the cholinergic amacrine cells, which are highly overlapping themselves (Vaney et al., 1989; Vaney and Pow, 2000). Thus the SBAC and DSGC dendrites run in fasciculi around the borders of gaps or lacunae approximately 10-50 um in the plane of the sublamina a or b (Brandon, 1987b; Famiglietti, 1987; Tauchi and Masland, 1984). This intimate association of SBAC and DSGC dendrites was the initial basis for the suggestion that SBACs are involved in forming directional selectivity.

The SBAC. The SBAC has a unique morphology getting its namesake from its resemblance to a burst of fireworks (Figure 3b). It has thin radial dendrites projecting symmetrically outward from the soma which terminate in an increased branching pattern and has a greater density of varicose swellings near the distal tips (Famiglietti, 1983c)There are two populations of SBAC in the retina, an ON type and an OFF type. The OFF type has its soma located in the INL and projects its dendrites to sublamina a, and the ON type has a displaced soma located in the ganglion cell layer and projects its dendrites to sublamina b. These two layers of dendrites are the basis for the cholinergic staining pattern in the IPL. Starburst amacrine cells are unique in the retina in that they are the only cell to synthesize and release Ach (Hayden et al., 1980; Masland and Mills, 1979) and they are unique in the nervous system in that they are both cholinergic and GABAergic (O'Malley and Masland, 1989; Vaney and Young, 1988). Furthermore, SBACs are axonless, as are many amacrine cells, so their dendrites must both receive input and mediate neurotransmitter output (Famiglietti, 1983b). It has been determined from ultrastructural work, as well as physiology, (Famiglietti, 1983a; Famiglietti, 1991 Lee, 2006; Hausselt et al., 2007)] that SBACs receive synaptic input over their entire dendritic arbor. These synapses in the adults retina appear to be limited to glutamatergic and GABAergic input, though in the developing retina, SBACs receive nicotinic input from neighboring SBACs (Peters and Masland, 1996b; Zheng et al., 2004a; Zhou and Fain, 1995). In contrast to the homogenous distribution of synaptic inputs, outputs are restricted to the distal ends of the dendrites though it is still unknown if there are

any differences in output location between, Ach and GABA. Paired recordings from SBAC and DSGCs suggest that GABA and Ach release sites are at least functionally distinct from each other because depolarization of the SBAC revealed a GABAergic input to the DSGC, but not a cholinergic input, despite the DSGCs relatively high level of sensitivity to Ach (Fried et al., 2002b; Kittila and Massey, 1997a).

While many retinal neurons are distributed so that they tile the retina with little overlap, the SBAC distribution displays an extremely high degree of overlap, up to 70 fold (Wässle and Riemann, 1978), as mentioned above these overlapping dendrites and the dendrites of DSGCs cofasciculate forming bundles of dendrites traversing the retina around lacunae. The intimate associate of the SBAC with the DSGC lead researchers to postulate a role of SBACs in the direction selective circuit. For this reason, and the observation that the SBAC is the only cholinergic neuron in the retina, much work has been done to describe these cells, though most of the studies have examined the ON type SBAC because of the easy experimental accessibility of its displaced soma.

Physiological recordings of SBACs were first made using sharp electrode recording by Miller and Bloomfield, (1983), who characterized the ON and OFF responses of the two subtypes. Subsequent physiological descriptions described a retinal neuron with a classic center surround organization, a glutamatergic light evoked synaptic input, and a receptive field delimited by the extent of the dendritic arbor (Bloomfield, 1992b; Peters and Masland, 1996a; Taylor and Wässle, 1995a). Another key feature of these cells is their tonic excitatory input, charac-

terized by a high variance, and large, fast synaptic events that are mediated by AMPA/Kainate receptors (Peters and Masland, 1996a; Taylor and Wässle, 1995a). Initially directional voltage responses to the SBAC could not be detected (Peters and Masland, 1996a); however, in 2002 Euler et al, discovered that directional calcium transients could be detected in the dendrites for motion directed from the cell soma towards the distal tip of the dendrite, but not for movement in the opposite direction. They found that these directional calcium signals reflected weak directional voltage signals recorded at the soma. After further refinement of visual stimuli, namely stimuli that move in a radially symmetric pattern, directional responses could be detected at the SBAC soma (Gavrikov et al., 2003; Gavrikov et al., 2006; Hausselt et al., 2007; Lee and Zhou, 2006).

DSGC synaptic inputs and pharmacology. DSGCs have been shown to be responsive to a variety of neurotransmitters including glutamate through AMPA/Kainate, (Jensen, 1999; Kittila and Massey, 1997b) and NMDA receptors (Cohen and Miller, 1994; Kittila and Massey, 1997b), acetylcholine, through nicotinic receptors (Ariel and Daw, 1982a; Ariel and Daw, 1982b; Masland and Ames, 1976) and the inhibitory neurotransmitter GABA, through GABAa receptors (Caldwell and Daw, 1978; Chiao and Masland, 2002b; Kittila and Massey, 1997b; Wyatt and Daw, 1976). A physiological role for $GABA_a$ receptors in the direction selective circuit was identified early on when it was discovered that the traditional $GABA_a$ receptor antagonist picrotoxin abolished the direction selectivity of DSGCs by causing the cell to fire an equal number of spikes in the preferred and

null directions (Wyatt and Daw, 1976), This initial result has been confirmed by a number of groups (Caldwell and Daw, 1978; Chiao and Masland, 2002b; Kittila and Massey, 1997b).

Because of the SBAC DSGC relationship and the observation that SBACs are the only cholinergic cells in the retina, a role for Ach in direction selectivity has long been favored. Despite DSGCs being highly sensitive to Ach through nicotinic receptors (Ariel and Daw, 1982a; Kittila and Massey, 1997b; Masland and Ames, 1976), Ach does not appear to be required for generating the DS signal. When nicotinic antagonists are applied to the retina, the number of spikes to stationary stimuli and preferred direction stimuli is reduced, but direction selectivity remains robustly intact for a wide range of stimulus conditions. Based on the observation that light evoked spiking is reduced in the DSGC in the presence of nictotinic receptor antagonists, it was postulated that Ach provides the majority of the excitatory drive to the DSGC (Ariel and Daw, 1982a; Cohen and Miller, 1995; Kittila and Massey, 1995; Kittila and Massey, 1997b). More recent observations, including work presented here, has called into question the existence of a direct cholinergic input to the DSGC and suggested that all the synaptic input to the DSGC is mediated by glutamate, through AMPA/kainate and NMDA receptors. Grzywacz et al (1998) did find that direction selectivity to low spatial frequency gratings had a component that was mediated by nicotinic receptors and more recently work by Fried et al (2005) described that nicotinic receptors are involved in the pathway that shapes preferred direction inhibition in the DS. Despite these

hints at possible roles for Ach in direction selectivity, the mechanism through which Ach contributes to direction selectivity remains unknown.

Mechanisms of Direction Selectivity

Proposed mechanisms to describe direction selectivity can be grouped into two categories, pre and post synaptic. Neither model is mutually and, given that DS is a robust phenomena, it seems likely that DS may be formed by multiple overlapping or redundant mechanisms. Indeed, it is clear that at least two mechanisms contribute to DS as both the excitatory and inhibitory inputs to the DSGC are directional, so it follows that each modality must have a mechanism. Regardless of the locus at which DS is computed in the retinal circuitry it is clear from antagonism of GABAa receptors that the DS signal in the retina relies on a feed-forward inhibitory mechanism (Amthor and Grzywacz, 1993; Barlow and Levick, 1965a; He et al., 1999a). For this reason, many proposals have focused on inhibition in the DSGC, either how inhibition generates direction selectivity in a post-synaptic model, or how directional inhibition is formed in presynaptic models.

It was first postulated that direction selectivity arose as a post-synaptic computation in the DSGC dendrites based on the observation that DS appeared to be computed locally in the DSGC receptive field, as described above. Theoretical modeling suggested that local postsynaptic discrimination could be achieved with non-linear interactions in the dendrites of the DSGC. The non-linear interaction typically invoked in this kind of model is shunting inhibition. This

type of interaction is favored, because it operates in a spatially localized manner, and is sensitive to the spatial arrangements of the excitatory and inhibitory synapses (Koch et al., 1982; Koch et al., 1983). In these models, inhibition can effectively shunt excitatory inputs when it meets certain spatio-temporal requirements. It must be located near the excitatory current source, be sufficiently large (10 to 50 nS), and last long enough to sufficiently overlap with the time course of the excitatory input (Koch et al., 1983; Segev and Parnas, 1983). While these models reproduce certain aspects of direction selectivity, other theoretical considerations demonstrate that robust direction selectivity based on shunting inhibition is difficult to achieve except in very limited areas of parameter space, which may not match biological constraints (Grzywacz and Koch, 1987). Furthermore, experimental evidence to support postsynaptic shunting inhibition has been limited (Taylor et al., 2000). With the demonstration that synaptic inputs to the DSGC were already directional, a postsynaptic model of direction selectivity has fallen out of favor, and increasingly experimental evidence has supported presynaptic models of direction selectivity.

The major support for a presynaptic mechanism comes from the observation that the synaptic inputs to the DSGC are themselves directional, with inhibitory inputs being 2 to 10 times larger in the null direction and excitatory inputs being larger in the preferred direction (Borg-Graham, 2001b; Fried et al., 2002a; Fried et al., 2005a; Taylor and Vaney, 2002). This observation has focused the attention of researchers on finding the source or sources of the presynaptic mechanism. Several lines of evidence suggest that the SBAC may be involved in

generating some or all of the presynaptic inputs. When the SBAC is selectively ablated using toxins, DS in the retina is abolished (Amthor et al., 2002; Yoshida et al., 2001). When a variation of this experiment was performed by ablating a limited population of SBACs with a laser, direction selectivity remained (He, 1999). The laser ablation experiment is widely viewed as evidence that the SBAC network is highly redundant, as evidenced by the high degree of SBAC overlap, and not as evidence that SBAC do not contribute to direction selectivity. Further evidence for the SBACs role in direction selectivity comes from observations by Fried et al (2002), where they made paired recordings between DSGCs and neighboring SBAC cells. The found that they could evoke GABAergic inhibition in the DSGC by depolarizing SBACs located on the null side of the DSGC, but not on the preferred side. This piece of evidence is the basis for the notion that the DSGC is selectively contacted by GABAergic SBAC synapses on the null side of the cell, which generates the spatial asymmetry needed for directional selectivity in the DSGC. At the time, it was also surprising to find that depolarization of the SBAC did not evoke nicotinic synaptic input, as it was commonly though that the SBAC provided the majority of the excitatory input through nicotinic receptors.

The realization that direction selectivity is computed presynaptically to the DSGC and that SBACs are likely involved, roughly coincided with the observation that SBAC dendrites could elicit directional calcium transients in their dendrites (Euler et al., 2002a). This has lead many researchers to search for the mechanisms that generate directional signaling in the SBAC, and therefore directional

inhibitory input required for direction selectivity in the DSGC. Two types of models to explain direction selective signals in the SBAC have been proposed. The first model relies on the intrinsic properties of the SBAC dendrite to generate directional signals in the dendrites; however, theoretical work indicated that DS would occur over only limited ranges of stimulus conditions for a given parameter set (Tukker et al., 2004). Another prediction from the modeling that contradicted experimental observation was that the voltage signal at the soma would be non-directional or have a reversed directionality from what was observed (Tukker et al., 2004).

A second type of mechanism proposed was one that relied on inhibitory synaptic connections to generate the SBAC DS signal (Borg-Graham and Grzywacz, 1992; Lee and Zhou, 2006). Lee and Zhou recently provided evidence suggesting that SBAC signals were generated by reciprocal GABAergic contacts between neighboring SBACs. The arrangement of inhibitory inputs from neighboring SBAC can form a spatially asymmetric pattern of inhibition and excitation for a given point near the distal tips of the SBAC dendrites. Work by Gavrikov et al, (2006) has suggested an alternate mechanism to the one proposed by Lee and Zhou, where an asymmetry is set up in the GABA inputs themselves through a chloride gradient in the SBAC dendrites; however, it is not clear how such a mechanism could generate the temporal differences needed to compute direction, nor is it clear how the chloride gradient mechanism could maintain asymmetric GABA currents near the membrane potential needed for synaptic release (Gavrikov et al., 2003; Gavrikov et al., 2006).

Most recently Hausselt et al (2007) has provided experimental and modeling evidence for a variation on the dendritic mechanism of DS, where instead of passive membrane properties, active conductances and a voltage gradient interact to produce directional voltage signals at the soma and distal dendritic tips. They found that SBAC DS could be generated for stimuli which were restricted to the dendrites of the SBAC, thereby excluding the neighboring SBACs proposed to be involved in the Lee and Zhou model. Furthermore, they found that SBAC DS was independent of involvement of GABAa receptors. Their observation that directional signaling could be modulated by the holding potential of the membrane suggested a role for voltage gated calcium channels in generating SBAC DS as had been previously proposed (Jensen, 1995b).

While it is clear that the SBAC responds differentially to directional stimulation, the possibility of directional excitatory inputs to the SBAC as an explanation for DS signals in the SBAC has not been investigated in much detail. In this thesis, I present data which argues that excitation to the SBAC is itself directional, and that an AMPAergic voltage-gradient does not play a significant role in generating direction selectivity. We did find that tetrodotoxin-resistant voltage-gated sodium channels (TTX-R VGSC) contribute to the directional response by preferentially activating during centrifugal motion and increase the response to centripetal. While it may seem surprising that DS at only the second synaptic relay point in the retina, it is clear that directional excitation exists in the DSGC. Since the DSGC receives a majority, if not all, of its excitatory inputs from bipolar cell terminals and directional excitation persists in the presence of nicotinic an-

tagonists, it follows that bipolar cells must directionally release glutamate onto DSGC dendrites.

While synaptic conductances are clearly directional and direction selectivity is certainly formed prior to the DSGC dendrites, the DSGC is the final generator of the directional signal and it is clear that it must have some role in integrating these directional inputs. Current-clamp recordings presented in this thesis, show that the directional difference in postsynaptic potential is often small and cannot reliably account for the robust directional spike output over a wide range of conditions (Oesch et al., 2005a). This indicates that postsynaptic mechanisms play an important role in processing the synaptic input to the DSGCs. The most obvious postsynaptic mechanism that could be employed by the DSGC is a simple axosomatic spike threshold. When we investigated the role of the axosomatic spike threshold in the DSGC we discovered that voltage at the soma was a poor predictor of the light evoked spiking behavior of the cell, and could not produce robust directional discrimination. In this thesis, I provide evidence that the critical spike threshold for generating direction selectivity is located at multiple points in the dendrites by dendritically located voltage gated sodium channels. The discovery of dendritic action potentials in the DSGC provides a substrate for local direction subunits that have long been observed in the DSGC and provide a mechanism capable of generating robust direction selectivity over a wide range of stimulus conditions. Furthermore, the existence of dendritic spikes provide an description of the local computational subunit that is consistent with the existence of the non-DS zone.

Non-linear dendritic processes

Dendrites represent the first point where integration of synaptic inputs can occur in a neuron, and for over a century dendritic properties have been the subject of intensive study (for review see, Hausser, 2005). How a dendritic arbor integrates these PSPs depends on the electrical membrane properties of the neuron. Classically, the electrical properties of dendrites were thought to be passive, so that post-synaptic potentials would sum at the action potential initiation zone according to simple arithmetic rules. This model is commonly referred to as the point neuron model. Even in passive dendrites non-linear interactions can violate the ideal point neuron model (Rall, 1964). More recently, the dendrites of many neurons have been observed to possess active electrical properties, further extending the repertoire of non-linear processes the dendrite is capable of using to perform neural computation. A more complicated alternative model of synaptic integration to the simple point neuron model that takes into account one type of active dendritic property, dendritic spiking, is the multi-subunit model, where multiple action potential initiation zones independently threshold synaptic information in the dendritic arbor before the signal is passed to the soma and subsequently travels down the axon (Poirazi et al., 2003). In other similar models this arrangement increases the computational capability of the neuron (Mel, 1993; Poirazi et al., 2003; Poirazi and Mel, 2001).

Non-linear interactions can take place in dendrites with only passive membrane properties at work and the passive properties may dominate dendritic computations even when the dendrite is electrically active (London et al., 1999).

The most common type of passive non-linear interaction is so called “shunting” inhibition. Fatt and Katz (Fatt and Katz, 1953), first noted that inhibition can have a divisive effect on excitatory inputs. A key feature of this type of interaction that makes it an attractive theoretical tool for dendritic computation is that it can be highly spatially localized. When inhibitory and excitatory inputs are located near each other in space and time the interaction can be highly non-linear; however, when excitation and inhibition are widely separated, linear summation at the soma will dominate (Rall, 1964). Recently Liu et al. (2004) provided experimental evidence that shunting inhibition could take place in a spatially located region of hippocampal dendrites, validating a significant amount of theoretical work (Koch et al., 1982; Koch et al., 1983) Theoretical studies extended these findings to demonstrate that not only is the non-linear interaction dependent on the proximity of inputs, but also on the spatial order relative to the soma, with on the path inhibition having a significantly larger effect, than inhibition located outside the path between the excitatory inputs and the observer (Jack, 1975; Koch et al., 1982; Segev and Parnas, 1983; Torre and Poggio, 1978). Early modeling showed that this effect could be powerful enough to block the propagation of action potentials (Koch et al., 1983). These models have some interesting implications for direction selectivity, since spatial and temporal asymmetries are a key requirement of a direction selective mechanism. Furthermore, with the demonstration that DSGCs exhibit dendritic action potentials, action potential failure, could be a possible mechanism sharpening directional tuning. Later modeling presented in this thesis using a compartmental biophysical model of the DSGC, demonstrated that

shunting inhibition could not adequately block propagating spikes in the DSGCs model, and its effect had considerably less spatial dependance than was initially predicted (Koch et al., 1983).

The idea that dendrites function primarily as passive collectors of synaptic information has long been discarded; however, this notion persisted long past the first evidence of active membrane properties in the dendrite. The first suggestion that dendrites might have active properties came from the observation of fast pre-potentials in hippocampal neurons (Spencer and Kandel, 1961) and the very first direct dendritic recordings provided confirmation that dendrites posses active conductances (Fujita, 1968; Llinas and Hess, 1976; Llinas et al., 1968; Llinas and Sugimori, 1980; Wong and Prince, 1978; Wong et al., 1979). It now appears that dendrites can posses a wide range of voltage-gated ion channels including voltage-gated sodium channels, voltage-gated calcium channels, voltage-gated potassium channels, and Ih channels (Magee and Carruth, 1999).

Much research into active dendritic conductances have focused on voltage-gated sodium, and voltage-gated calcium channels, and to some extent NMDA receptors. While subtypes and distributions vary widely among neurons, they have been described on the dendrites of many neurons, including retinal ganglion cells (GC specific reference. for review see, (Gulledge et al., 2005). Typically, these two types of voltage-gated ion channels function to either boost synaptic (Lipowsky et al., 1996; Oviedo and Reyes, 2002; Schwindt and Crill, 1995), or generate dendritic action potentials (Golding and Spruston, 1998; Stuart et al., 1997b; Wong et al., 1979, Chen, 1997 #2741) or NMDA spikes

(Schiller et al., 2000; Schiller and Schiller, 2001). In addition, calcium entering through voltage-gated calcium channels can activate a wide range of second messenger systems (Berridge, 1998; Zucker, 1999).

A large portion of research on active excitatory dendritic conductances has focused on dendritic action potential initiation or propagation. The existence of dendritic spikes was first suggested by Spencer and Kandel (Spencer and Kandel, 1961) and extended by many others (Llinas and Nicholson, 1971; Schwindt and Crill, 1997; Turner et al., 1991). Direct dendritic recordings have corroborated and extended these findings using electrophysiological (Chen et al., 1997; Golding and Spruston, 1998; Hausser et al., 2000; Llinas and Sugimori, 1980; Martina et al., 2000; Schwindt and Crill, 1997; Stuart et al., 1997b; Velte and Masland, 1999b) and optical techniques (Djurisic et al., 2004; Kasuga et al., 2003). Dendritic action potentials raise numerous important implications for dendritic computation. Perhaps most importantly this arrangement can form multiple integration subunits within the dendrites, increasing the computational abilities of the neuron (Mel, 1993; Poirazi and Mel, 2001).

Alternatively, voltage gated sodium channels could support the retrograde propagation of an action potential at the soma into the dendritic arbor. Direct dendritic recordings have also shown that action potentials initiated in the soma can back-propagate into the dendrites of several types of neurons (Spruston et al., 1995; Stuart et al., 1997b; Stuart and Sakmann, 1994). This has important implications for synaptic plasticity (Linden, 1999; Magee and Johnston, 1997) as

well as for burst firing at the soma (Magee and Carruth, 1999; Williams and Stuart, 1999).

Other dendritic conductances besides synaptic inhibition and voltage gated sodium channels can exert control over the membrane potential and spike output of a cell. A growing body of work suggests that in many neurons I_h functions primarily to control the electrical compactness of a neuron, which in turn controls the properties of spatial and temporal summation of synaptic inputs (Berger et al., 2003; Magee, 1999). They have been implicated in contributing to the resting membrane potential, and evidence from pyramidal neurons suggests that their main function is to adjust the membrane time constant of the cell to affect the degree of signal attenuation between the somatic and dendritic compartment, which in turn changes the properties temporal summation of synaptic inputs (Magee, 1998; Williams, 2000; Migliore, 2004). In addition to Ih, other more traditional voltage-gated potassium channels can play a role in regulating dendritic excitability (Goldberg et al., 2003; Hoffman et al., 1997).

Work presented in this thesis and work by others demonstrates multiple roles of active dendritic non-linearities in a well-known neural computation, direction selectivity in the retina. Our results on dendritic spikes in the DSGC demonstrate a clear role of orthograde dendritic spiking under physiologically relevant conditions. While previous studies have demonstrated the existence of orthograde dendritic spiking, it is not clear if the stimulus conditions under which this behavior is evoked are relevant to the normal conditions experienced by the cell.

In the SBAC we demonstrate how subthreshold active conductances act as a non-linear amplifier of differences in synaptic input. Furthermore, we add another channel, the TTX-resistant voltage-gated sodium channel, to the list of active dendritic conductances that contribute to the computational repertoire of dendrites. Prior to the description presented here, roles for TTX-R VGSCs had been described in dorsal root ganglion (DRG) neurons. However, the computational role of DRG signaling remains unclear. In our preparation, we were able to demonstrate that a TTX-R VGSC performs a clear computational task in a well-defined neural computation.

CHAPTER 2 DIRECTION SELECTIVE DENDRITIC ACTION POTENTIALS IN RABBIT RETINA

Abstract

Dendritic spikes that propagate towards the soma are well documented, but their physiological role remains uncertain. Our *in vitro* patch-clamp recordings and two-photon calcium imaging show that direction-selective retinal ganglion cells (DSGCs) utilize orthograde dendritic spikes during physiological activity. DSGCs signal the direction of image motion. Excitatory sub-threshold postsynaptic potentials are observed in DSGCs for motion in all directions and provide a weakly tuned directional signal. However, spikes are generated over only a narrow range of motion angles, indicating that spike generation greatly enhances directional tuning. Our results indicate that spikes are initiated at multiple sites within the dendritic arbors of DSGCs, and that each dendritic spike initiates a somatic spike. We propose that dendritic spike failure, produced by local inhibitory inputs, might be a critical factor that enhances directional tuning of somatic spikes.

Introduction

More than 40 years ago, electrophysiological recordings documented the presence of fast prepotentials in hippocampal neurons (Spencer and Kandel, 1961). Subsequent work suggested that such events represent spikes initiated within the dendrites, and that these spikes propagate to the soma and initiate ac-

tion potentials at the soma or initial axonal segment (Llinas and Nicholson, 1971; Schwindt and Crill, 1997; Spencer and Kandel, 1961; Turner et al., 1991). Direct dendritic recordings have corroborated and extended these findings using electrophysiological (Chen et al., 1997; Golding and Spruston, 1998; Hausser et al., 2000; Martina et al., 2000; Schwindt and Crill, 1997; Stuart et al., 1997a; Velte and Masland, 1999a) and optical techniques (Djurisic et al., 2004; Kasuga et al., 1993). It is evident that the site of action potential initiation can depend on the characteristics of the stimulus driving the neuron (Chen et al., 1997; Martina et al., 2000). Moreover, dendritic spikes initiated within functionally isolated dendritic compartments, can propagate to the soma even in the presence of continuous synaptic activity (Williams, 2004). Direct dendritic recordings have also shown that action potentials initiated in the soma can back-propagate into the dendrites of several types of neurons (Spruston et al., 1995; Stuart et al., 1997a; Stuart and Sakmann, 1994). The extent to which dendritic action potentials contribute to neural computation remains unresolved.

Fohlmeister and Miller (1997) predicted from their modeling studies that the dendrites of retinal ganglion cells are active. Dendritic spikes have been observed in a- ganglion cells, which have large somas and thick primary dendrites (Velte and Masland, 1999a). In that study, spikes were elicited by current injection into either the soma or dendrite, and therefore it is not known whether dendritic spikes are generated during light-evoked activity. In this study we provide evidence for light-evoked dendritic spikes in a well-defined class of retinal gan-

glion cell, the direction-selective ganglion cell (Taylor and Vaney, 2003; Vaney and Taylor, 2002).

Direction-selective ganglion cells (DSGCs), which make up about 10% of the ganglion cells in the rabbit retina (Vaney, 1994b), signal the direction of image motion across their receptive fields by firing action potentials in a preferred direction, and not in the opposite, or null direction. These cells are ON/OFF ganglion cells, meaning that the cell responds to the onset and termination of a light flash. The ON- and OFF- postsynaptic potentials (PSPs), which comprise excitatory and inhibitory components (Taylor and Vaney, 2002), are received through two separate dendritic arbors that stratify narrowly at distinct levels within the inner plexiform layer. The extents of these two dendritic arbors define the extent of the receptive fields for ON and OFF responses (Yang and Masland, 1992). The outer, or OFF-dendritic arbor, is furthest from the soma and responds only to light decrements, while the inner, or ON-dendritic arbor responds to light increments. A practical consequence of the dendritic structure is that the experimenter can selectively stimulate only one dendritic arbor by the choice of stimulus contrast. For example, the leading edge of a dark stimulus bar moving across the receptive field will activate the OFF dendritic arbor, while the trailing edge of the same stimulus bar will activate the ON dendritic arbor. Because the axon arises from the soma in these cells, signals must pass through the soma before reaching the axon.

Under some conditions we observed small spike-like events elicited in response to physiological stimulation of DSGCs, and therefore we postulated that

these events might represent dendritic spikes. In this paper, we investigate the properties of these putative dendritic spikes, and show that spike generation allows transmission of salient sensory inputs and precludes the transmission of information during inappropriate stimuli. We propose that dendritic spikes have a clear physiological role in dramatically increasing the directional tuning of these cells.

Results

Action Potentials Sharpen Directional Tuning in DSGCs

The strength of the directional tuning can be quantified using a directional tuning index, DSI (see methods) that ranges between zero and one, with larger values being more directional. The DSI measured from spikes in current-clamp recordings averaged 0.67±0.13 for the ON response and 0.74±0.13 for the OFF response, similar to DSIs of 0.53±0.13 and 0.64±0.12 obtained from extracellular spike recordings in the same 12 cells (Figure 1A). The angle of the preferred direction did not differ between current-clamp and extracellular recording conditions ($p>0.6$, paired t-test). The DSI was also estimated from the post-synaptic potential (PSP) amplitude under current-clamp conditions. In order to measure the PSP amplitude, we removed spikes either digitally during off-line analysis, or pharmacologically by adding 0.5μM TTX to the superfusion solution (Fig. 1B). The directional difference in the amplitude of PSPs varied widely in the group of cells. In the same group of cells used to estimate DSI from spikes, DSI measured from spike blanked PSPs was 0.09±0.05 for the ON-response and 0.14±0.08 for the OFF-response (N=12). When TTX was applied, DSI was 0.11±0.05 for the

ON response and 0.16±0.04 for the OFF response (N=10). These low DSI values corresponded to PSP amplitude differences between preferred and null direction stimuli that ranged from 0 to 7.8mV with a mean of 3.7±1.7mV for the ON response, and -3.7 to 10.1 mV with a mean of 3.8±3.0mV for the OFF response (Fig. 1C). The spike DSI displayed a weak positive correlation with the PSP DSI measured from blanked PSPs, (regression coefficient of the best fit line was 1.3, r^2=0.53), however, the spike DSI was not dependent on PSP DSI recorded during bath application of TTX, (regression coefficient was 0.39, r^2=0.04, Fig. 1D). The reason for the weak correlation is unclear, but may relate to the presence of voltage-gated sodium channels in the dendrites. On average, the DSI observed for spikes was about six-fold higher than the PSP DSI. The enhanced directional tuning is also evident from the close correlation in the preferred directions for the ON and OFF responses. The difference in the preferred directions between the ON spikes and OFF spikes was 12±9°, while this difference for PSPs was 38±52° (N=12). These results indicate that spike initiation is a potent mechanism for sharpening directional tuning in these cells.

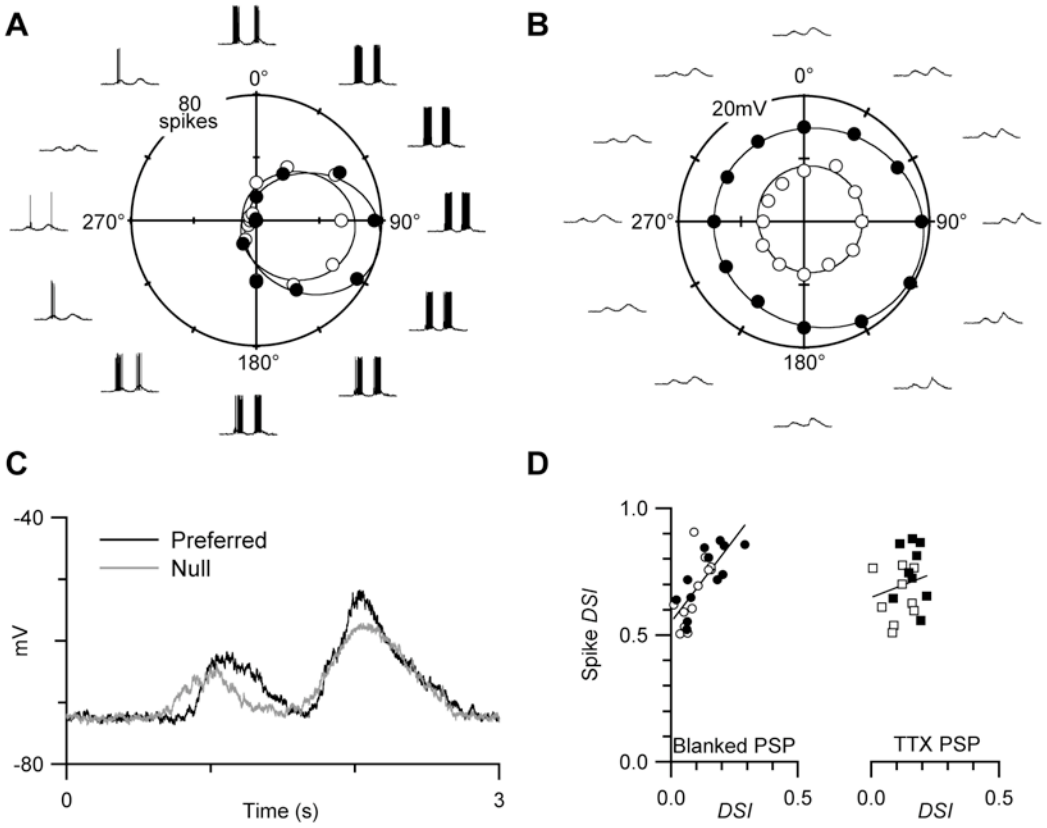

Figure 2.1:

Spike generation sharpens directional tuning. A) Current clamp recordings are shown adjacent to the stimulus angle. Spikes are observed during the leading and trailing edge of the stimulus. Since the stimulus was a bright bar, the leading edge response activated the ON-dendritic arbor (solid symbols), while the trailing edge activated the OFF-arbor (open symbols). Each point on the polar plot shows the total number of spikes elicited during each response. The ON and OFF responses have essentially the same preferred direction. The continuous line shows best-fit von Mises distribution for the ON and OFF responses. The preferred directions obtained from the fits were 97° and 103° for the ON and OFF responses respectively. The DSI values for the ON and

OFF responses were 0.5 and 0.63 respectively. B) 0.5 μM TTX was added to the bath solution to block spiking. The continuous line shows best-fit von Mises distributions for the ON and OFF responses. The preferred directions obtained from the fits were 83° and 110° for the ON and OFF responses respectively. The DSI values for the ON and OFF responses were 0.04 and 0.21 respectively. C) Current clamp responses from the same cell to preferred (solid line) and null direction motion (dotted line). The first PSP represents the leading edge, ON response, and the second PSP the trailing edge OFF response. D) DSIs measured from spike counts plotted against DSIs measured from PSP amplitudes in 12 cells (open symbols = ON responses, closed symbols = OFF responses). Left panel (circles) shows the DSIs of the PSPs determined by blanking the spikes, as described in the Methods. The regression coefficient for the best-fit line was 1.31 (r^2=0.53). In 9 of the 12 cells (right panel, squares), PSP DSIs were measured during bath application of TTX. The regression coefficient for the best-fit line was 0.39 (r^2=0.04).

Spike Initiation Does Not Occur at the Soma for Light-evoked Spikes

Dark-adapted DSGCs had a resting potential of -70.7±1.6 mV (N=13), and an input resistance of 82.0±20.6 MW (N=9). They displayed little spontaneous synaptic input, and had no background spiking. Depolarizing current steps elicited sustained trains of action potentials that displayed prominent after-hyperpolarizations. During hyperpolarizing steps an early transient component was observed suggesting the presence of I_h currents in the DSGCs (Fig. 2A).

Above threshold, spike frequency was a linear function of injected current, with a slope of 0.31±0.18Hz/pA (N = 9, Fig. 2C).

Light stimuli were more potent than direct somatic depolarization for generating spikes in DSGCs (Fig. 2B, D & E). The peak of light-evoked PSPs reached -59.1±1.5 mV, or 11.6±1.5 mV depolarized from the resting potential, and generated 59±21 spikes/stimulus. The mode of the inter-spike interval (ISI) distribution corresponded to a spike rate of 148±30Hz (Fig. 2D open squares, N = 13 cells). In each cell we also injected current through the recording electrode with a waveform generated from PSPs recorded in response to light stimuli for that cell (Fig. 2B, see methods). Using this PSP current command waveform we generated a series of somatic PSPs that bracketed the amplitude of the light-evoked PSP. Invariably, one of these current-injected PSPs would closely match the light-evoked PSP in both amplitude and shape. Injected current waveforms that depolarized the soma to equivalent or slightly more depolarized potentials as the light-evoked PSPs produced 11±9 spikes/stimulus at a modal ISI corresponding to a spike rate of 41±47 Hz (Fig. 2D closed squares). The average peak depolarization reached –56.8±1.3 mV, or 13.9 mV depolarized from the resting potential. This value is 2.3 mV more depolarized than the peak depolarization for the light-evoked PSPs in the same cells, yet produced a significantly lower spike rate and absolute number of spikes ($p<0.001$, paired t-test).

These results suggest that the membrane potential at the soma is a poor predictor of spike initiation during light-evoked PSPs. Direct analysis of the spike threshold confirms this expectation. The spike threshold (see methods) was

measured during current-injected and light-evoked PSPs in 10 cells. In order to obtain a comparable number of spikes under the two conditions, current-injected PSPs that reached more depolarized mean potentials were also analyzed. The probability density distribution of light-evoked spike thresholds was symmetric with a broad monotonic peak at -56mV, and a width at half height of ~8 mV (2117 spikes, Fig. 2E). The peak was approximately centered on the mean PSP amplitude, suggesting that spikes are most likely to occur during a PSP, but the broadness and symmetry of the distribution indicates that spike initiation is essentially uncorrelated with membrane potential during the PSP. The probability density distribution for spike thresholds during current-injected PSPs displayed a narrower peak at -49 mV, and a width at half height of ~4 mV (1233 spikes, Fig. 2E). The distribution was skewed, with a tail towards negative potentials that arose because spike threshold was initially low and in some cells increased during the current-injected PSPs. The increase in threshold presumably resulted from sodium channel inactivation during the depolarization. The results indicate that somatic spike threshold, probed with depolarizing current injection, is considerably more depolarized than the mean light-evoked PSP amplitude, demonstrating that the PSP amplitude at the soma is not the critical factor for generating directional spike discharge. Therefore, we considered the possibility that spike initiation might occur in the dendrites.

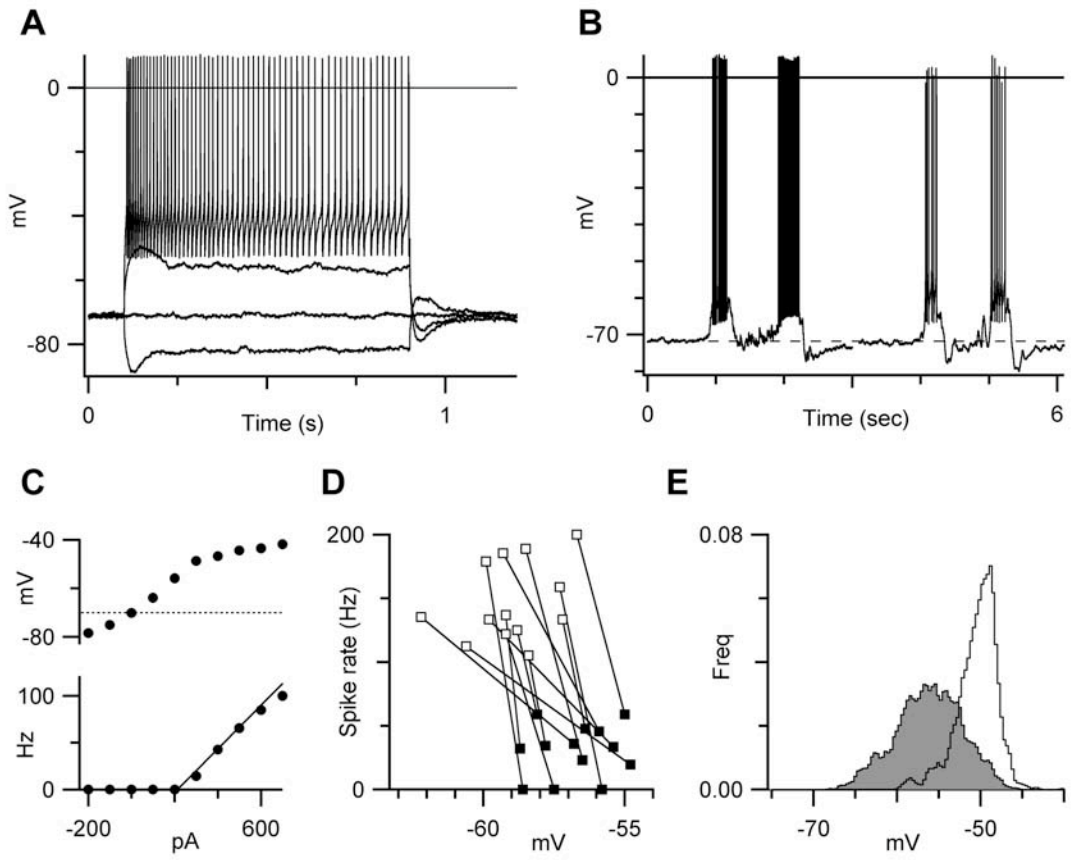

Figure 2.2:

Light stimuli are more potent at generating spikes than direct current injection. A) Current-clamp recordings showing responses to -100, 0, 100, 200pA current steps. B) Response to a bright bar moving in the preferred direction (left trace) and a response from the same cell to direct current injection of a PSP waveform into the soma (right trace). The PSP waveform for the injected current was taken from a previously recorded light response in the same cell. In this example the light stimulus generated 130 spikes/sec while the current injected response produced 36 spikes/sec. C) The upper panel shows the average membrane potential reached during 800ms depolarizing current pulses. The dotted line shows the resting membrane potential. The lower

panel shows the mean spike rate during depolarizing pulses. Above spike threshold, injected current generated 0.28 Hz/pA. The average for 9 cells was 0.31 ± 0.18 Hz/pA. D) Spike-rate versus mean depolarization level. Light stimuli (open circles) produced higher spike rates at similar or less depolarized levels than responses to direct current injection, which mimicked the light-evoked PSP in the same cells. E) Light-evoked spikes and current-injection evoked spikes were generated as described in *B*. Spike threshold measurements from 10 cells were combined to produce probability density distributions for light-evoked spike thresholds (shaded histogram) and depolarization evoked spike thresholds (open histogram).

Spike Initiation Occurs in the Dendrites

Previous work has shown that it is possible to reveal the presence of active dendritic responses when somatic spiking is suppressed by local application of TTX to the soma (Huguenard et al., 1989b; Regehr, 1993; Turner, 1991; Turner, 1989). To investigate the active properties of the dendrites, preferred direction stimuli were presented to a cell every 16 seconds, while a pipette filled with extracellular solution containing 1μM TTX was moved to within about 10μm of the cell soma. Positive pressure was applied to the pipette to eject the TTX solution onto the soma. During somatic TTX application, action potentials were suppressed and replaced by smaller fast-potentials (Fig 3A). The effect of TTX was rapid and reversible (Fig. 3B). The directional tuning of the small spikes was identical to the large spikes (Fig. 3C). The large spikes were brief and displayed

an after-hyperpolarization, whereas the small spikes were broader and lacked the after-hyperpolarization (Fig. 3D). The large and small spikes are clearly separated in amplitude histograms (Fig. 3E). In all cells, the spike amplitudes showed a strong bimodal distribution, with one peak at 7.4±1.9 mV representing the small spikes and a second peak at 54.8±3.5 mV representing the large spikes. It is important to note that inclusion of TTX in the bath solution completely eliminated both large and small spikes, (Fig. 1B,C) indicating that TTX-sensitive sodium channels in the dendrites mediate the putative dendritic spikes.

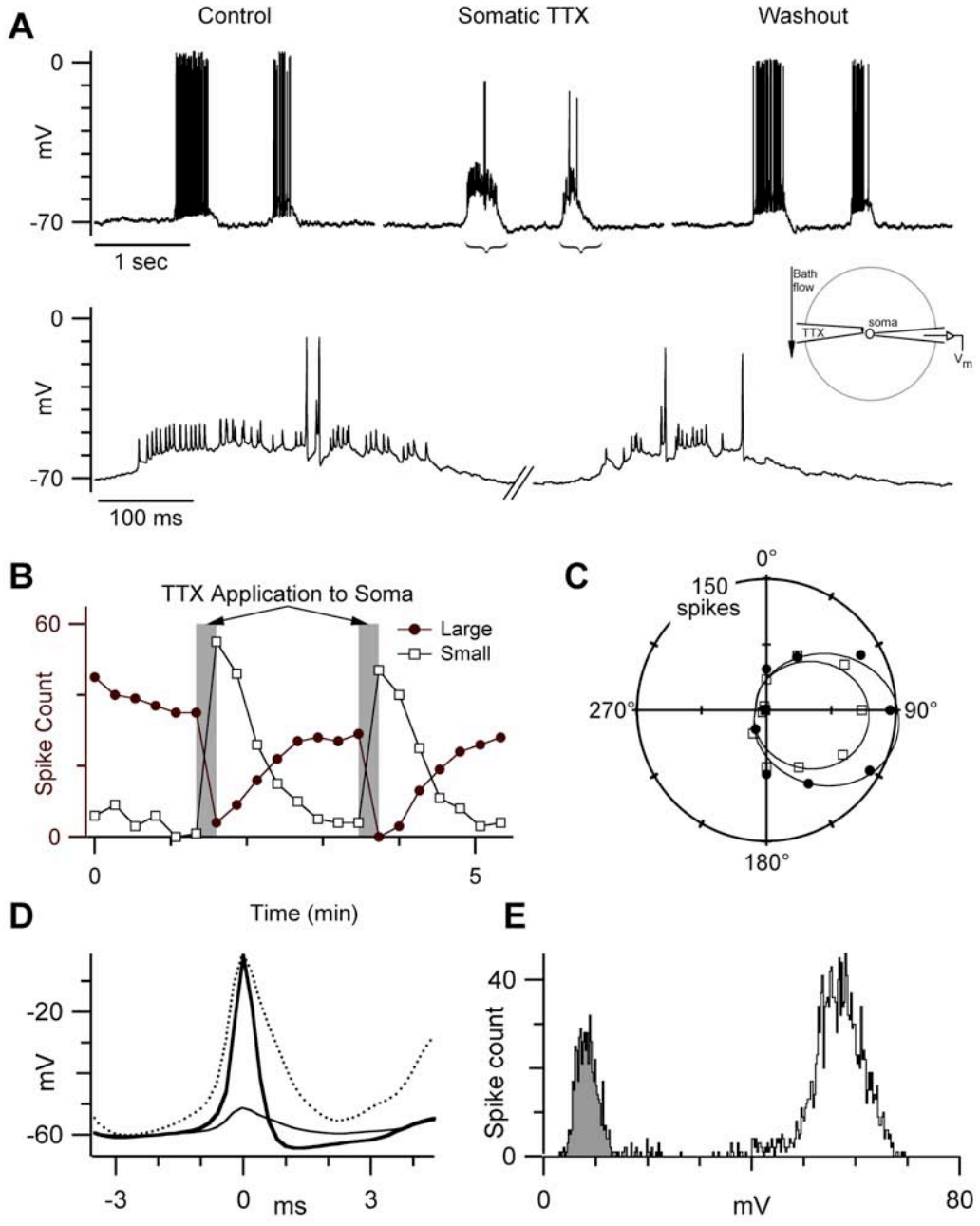

Figure 2.3:

Local TTX application to the soma reveals dendritic spikes. A) Current clamp responses to a dark bar moving in the preferred direction before, during, and after local application of 1 μM TTX to the soma. The lower panel shows, on

an expanded time axis, sections of the upper middle trace denoted by brackets. The inset schematic shows the positions of the TTX and recording electrodes in relation to the soma and the dendritic arbor (outer circle). B) Total spike counts for ON and OFF responses during preferred direction stimuli presented every 16 seconds. Gray regions indicate periods of 1 μM TTX application to the soma. C) Polar plot of the total spike count for somatic spikes during a control period (open squares) and dendritic spikes during a period of 1μM local TTX application (solid circles). The solid lines show the best-fit von Mises distributions, with preferred directions of 96° and 98° degrees for the control and TTX data and DSI values of 0.56 and 0.62. D) The thick trace shows the average of 679 somatic spikes and the thin trace shows the average of 515 dendritic spikes from one cell. The broken line shows the dendritic spike scaled to match the somatic spike amplitude. Spikes were averaged by aligning the peaks at time zero. E) Amplitude distribution histograms of 1726 somatic spikes (black) and 582 dendritic spikes (grey) derived from preferred direction stimuli before, during and upon washout of local TTX application to the soma. Twelve other cells displayed similar results.

If the large spikes are somatic and small spikes dendritic, then it should also be possible to block somatic spikes, and reveal dendritic spikes using the intra-cellular sodium channel blocker QX-314, a lidocaine derivative (Pinato and Midtgaard, 2005). In order to obtain sufficient control responses, the tip of the

patch electrode was filled with drug free solution, and the electrode was back-filled with intracellular solution containing 1-10mM QX-314. At the higher concentrations, all spike activity was quickly suppressed. At concentrations of 1-2mM, somatic spikes were suppressed, revealing the presence of smaller dendritic spikes. Similar to bath application of TTX, spiking was completely suppressed in five of the seven cells. In two cells the recording was lost before complete suppression could be observed. We will provide further evidence supporting our hypothesis that the small spikes are initiated in the dendrites and propagate to the soma where they initiate the larger spikes. In the following we will refer to the small and large spikes as dendritic and somatic, respectively.

If dendritic spikes can be independently initiated in separate dendritic branches, then spikes from separate dendrites should not be refractory to each other and should be able to superimpose (Larkum et al., 2001). In contrast, somatic spikes should display an absolute refractory period. These expectations are borne out by analysis of the inter-spike interval distributions during experiments similar to that shown in Figure 3. Responses included control periods, where no dendritic spikes were seen, and periods of local somatic TTX application where a mixture of somatic and dendritic spikes was seen. The somatic spikes displayed an absolute refractory period of 3.5±0.7ms (N=9, gray bars Fig. 4A). Analysis of dendritic spikes revealed a shorter refractory period (open bars Fig. 4A). The decline in the dendritic inter-spike interval histogram near zero is due to a limit on the shortest resolvable inter-spike interval (see methods). Examination of the raw responses (Fig. 4C, D) shows superposition of the dendritic

spikes indicating that many dendritic spikes were not refractory. Similar results to Figure 4 were obtained in all 9 cells analyzed.

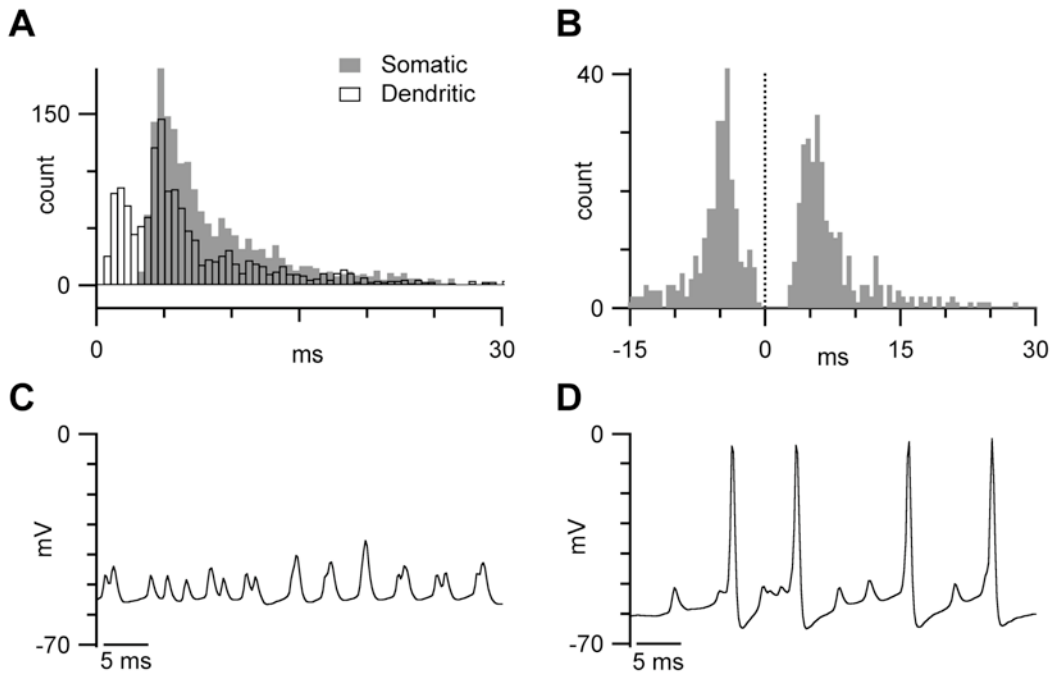

Figure 2.4:

Inter-spike interval analysis shows that many dendritic spikes are not refractory.

TTX was applied locally to the soma to reveal dendritic spikes during preferred direction stimuli. A) Inter-spike interval distributions for somatic spikes under control conditions (grey bars) and dendritic spikes during local TTX application (open bars). B) Analysis of inter-spike intervals between somatic and dendritic spikes. During onset or washout of somatic TTX application responses often displayed a mixture of large and small spikes. The histograms show the timing of dendritic spikes relative to the somatic spikes that occurred at time zero. Negative inter-spike intervals indicate

dendritic spikes that precede the somatic spike; positive intervals represent dendritic spikes that follow the somatic spike. C) An expanded section of a light response during local 1μM TTX application showing superposition of dendritic spikes. D) An expanded section of a light response during local 1μM TTX application showing a mixture of large and small spikes.

If spikes are initiated in the dendrites and propagate to the soma, then it might be possible for somatic spikes to back-propagate into the dendrites. Moreover, a back-propagating somatic spike might render the dendrites refractory. We were able to confirm this prediction by analyzing the timing of dendritic spikes that preceded or followed a somatic spike in records where a mixture of events was seen. Dendritic spikes did not appear within the refractory period following a somatic spike (Fig. 4B); however, examination of the records shows directly that dendritic spikes can occur at any time before a somatic spike (Fig. 4B,D). Back-propagation of somatic spikes might explain why in some cells there were more dendritic spikes per stimulus during local TTX application than somatic spikes in control (Fig. 3B). Multiple spike initiation sites could generate dendritic spikes in different dendrites; however, the first dendritic spike to reach the soma will elicit a somatic spike, which will back-propagate and cancel any coincident dendritic spikes.

If dendritic spikes initiate somatic spikes, then injecting hyperpolarizing current into the soma should reduce the efficacy of somatic spike initiation and reveal the underlying dendritic spikes. Indeed, progressively larger hyperpolariz-

ing current steps reduced the number of somatic spikes with a concomitant increase in the number of dendritic spikes (Fig. 5A,B). Similar to dendritic spikes observed during local TTX application, the small spikes revealed during hyperpolarizing pulses could be clearly distinguished from the somatic spikes based on amplitude (Fig. 5C). Overall, there was a tendency to observe more ON than OFF dendritic spikes. In some cells we observed dendritic spikes only during ON-responses, and not during OFF-responses (data not shown). The observation that the spiking properties of the DSGCs are dependent on the contrast of the light stimulus, and thus the dendritic origin of the signals, provides further evidence for multiple spike initiation zones in the dendrites.

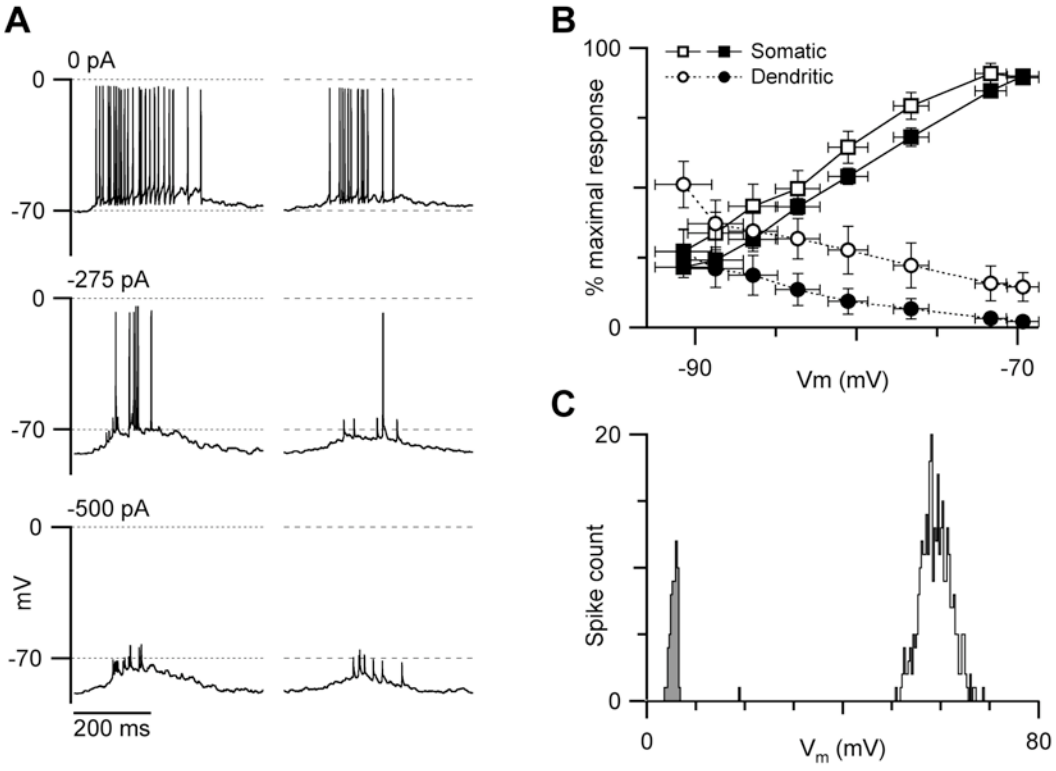

Figure 2.5:

Hyperpolarizing the soma unmasks dendritic spikes. A) Evoked responses from

preferred direction motion during hyperpolarizing current injection. The left traces are OFF-responses and the right traces are ON-responses. B) Preferred direction stimuli were presented during current pulses between +25 and –500 pA. The x-axis shows the average baseline potential during the current step. The y-axis shows the percentage of somatic ON and OFF spikes and dendritic ON and OFF spikes relative to the number of somatic spikes recorded at the resting potential (solid and open symbols are OFF and ON responses respectively, square and round symbols are somatic and dendritic spikes respectively). Each point represents the averaged data from 10 cells. C) Amplitude histograms of the spikes elicited by preferred direction stimuli presented during current pulses that hyperpolarized the cell over the potential range shown in *B*. The dendritic spikes are well separated from the larger somatic spikes. Similar results were obtained in nine other cells.

If light-evoked spikes are first initiated in the dendrites then we should be able to block light evoked somatic spikes by applying TTX to the dendrites (Huguenard et al., 1989a; Regehr et al., 1993; Turner et al., 1989; Turner et al., 1991). We tested this prediction by placing a pipette containing TTX in the inner plexiform layer, 10-20 mm beneath the inner limiting membrane of the retina, and approximately 80-200 mm from the cell soma. We applied 30-60 second pulses of 0.5 mM TTX to the dendrites. To monitor the excitability of the soma, a depolarizing current pulse followed each preferred direction stimulus. In all 8 cells, we were able to observe a selective reduction from 13-73% (average 41.5±15%) in

the number of light-evoked spikes (Fig.6A,B). In every case there was a smaller concomitant reduction (25.2±7.8%) in the depolarization-activated spikes, which we attribute to the spread of TTX. However, it is important to emphasize the qualitative difference between somatic and dendritic TTX application. In contrast to somatic TTX application, dendritic TTX application, which selectively reduced light-evoked spiking, did not promote the unmasking of dendritic spikes; it simply reduced the number of spikes (Fig. 6A). These results are consistent with the hypothesis that orthograde dendritic spikes initiate somatic spikes.

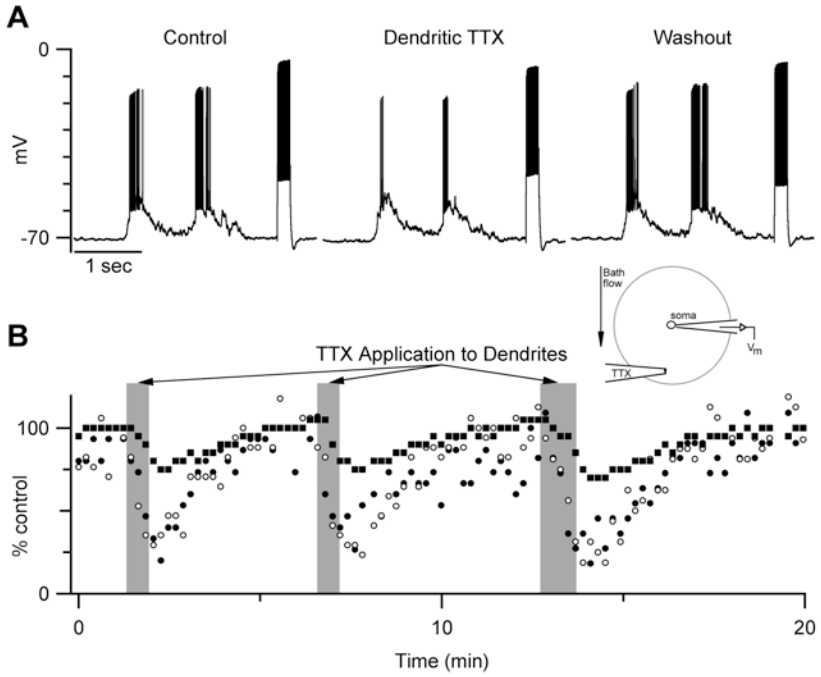

Figure 2.6:

TTX application to the dendrites blocks light-evoked spikes. A) Current clamp responses to a dark bar moving in the preferred direction followed by a 500 pA current step 200 ms long. The inset schematic shows the positions of the TTX and recording electrodes in relation to the soma and dendrites (outer

circle). B) Normalized spike counts expressed as percent spikes relative to pre-TTX application for ON spikes (open circles), OFF spikes (filled circles) and depolarization spikes (filled squares). Gray regions indicate periods of TTX application to the dendrites.

DSGC Dendrites are Excitable

In order to directly test whether the dendrites of DSGCs are electrically excitable we performed calcium imaging experiments. DSGCs were filled with the calcium indicator Oregon-green BAPTA-1 by passive diffusion from the patch-electrode during current-clamp recordings. The DSGC was simultaneously stimulated with visible light along the preferred-null axis while measuring calcium signals using 930nm excitation from the infrared laser. As noted above, DSGCs comprise two planar dendritic arbors; an ON-dendritic arbor (colored green in Fig. 7A) and an OFF-dendritic arbor (colored red in Fig. 7A). Changes in the dendritic calcium concentration were measured as changes in fluorescence intensity relative to the background. Calcium transients showed the same dependence on stimulus direction as the somatic spikes recorded in the same cell (Fig. 7B), indicating that the fluorescence signal scaled linearly with the number of somatic spikes.

Leading and trailing edge responses produced calcium transients in both dendritic arbors (Fig. 7C), indicating that a somatic spike resulting from stimulation of one dendritic arbor back-propagates and generates a calcium transient throughout the cell. Bath application of TTX, which blocks all spikes, reversibly

abolished the calcium signals (Fig. 7D), demonstrating that the depolarization produced by the PSPs was not sufficient to activate the dendritic calcium channels. Similarly, direct depolarization of the soma did not elicit calcium transients, until somatic spike threshold was reached at which point calcium transients were again observed throughout the cell (data not shown).

The results indicate that the dendrites of DSGCs are electrically active. To directly test this, we applied TTX locally to a dendrite while presenting preferred direction light stimuli (N=4 cells; Fig. 7E). The TTX suppressed calcium transients in dendrites close to the site of application, but not at more distant sites, providing direct evidence for the presence and physiological activation of TTX-sensitive sodium channels in the dendrites of the DSGCs.

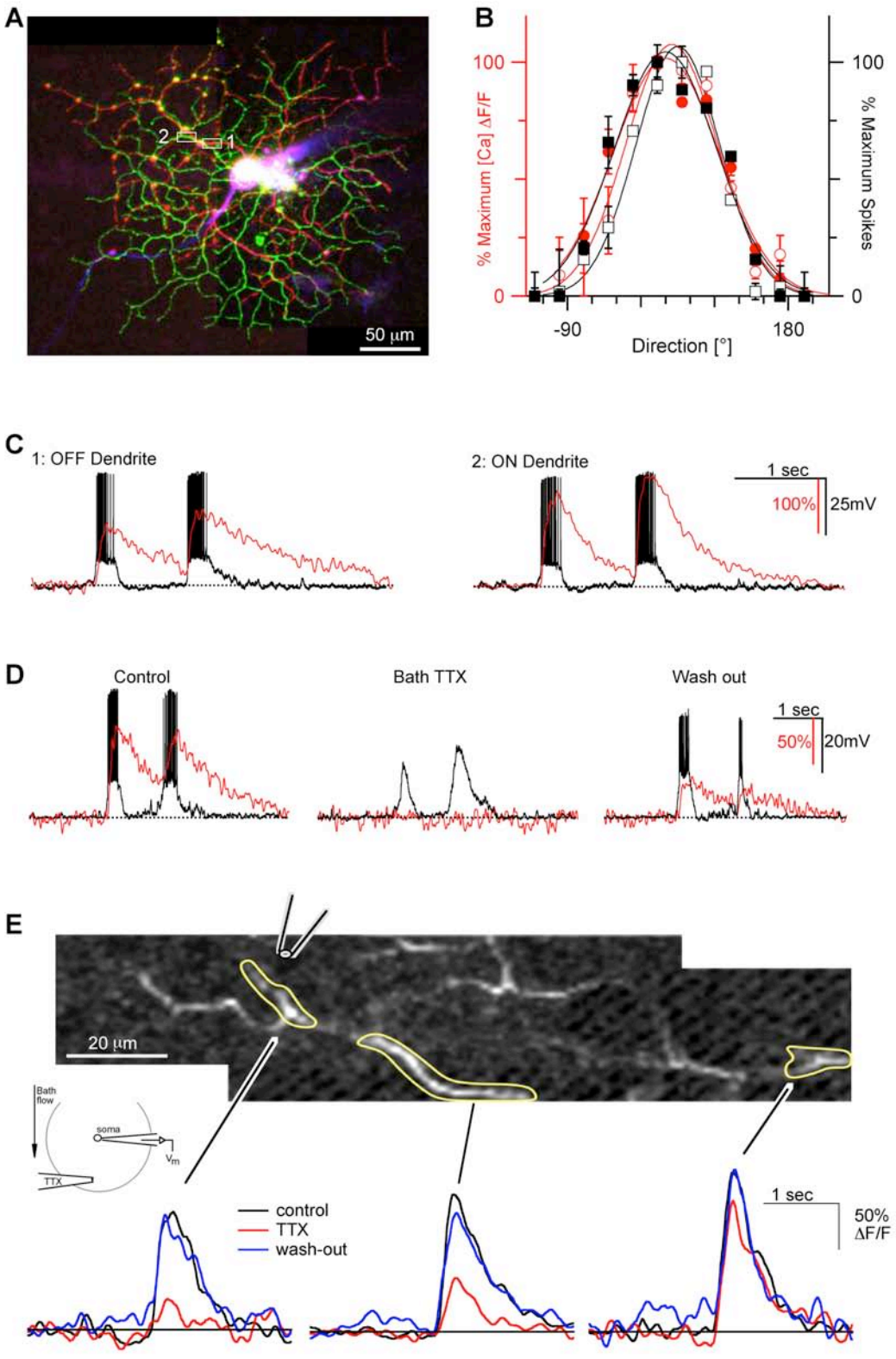
A
2
1
50 µm
B
100
0
% Maximum [Ca] ΔF/F
100
0
% Maximum Spikes
-90
180
Direction [°]
C
1: OFF Dendrite
2: ON Dendrite
1 sec
100%
25mV
D
Control
Bath TTX
Wash out
1 sec
50%
20mV
E
20 µm
Bath flow
soma
Vm
TTX
control
TTX
wash-out
1 sec
50%
ΔF/F

Figure 2.7:

Dendrites are electrically excitable. Calcium imaging data is shown in red, and current-clamp data is shown in black. A) Cell morphology showing the imaging locations in the OFF-dendrites (1) and ON-dendrites (2). In this pseudo-color image the OFF dendrites are colored red and the ON-dendrites are colored green. The images of the two arbors have been overlaid for this illustration. During the experiments only one dendritic arbor is visible, since the other lies well above or below the optical section. B) The normalized magnitude of the calcium transients (left axis, red), and the number of action potentials (right axis, black), are plotted against the direction of stimulus motion. C) Responses were elicited by a preferred direction positive contrast stimulus. C1 and C2 show calcium transients and current clamp responses in the OFF and ON dendritic arbor respectively. D) Voltage records and calcium signals in response to preferred direction stimuli, during control, 0.5μM bath TTX application, and washout. E) TTX was applied to a section of dendrite as shown and calcium transients measured for each region of interest delineated by the white lines. Calcium transients were recorded during preferred direction stimuli before (black trace), during (red trace), and after (blue trace) TTX application.

Modeling Supplement: Leading inhibition prevents spike initiation

Using our compartmental model of the DSGC, we explore the ability of inhibition to modulate excitability of the DSGC, we ran simulations with different spatial arrangements of inhibitory synapses. In one set of simulations, we applied

a 75µm “spot” of shunting inhibition (~40 synapses, 3nS/synapse, reversal potential ~V_{rest}) over an area that covered the soma and proximal dendrites, while stimulating a distal region with a spot of excitatory input (~40 synapses, reversal potential=0mV, ~3nS peak conductance) (Fig. 2.8a). To effectively prevent spike propagation a total inhibitory conductance greater than 50nS was required (Fig. 9c), far more than the physiologically estimated range of 3-10nS. In this case, spikes were heavily attenuated by on-path inhibition as they propagated through proximal areas, and appeared at the soma as low amplitude “spikelets” (Fig. 8c, black trace). The on-path inhibition also reduced the local PSP produced by excitatory input. Given that dendritic spikelets are rarely observed at the soma of the DSGC during light stimulation and that an unrealistically-high inhibitory conductance was needed to shunt propagating dendritic spikes, our conclusion from this set of experiments was that inhibition served to block spike initiation more effectively than propagation.

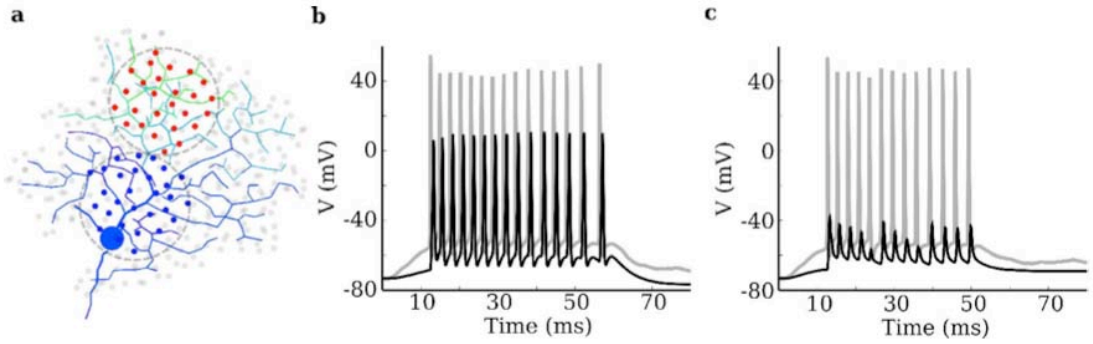

Figure 2.8:

Unrealistically-strong on-path inhibition only attenuates propagating spikes. **(a)** The model was stimulated with ~30 identical excitatory inputs (red dots)

producing a peak conductance of ~3nS and located randomly over the distal dendrites. The strength of ~30 identical inhibitory inputs located randomly within a spot of the same size and placed over the soma (blue dots) was modulated to explore the requirements for on-path shunting inhibition of dendritic spikes. **(b)** Inhibitory input with a peak total conductance of ~50nS distributed equally amongst the synapses did not prevent dendritic spike propagation. Gray traces show voltage in the dendrites, black is the soma. **(c)** When the total peak inhibition was raised to an unrealistic conductance (~85nS), dendritic spikes (gray trace) were severely attenuated and appeared as small “spikelets” at the soma (black trace), which are not observed except during somatic TTX application.

Discussion

We conclude from this study that spikes in DSGCs are initiated within the dendrites at more than one location, and that these dendritic spikes propagate towards the soma where they trigger somatic and axonal spikes. Dendritic spikes are not seen under control conditions because they masked by the somatic spikes that they trigger. Generation of spikes locally within the dendrites enhances the directional tuning of the DSGCs.

Evidence for dendritic spikes

Key evidence was obtained by the local application of TTX to the soma, which blocked large spikes and revealed the presence of dendritic spikes. An al-

ternative explanation for the appearance of these small spikes is that TTX effectively reduces the sodium channel density at the soma and initial segment, with the result that action potentials do not reach the full amplitude. Under these conditions, one might expect to see a continuous variation of spike sizes due to the variable concentration of TTX present. However, examination of the spike amplitude distribution shows two discrete populations of spike amplitudes (Fig. 3). The appearance of large and small spikes within the same record suggests that local somatic TTX application can decrease the probability of somatic spike initiation before it has significant effects on the amplitude of the somatic action potentials.

Further evidence is the finding that hyperpolarization also suppresses large spikes and reveals small spikes. The same bimodal distribution in spike amplitudes is seen during this experimental condition as for the TTX application to the soma. This suggests that small spikes are not simply an artifact due to TTX reducing the number of active sodium channels, but are always present and can be revealed if somatic spike initiation can be selectively suppressed. Moreover, hyperpolarization more readily unmasked dendritic spikes during ON responses. Such an observation provides strong evidence for the presence of at least two distinct spike initiation zones, one in each dendritic arbor.

Certain types of retinal ganglion cells that are coupled through gap junctions show evidence of electrical coupling, which can cause correlated firing (Bennett and Zukin, 2004; Brivanlou et al., 1998; Hidaka et al., 2004; Hu and Bloomfield, 2003; Mastronarde, 1983). However, several lines of evidence indicate that the dendritic spikes we recorded in DSGCs are not remnants of spikes

activated in neighboring, electrically coupled neurons (MacVicar and Dudek, 1982; Valiante et al., 1995). Firstly, there are four sub-types of DSGCs with distinct preferred directions corresponding to the four ocular cardinal directions. However, only one subset of DSGCs shows dye coupling (Vaney, 1994b), whereas dendritic spikes are observed in all cells. Secondly, if DSGCs could transmit spikes to adjacent cells through gap junctions, then their receptive fields should be considerably larger than the dendritic extent; however, the receptive fields of the DSGCs are delineated by the extent of the dendritic arbors (Yang and Masland, 1994a). Finally, the dendritic spikes have precisely the same preferred direction and directional tuning as the somatic spikes, which excludes the possibility that they originate in overlying DSGCs that have overlapping dendritic and receptive fields, but different preferred directions.

Dendritic spikes trigger somatic spikes

By applying TTX locally to the dendrites of the DSGC we were able to block a portion of the light-evoked spikes (Fig 6), which supports our hypothesis that dendritic action potentials propagate to the soma where they initiate somatic spikes. Dendritic spikes are rarely seen under normal conditions indicating that the probability that a dendritic spike will trigger a somatic spike is close to one.

Our results also indicate that the spike threshold at the soma is set high, so that somatic spikes cannot be elicited by somatic PSPs, which are generated by the global summation of dendritic inputs, and are similar in amplitude in the preferred and null directions (Fig 1&2). While spikes were clearly correlated with

the occurrence of preferred direction PSPs, the apparent spike threshold was broadly distributed during the PSPs, suggesting that spike initiation was not strongly influenced by somatic membrane potential. This is consistent with the idea that incoming dendritic spikes have a very high probability of initiating a somatic spike, and that the depolarization represented by the somatic PSP does not significantly increase the probability of spiking.

A role for dendritic spikes

DSGCs receive directional excitatory and inhibitory synaptic inputs, with inhibition being larger in the null direction and excitation larger in the preferred direction (Borg-Graham, 2001a; Fried et al., 2002a; Taylor and Vaney, 2002). Directional inhibitory inputs are GABAergic and likely originate from starburst amacrine cells (Euler et al., 2002a; Famiglietti, 2005a; Fried et al., 2005a). We show that the directional inputs produce PSPs that are weakly directional at the soma. We propose that the excitatory inputs will initiate dendritic spikes at local regions within the dendrites, but that dendritic spikes generated during null direction motion will fail to propagate successfully to the soma due to directional inhibitory inputs from the starburst amacrine cells interposed between the spike initiation site and the soma. Precedence for this type of interaction has been shown in mitral cells (Chen et al., 1997; Kim et al., 1995; Lowe, 2002; Tsubokawa and Ross, 1996; Xiong and Chen, 2002), and pyramidal cells (Kim et al., 1995; Tsubokawa and Ross, 1996). The actual spike thresholds in the dendrites may be less important than judicious activation of postsynaptic inhibition,

which should make the system more robust when the signal-to-noise ratio is unfavorable. Direct supporting evidence for this idea in DSGCs requires electrical recordings from the dendrites, a challenging prospect since the dendrites are typically 0.5μm in diameter (Amthor et al., 1984; He et al., 1999a); however, other results support this interpretation of our findings.

DSGCs display a non-directional zone that occurs on the preferred side of the receptive field (the side first encountered during preferred direction motion), and is evident by the appearance of spikes during null-direction stimuli that traverse only the non-directional zone (Barlow and Levick, 1965a; He et al., 1999a). Since inhibition is spatially offset toward the null direction (Barlow and Levick, 1965a; Wyatt and Daw, 1975), inhibitory inputs will be interposed between the excitatory inputs and the soma on the null side of the dendritic arbor, but not on the preferred side (Fig. 8). As a stimulus edge moves across the dendritic arbor in the null direction, the PSPs at local dendritic inputs near the edge will be mainly excitatory, and inputs onto dendrites ahead of the moving edge will be inhibitory (Fig. 8, stimulus at N2). Dendritic spikes initiated by the excitatory inputs and propagating into the region of inhibition may fail due to the local shunting effect of the inhibitory conductance. However, if the null direction stimulus commences on the preferred side of the dendritic arbor (at P2), the inhibition will be activated distal to the excitation, and the dendritic spikes will propagate successfully to the soma. Thus, the existence and location of the non-directional zone is consistent with the spatial arrangement of inhibition and excitation, and with our hypothesis that dendritic spike failure is more likely if the inhibition is on-the-path

to the soma. These marked spatial differences in synaptic input are not reflected in current or voltage recordings from the soma, which comprise the summed input from all dendritic locations.

These same arguments can account for a systematic offset of the receptive field towards the preferred side of the dendritic field (Yang and Masland, 1994a). While mapping the receptive field, a stimulus spot flashed on the null side of the dendritic arbor will activate on-the-path inhibition (Fig. 8, stimulus at N2), and therefore will tend to produce fewer spikes than at the same relative location on the preferred side of the dendritic arbor (Fig. 8, stimulus at P1). Thus, the receptive field will tend to be offset towards the preferred side, in agreement with observations (Yang and Masland, 1994a).

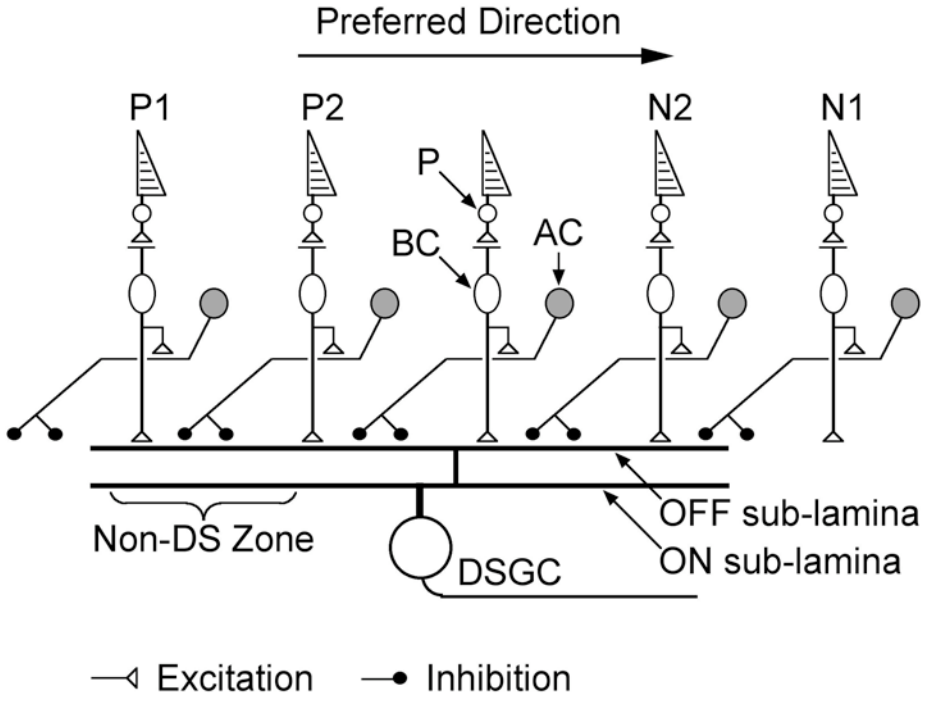

Figure 2.9:

Synaptic scheme. P: photoreceptor, BC: bipolar cell, AC: amacrine cell, DSGC: direction-selective ganglion cell. As the stimulus edge activates N2 during null-direction motion the inhibition activated ahead of the stimulus will cause spike failure. During preferred direction motion, the inhibition will be distal to the excitation over much of the receptive field, and dendritic spikes will successfully propagate to the soma. Within the non-DS zone, a stimulus moving in the null-direction will first activate P2, and since inhibition is not activated between the excitatory inputs and the soma, dendritic spikes will generate somatic spikes. These spatio-temporal effects for motion in both directions will be complemented by presynaptic mechanisms, which generate directional inhibitory and excitatory inputs. Inhibition is larger in the null direction than the preferred direction, which will promote null direction dendritic spike failure. Excitation is smaller in the null direction than the preferred direction, which will tend to produce less null direction spikes. However, these motion-dependent presynaptic mechanisms cannot contribute to the offset in the spot-mapped receptive field towards the preferred side, as has been observed (see Discussion).

Other results appear consistent with dendritic spike initiation. Excluding the non-directional zone, directional spikes are generated by movements as small as ~40μm, about 20% of the receptive field diameter (Barlow and Levick, 1965a). A more recent study contends that the spatial resolution is tenfold finer (Grzywacz et al., 1994). Thus, it seems that the critical directional mechanism is

replicated many times across the receptive field. It is difficult to see how a single spike threshold at the soma could effectively discriminate preferred and null PSPs both for full field stimuli that produce large PSPs, and for restricted stimuli that produce smaller PSPs. A model that allows for local dendritic spike initiation can more easily explain these results.

The idea that directional selectivity may be the result of local, post-synaptic, non-linear interactions in the DS cell was first introduced by Barlow and Levick (1965a), and has received subsequent experimental (Amthor and Grzywacz, 1991; Amthor and Grzywacz, 1993; Taylor et al., 2000) and theoretical support (Grzywacz et al., 1990; Grzywacz and Koch, 1987; Koch et al., 1982; Koch et al., 1983; Poggio and Reichardt, 1973; Torre and Poggio, 1978). The non-linearity invoked in these studies was shunting inhibition and it was generally agreed that such inhibition would need to be large, and in close proximity to excitatory inputs, to significantly shunt excitatory PSPs. In has been well documented that direction selectivity in the DSGC is dependent on $GABA_A$ receptors (Ariel and Daw, 1982b; Caldwell et al., 1978; Kittila and Massey, 1997a; Massey et al., 1997), however, anatomical analysis has shown that the patches of GABA receptors on DSGCs are not located immediately adjacent to the excitatory receptors (Jeon et al., 2002a), and the present results show that depolarizing PSPs are seen during null-direction motion. While our proposed model also invokes inhibitory shunting, since the inhibition promotes failure of dendritic spikes, it does not need to be close to the original excitation.

Recent work has emphasized the importance of presynaptic mechanisms for generating directional inputs to DSGCs (Borg-Graham, 2001a; Euler et al., 2002a; Fried et al., 2002a; Taylor and Vaney, 2002). While directional signals are generated in the presynaptic circuitry, the current results show that local, post-synaptic processing within the dendrites of the DSGC is also important for producing sharply tuned directional signals.

Methods

Tissue Preparation and Maintenance

Experiments were conducted in accordance with protocols approved by the Institutional Animal Care and Use Committee at OHSU and NIH guidelines. Dark-adapted, Dutch-belted rabbits were surgically anaesthetized and the right eye removed under dim-red illumination. The animal was then killed by anesthetic overdose. All subsequent manipulations were performed under infrared illumination (>900nm) or under dim red light during the imaging experiments. The anterior portion of the eye was removed, the eyecup transected just above the visual streak, and the dorsal piece discarded. The retina was dissected from the sclera, and a 5 by 5 mm section of central retina was adhered, photoreceptor-side down, to a glass cover-slip coated with poly-L-lysine (Sigma) or Cell-Tak (Becton Dickinson GmbH, Germany). The preparation was placed in a recording chamber (~0.5 ml volume) and continually perfused (~4 ml/min) with oxygenated bicarbonate-buffered Ames medium (Ames and Nesbett, 1981), pH 7.4 maintained at 34–36 ºC. The major electrolytes in Ames medium are (mM): 120 NaCl, 23 $NaHCO_3$, 3.1 KCl, 1.15 $CaCl_2$ and 1.24 $MgCl_2$.

Electrophysiology and Light Stimulation

Patch electrodes were pulled from borosilicate glass to have a final resistance of 4–8 MΩ. For extracellular recording, the electrodes were filled with Ames medium. For intracellular recording, the electrodes were filled with the following electrolytes: 110 mM K-methylsulfonate, 10 mM NaCl, 5 mM Na-HEPES, 1 mM K-EGTA, 1 mM Na-ATP, 0.1 mM Na-GTP. The liquid-junction-potential of 10 mV was subtracted from all voltages during analysis. Ganglion cells with a medium soma diameter and a crescent-shaped nucleus were targeted as potential DSGCs (Vaney, 1994b). The extracellular electrode was applied to the soma under visual control through a small hole in the overlying inner limiting membrane, and a loose patch recording was formed. After establishing that the ganglion cell was a DSGC and determining its preferred direction (see below), the extracellular recording electrode was removed and an intracellular patch-electrode applied to the same cell. During whole cell recordings voltage signals were filtered at 2kHz through the 4-pole Bessel filter of the Multiclamp 700A amplifier, and digitized at 5-10kHz. To minimize series resistance errors during whole-cell current-clamp recordings, 10ms hyperpolarizing current pulses were applied and the bridge-balanced to eliminate any instantaneous voltage offsets. Bridge balance was monitored periodically during the recordings.

TTX was applied locally to the soma or dendrites of the DSGCs from a patch electrode (4–8 MΩ) positioned just above the cell. TTX at 0.2 – 1μM was dissolved directly into the extracellular Ames medium. The TTX was pressure

ejected using a syringe. In some experiments, the lidocaine derivative, QX-314, was included in the patch electrode. To ensure adequate time to obtain control responses, the tip of the electrode was filled with drug free solution, and the electrode back-filled with intracellular solution containing 1-10mM QX-314. The drug diffused into the cell over a 10-20 minute time period, during which we monitored the responses of the ganglion cells to depolarizing current pulses, and preferred-direction light stimuli.

Light stimuli, generated on a CRT computer monitor (refresh rate, 85 Hz), were focused onto the photoreceptor outer segments through a 20x (NA 0.95) Olympus water-immersion objective. The percent stimulus contrast was defined as $C = 100 \times (L - L_{mean}) / L_{mean}$, where L is the stimulus intensity and L_{mean} is the background intensity. C was set between 30 and 100%. The standard moving stimulus comprised a light or dark bar, moving along its long axis at 800–1200 μm/s on the retina. All light stimuli were centered with respect to the tip of the recording electrode, and thus also with the soma of the ganglion cell. The bar's width was 250 μm, and its length was set to achieve a 1-2 second separation of the leading- and trailing-edge responses. The stimulus area was limited by the aperture of the microscope objective, and covered a circular region 1mm in diameter. Since the dendritic extents of DSGCs, which delimit the receptive field (Yang and Masland, 1994a), reach a maximum of about 400 μm across in rabbit retina (Vaney, 1994b), they were fully contained within the stimulus area. The leading edge of the stimulus bar commenced at one edge of the stimulus area and moved until the trailing edge reached the opposite edge. Thus, both leading

and trailing edges of the stimulus traversed whole receptive field of the recorded cell.

Multi-photon Microscopy and Calcium Imaging

A custom-built upright multi-photon microscope equipped with a 20x water immersion lens (20x 0.95 W, XLUMPlanFI, Olympus) was used to identify and view cells, and to image calcium signals in dye-labeled cells (Denk and Detwiler, 1999; Euler et al., 2002a). The tissue was counterstained with sulforhodamine 101 (2 to 4 mg/l; Sigma-Aldrich), which allowed us to visually identify the somata of DS ganglion cells with a high success rate. The sulforhodamine was usually washed out during recording periods to reduce fluorescence in the tissue and possible photo damage.

A mode-locked Ti/Sapphire laser (Mira-900; Coherent, USA) tuned to 920-930 nm was used to excite the dyes. The scanning laser beam caused moderate and transient excitation of the DSGCs that adapted rapidly. Light stimuli overlaid upon the scanned region produced robust responses in the DSGCs. Thus, it was possible to visually stimulate DSGCs and optically record calcium signals simultaneously. Filters in the stimulation light path and in front of the detectors ('green' calcium signal: D 535 BP 50; 'red' sulforhodamine counterstaining: HQ 622 BP 36) and dichroic mirrors in the optical path ensured that stimulus light did not interfere with fluorescence detection.

For calcium imaging DSGCs were filled with Oregon Green BAPTA-1 (100 to 200 µM in the pipette; Molecular Probes, USA) via the patch pipette. The dye

diffused rapidly into the dendritic tree so that imaging could commence within 3-5 minutes. The imaging software was developed at Bell Labs by R. Stepnoski and extended at the Max Planck institute by M Müller. Image regions (64x8 pixel blocks at 62.5 Hz) or line scans (64 pixel lines at 500 Hz) were acquired from short dendritic segments and analyzed off-line with IgorPro (Wavemetrics, USA). Fluorescence (F) data were spatially averaged over selected regions of interest and temporally filtered (line scans: box car, 10 ms window; image series: box car, 38 ms window). After background subtraction DF/F was calculated for each stimulus presentation. The maximal amplitude of the smoothed DF/F trace was used to quantify the size of the calcium response.

Light stimuli were generated on a miniature LCD monitor (30 Hz frame rate; 800x600 pixels with ~2.1 µm/pixel; i-visor DH-4400VP, Cybermind Interactive, Netherlands), which was illuminated by a yellow LED, band pass-filtered (578 BP 10) and projected through the objective lens (~ 1 mm field of view) onto the retina. An adjustable lens in the stimulus pathway offset the focal plane of the stimulus by about 100 mm relative to the imaging plane. This ensured that the stimulus was focused on the photoreceptor array while imaging the DSGC dendrites.

Analysis

The preferred direction of the cells and the strength of the directional tuning were calculated from responses to stimuli in each of 12 stimulus directions evenly spanning 360 degrees. Responses were represented as vectors with the

angle representing the direction of stimulus motion, and length equal to the number of action potentials or the peak amplitude of PSPs. The preferred direction was obtained from the angle of the resultant vector, obtained from the vector sum of all 12 responses. The directional tuning index (DSI) was calculated as the normalized length of the resultant vector. DSI can range from 0, when the magnitude of the response is the same in all stimulus directions, to 1, for perfect tuning when a response is produced only for a single stimulus direction (Taylor and Vaney, 2002). The directional tuning data in figures 2 & 3 is well described by a von Mises distribution, which is the circular analogue to the Gaussian distribution. The response *R*, as a function of stimulus direction is given as;

$R = R_{\max} e^{\left(\kappa \cos\left((x-\mu)\pi/180\right)\right)} \Big/ e^{\kappa}$, where R_{max} is the maximum response, μ becomes the preferred direction in degrees, and κ is the concentration parameter, which accounts for the width of the directional tuning.

In some cells recorded PSPs were used as a current-clamp command waveform. The somatic input resistance was measured by applying hyperpolarizing current pulses. Then a preferred-direction stimulus was applied and the spikes on the resulting PSPs were digitally blanked. Digital spike blanking was performed by replacing the action potential with a straight line connecting a point preceding the threshold crossing to a point about 2 ms later. The resulting PSPs were then smoothed by digital filtering. Using the measured somatic input resistance, the PSPs were scaled to produce a series of current-command waveforms that generated somatic PSPs, which bracketed the amplitude of the light-evoked PSPs.

Analysis was performed using custom procedures in IgorPro (Wavemetrics, USA). Unless otherwise noted, the mean ± standard deviation is quoted throughout the paper. Spikes were identified by threshold crossings of the second derivative of the current-clamp recordings. Differentiation effectively removed the slower PSPs, and allowed the same detection threshold to be used regardless of fluctuations in the amplitude of the PSPs in the original voltage record. Spikes times were detected as those events where the second derivative dropped below -2.10^5 V/s^2. A second threshold, usually set to 0 V/s^2 signaled the end of the event. Inter-spike intervals were determined from these spike times. The spike-threshold potential was defined as the membrane potential at the time point, prior to the peak, where the second derivative exceeded 2.10^5 V/s^2. Essentially the same results were obtained using an alternative method in which spike threshold potentials were measured as the membrane potential at a fixed time (usually about 1ms) before the peak. Spike amplitudes were calculated by subtracting the threshold potential from the membrane potential at the peak of the spike.

Modeling

Multi-photon microscopy. A Zeiss Axioskop 2 FS mot equipped with a LSM 510 meta NLO scanhead and a mode-locked Ti/Sapphire laser (Chameleon; Coherent, USA) was used to capture images of DSGC morphology. After break-in, Alexa Fluor 488 hydrazide (Invitrogen Corporation, USA) included in the recording pipette diffused rapidly into the dendritic tree. In some cases the re-

cording electrode was removed from the cell body after the cell had filled with dye before imaging took place. The dye was excited using mode-locked laser light from the chameleon laser tuned to 800-920 nm, and emitted light was collected through the objective, filtered through a BG 39 filter, and detected and digitized with the Zeiss LSM 510 system.

Digitization and construction of compartmental model. To aid with digitizing stacks of images of tracer-injected cell morphologies, we wrote additional software routines called from the “Image-J” image processing software package. Using Image-J the operator manually traced the cell's dendritic segments and branching pattern, measuring diameters with the caliper tool. Our software saved the morphologies as a collection of nodes and cables. The morphologies were then imported into the Neuron-C simulator (Smith, 1992), and endowed with voltage-gated channels (see “Channel densities” below). Semi-random arrays of presynaptic cells (see below) were constructed automatically by the simulator with a regularity (mean/SD) of 6-10, and synapses were connected between the presynaptic cells and the closest dendrite of the DSGC if it was within a threshold distance (typically 10 um). We set the compartment size small enough (0.03 lambda) so that each synapse from a presynaptic array was connected to a different compartment. Five morphologies were digitized from confocal stacks, and studied along with another more detailed morphology (“ds1e”), which had been traced with a Neurolucida system (Microbrightfield, Inc).

Calibration. The biophysical parameters provided for each morphology were calibrated to match the F/I curve, spike shape (via phase plot), and ISI curve produced by current injection recordings from the cell it was digitized. (Fohlmeister and Miller 1997a,b; Sheasby and Fohlmeister 1999; van Rosum et. al 2003). In total, five morphologies were digitized.

Ion channel densities and kinetics were calibrated to electrophysiological and pharmacological data. We calibrated voltage offsets and densities for $Na_v1.6$ and K_{dr} channels by matching phase plots of spikes from physiological recordings The $Na_v1.6$ and K_{dr} channel activation curves were offset depolarized by 4.5mV and 17mV, respectively. Offsets that significantly varied from these produced mismatched phase plots and a voltage threshold for spiking that differed from the real data.

Calcium channels of both high-voltage-activated (HVA) L-type, and transient low-voltage-activated (LVA) T-type have been found in the soma and dendrites of retinal ganglion cells (Karschin & Lipton 1989; Kaneda & Kaneko 1991; Huang & Robinson 1998; Henderson & Miller 2003). We included L-type Ca^{2+} channels, modeled as a discrete Markov channel with m^3-like kinetics (Armstrong & Matteson, 1984), and we set the Ca^{2+} channel density uniform across the soma and dendrites. In many types of ganglion cells, Ca^{2+}-activated K channels (K_{Ca}) reduce the firing rate during a prolonged current injection (Wang et. al 1998). We included two types of K_{Ca} channels, a small current, high [Ca^{2+}] affinity, voltage-independent sK_{Ca} channel with an activation time constant near 100ms simulated by a Markov model (Hirschberg et. al 1998), and another sK_{Ca}

channel with a higher [Ca^{2+}] affinity and activation time constant near 300ms (Sah & Clements, 1999). K_{Ca} channel densities were distributed uniformly across the soma and dendrites, set to match the cell's frequency-current and ISI curves produced by spike trains at various levels of current injection (Fig. 1ce). The calcium system (Ca^{2+} channels, pump, and K_{Ca} channels) was configured such that $[Ca^{2+}]_i$ never exceeded 1 μM during repetitive spiking (Van Rossum et al, 2003). Both K_{Ca} channel types were active during the inter-spike interval but did not significantly affect spike shape.

In some simulations, we added excitatory and inhibitory synaptic input from a moving bar stimulus (v_{bar}=1000μm/s), calibrated to evoke a response similar to physiological data (see above, and Fig. 10ab). We adjusted spatial separation of excitatory and inhibitory stimulus components and their corresponding synaptic conductances to approximate the wave shapes of currents (V_{hold} = -75 and 0 mV) recorded in a typical DSGC. We set the synaptic rise time (~1 ms) and the time constant of decay for excitatory and inhibitory synapses (250ms).

CHAPTER 3: STARBURST AMACRINE CELLS RECEIVE DIRECTIONAL INPUT FROM BIPOLAR CELLS AND ENHANCE DIFFERENCES WITH TETRODOTOXIN RESISTANT SODIUM CHANNELS

Abstract

The direction selective circuit of the retina has received much attention as a model circuit for study of the biophysical mechanisms of information processing

in the brain; however, the locus where the first directional signal in the circuit arises remains uncertain. It is currently thought that the starburst amacrine cell (SBAC) is the primary source of the directional inhibitory signal in the direction selective circuit of the retina. Using voltage-clamp recording, we measured the conductance of the synaptic inputs to the SBAC and found that excitatory synaptic inputs to the cell are themselves directional. Blockade of $GABA_a$ receptors had no influence on the directional excitatory inputs. By applying the tetrodotoxin-resistant sodium channel blocker ambroxol hydrochloride we found that tetrodotoxin-resistant sodium channels boost the directional difference in synaptic input. From these data we conclude that direction selectivity in the retina arises presynaptic to the SBAC, presumably at bipolar cell terminals, and that tetrodotoxin-resistant sodium channels in the SBAC enhance this directional signal, but do not generate it.

Introduction

Since the discovery of the retinal direction selective ganglion cell (DSGC) in the 1960's, much work has been done to elucidate the mechanisms generating direction selectivity in the retina. It is well known that GABAergic inhibition mediated by $GABA_a$ receptors on the DSGC are required for the discrimination of motion direction by the retina (Caldwell and Daw, 1978; Chiao and Masland, 2002b; Kittila and Massey, 1997b; Wyatt and Day, 1976). We now know that the DSGC receives directional GABAergic inhibition with the inhibitory synaptic conductance being two to tens times larger for null direction motion than for preferred direction

motion (Borg-Graham, 2001b; Fried et al., 2005a; Fried et al., 2002b; Taylor and Vaney, 2002). The most likely source for this directional inhibition is the starburst amacrine cell, an inhibitory interneuron that is both GABAergi and cholinergic (Amthor et al., 2002; Fried et al., 2002b; Yoshida et al., 2001).

The biophysical mechanisms that generate the directional asymmetry have not been shown definitively and remain controversial. It has been shown that the SBACs generate larger calcium transients at their dendritic varicosities for light stimuli that move from the cell soma towards the distal tips of the dendrites, referred to as centrifugal motion. Conversely calcium transients are smaller or absent for light stimuli that move from the distal tips of the dendrites towards the center of the cell, referred to as centripetal motion. Similarly voltage responses measured at the soma are larger for centrifugal motion and smaller for centripetal motion and these differences in the voltage responses presumably drive the differences in calcium transient. (Euler et al., 2002a; Hausselt et al., 2007; Lee and Zhou, 2006).

Recently, two mechanisms have been proposed to explain the asymmetries in the voltage responses and calcium transients. First, Lee et al (2006) demonstrated that neighboring SBACs make reciprocal GABAeric contacts and they suggested that an anatomical asymmetry in the reciprocal GABAergic contacts generated directional inhibition in the SBAC that was larger for centripetal motion. They found that this inhibition suppressed the voltage and calcium signals during centripetal motion originating outside the extent of the dendritic arbor. In contrast, Hausselt et al (2007) demonstrated that directional signals in the

SBAC were generated when the stimulus was restricted to the dendritic arbor of a single SBAC, arguing that the involvement of neighboring SBACs was not necessary; furthermore, they found that $GABA_a$ antagonists had no effect on the directional calcium or voltage signals they recorded in the SBAC (Hausselt et al., 2007) and they proposed that the directional asymmetry was due to a voltage gradient in the dendrites generated by a tonic AMPA receptor mediated synaptic current, acting in concert with a voltage-gated channel. SBACs lack voltage-gated TTX sensitive sodium channels (Hausselt et al., 2007; Kaneda et al., 2007; Ozaita et al., 2004; Peters and Masland, 1996b; Taylor and Wässle, 1995b; Zhou and Fain, 1996), and therefore Hausselt et al. proposed that voltage-gated calcium channels were important for generating the non-linearity as previously suggested by Jensen (1995). Given that retinal DS is robust over a wide range of stimulus conditions, it is likely that multiple synaptic and dendritic mechanisms work to generate the asymmetric SBAC response.

These hypotheses suggest that the SBAC is the critical locus of directional differentiation, but do not rule out a role for presynaptic mechanisms that may generate directional transmitter release from the bipolar cells that contribute to the excitatory inputs to the SBACs. In this report, we compared the excitatory synaptic inputs elicited in SBACs during centrifugal and centripetal motion and found that the excitatory synaptic inputs are larger during centrifugal motion. In addition, we found evidence that TTX-resistant voltage gated sodium channels enhance the differences in synaptic input during centrifugal and centripetal stimuli. Because the only known source for excitatory inputs to the SBAC in the adult

retina are bipolar cell terminals, we conclude that the bipolar cell terminals are the locus where directional signals are generated and that the SBAC employs a dendritic mechanism using TTX-resistant sodium channels to enhance this directional signal.

Results

To examine the synaptic processes that mediate directional signaling in the starburst amacrine cell (SBAC), we made whole-cell voltage-clamp recordings from ON SBACs in whole-mount retina and presented static and moving light stimuli. Figure 1a shows a representative current response to a static stimulus comprised of a 200μm spot of light centered over the cell soma. The response is characterized by a transient inward current at light onset, which rises from 10% to 90% of the peak response of 117±7.13 pA, in 30±10 ms. The peak response is transient and decays to a sustained inward current that lasts the duration of the light stimulus, followed by a marked suppression of the inward current at the termination of the light stimulus. The response to the stimulus termination is concomitant with a decrease in the membrane current noise present in the baseline recording. These responses accord well with previous observations (Lee and Zhou, 2006; Peters and Masland, 1996b; Taylor and Wässle, 1995b).

SBACs respond differentially to centrifugal and centripetal motion

To study the asymmetric response between centrifugal and centripetal motion in our preparation, we stimulated the SBAC by drifting two bright

rectangles either away from or towards the cell soma (see methods, Fig. 1c & e). The responses were qualitatively similar to the flash responses shown in Fig 1a; there is a transient inward current as the stimulus crosses the receptive field, a sustained inward current while the light intensity remains elevated, and an outward current with a concomitant reduction in current noise levels as the trailing edge of the stimulus exits the receptive field, though for centripetal motion the initial transient response was greatly reduced. For centrifugal motion the peak amplitude of the response was -103±30.2 pA and the 10-90% rise-time was 38.2.0±6.9 ms. For centripetal motion the peak amplitude was -66.2±22.4 pA and the 10-90% rise time was 196±83 ms. The directional difference in peak amplitude was 36.9± 14.8 pA while the difference in rise time was 158±85 ms. Both peak amplitude and rise time were significantly different between centrifugal and centripetal motion ($p<0.001$, paired t-test, $n=30$). To quantify this directional difference we calculated an asymmetry index (AI) of the response for both peak amplitude and rise time where the directional difference is represented by a value between 0 and 1, with larger values representing a larger or faster response for centrifugal motion (see methods). For peak current amplitude the AI was 0.22±0.07 and for rise time the AI was 0.67±0.14. The directional asymmetry observed here, characterized by larger responses for centrifugal motion, are qualitatively similar to previous observations (Euler et al., 2002a; Hausselt et al., 2007; Lee and Zhou, 2006). Current-clamp recordings indicated that the directional asymmetry of the voltage response was quantitatively similar to the asym-

metry observed for the currents under voltage-clamp (AI = 0.175±0.064 for amplitude and 0.634±0.059 for rise time, n=4).

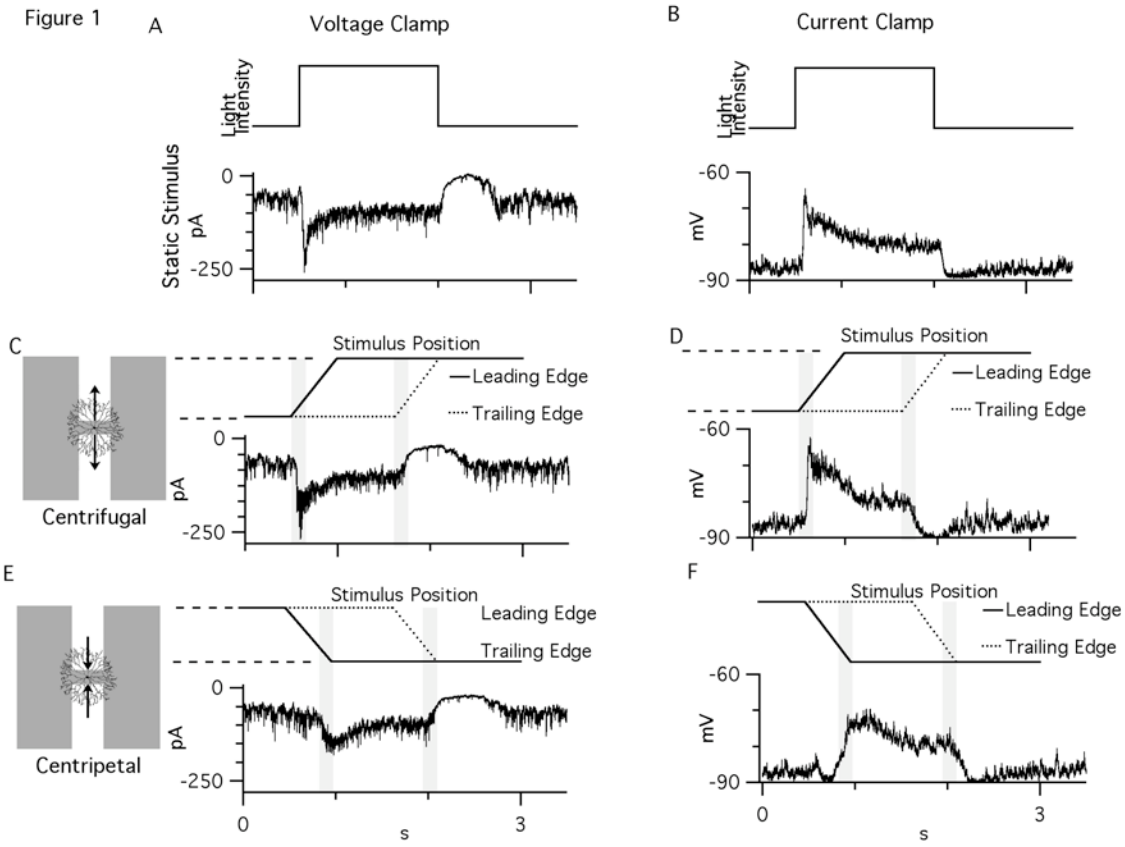

Figure 3.1:

Voltage and current responses to static and moving stimuli. A. Currents recorded in response to a 200 μm spot of light centered over the cells receptive field against a gray backgroud, contrast 100%. B. Vresponse to an identical stimuli. C and E show currents in response to a centrifugal and centripetal moving stimuli, respectively (see Methods). The solid line and dotted lines above the trace indicates the position of the leading and trailing edge, respectively of the stimuli on the y-axis plotted against time. The schematic to the left represents the position of SBAC and the stimulus bars in the stimulus

window. D and F, show voltage responses to the same stimuli shown in C and E.

Calculation of the total charge transferred during the time while the leading edge of the stimuli traversed the stimulus field for centrifugal and centripetal motion, suggests that more or larger synapses are activated during centrifugal stimulation than during centripetal stimulation. For centrifugal motion the integral of the synaptic current during leading edge motion was 24.0±8.7 pA/s and for centripetal motion the integral was 12.5±4.5 pA/s. The difference between centrifugal and centripetal was significant ($p<0.001$, $n=30$). This difference corresponded to a AI for integral during leading edge motion of 0.331±0.137. This indicates that, not only is the waveform of the synaptic input different between preferred and null directions, but the total amount of synaptic input underlying the EPSC is different between centrifugal and centripetal motion.

The highly symmetric dendritic arbors of the SBACs and our ability to precisely align the somas with the light stimulus allow us to correlate the synaptic responses with the stimulus position within the receptive field. For centrifugal motion the response passes 10% of its rise to peak after a 48±6.0 ms delay during which the stimulus edge had moved 43 μm from its starting point 75μm from the soma. As noted above, the 10-90% rise time of the centrifugal response was ~38ms, which corresponds to only ~34 μm of movement of across the retina. Therefore, the peak response was reached after the leading edge of the stimulus had traveled only 80 μm, or between 66-100% of the remaining distance from the

soma to the distal dendritic tips, assuming a dendritic diameter of of 300-400 μm (Bloomfield, 1992c; Taylor and Wässle, 1995b). In contrast, the response during centripetal stimulation passes 10% of its rise to peak after 185±95, this corresponds a movement of 167 μm from its starting point. Given than the centripetal stimulus began 450 μm from the center of the cell this indicates that the response passes 10% of the peak when the stimulus is still approximately 75 to 100 μm from the distal tips of the dendrites. During the 10-90% rise-time of the response the stimulus moves 175 μm, or approximately 190 μm, so the leading edge of the stimulus has nearly traversed the distance across the dendritic field. However during the time that the stimulus is directly over the dendritic field the response does not rise as fast or to as large of a peak as it does during centrifugal motion. This implies that the response to centripetal stimuli begins to rise before the stimuli reaches the edge of the SBAC dendrites, however it is possible that this is due it imprecision in our stimulus alignment.

Anatomical analysis suggests that synaptic inputs are distributed along the length of the dendritric branches (Famiglietti, 1987; Famiglietti, 1992). Furthermore, previous evidence has suggested that the receptive field of the SBAC during static light stimulation is limited to the extent of the dendritic arbor (Bloomfield, 1992c; Peters and Masland, 1996b; Taylor and Wässle, 1995b). Thus the centrifugal response appears consistent with the sequential activation of the synaptic inputs as the edge moves along the dendrite, while centripetal motion evokes inputs from outside the extent of the dendritic field, and subsequently inputs evoked over the dendritic arbor appear to contribute little to the

response, unlike centrifugal motion. Centripetal motion must selectively engage circuitry different from that activated by static stimuli, to account for the observation of excitatory inputs evoked by motion outside the cells dendritic arbor. This indicates that centrifugal and centripetal differentially activate inputs to the SBAC (fig. 2).

Figure 2

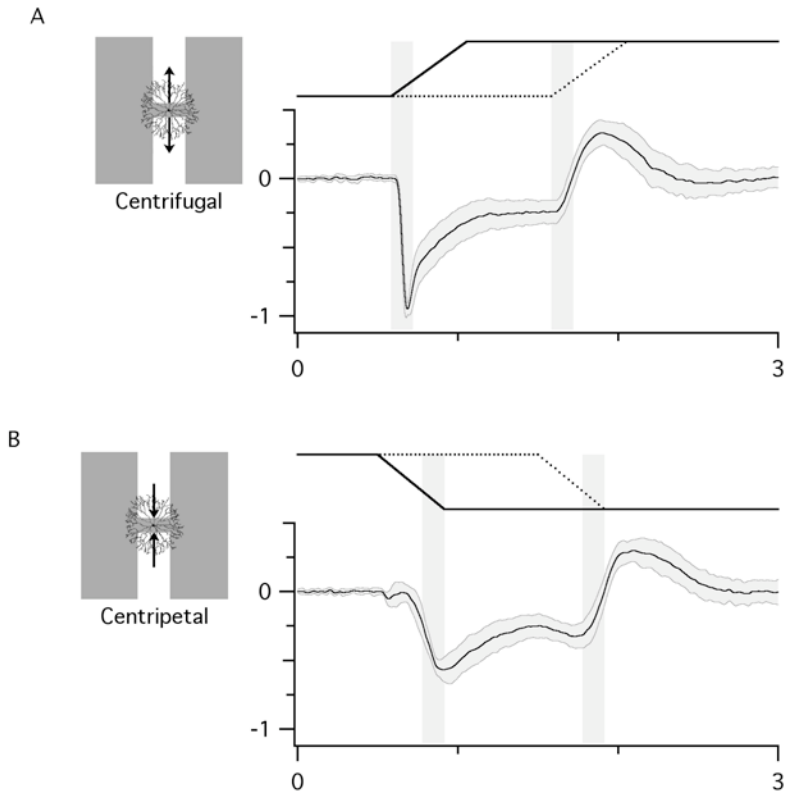

Figure 3.2:

Alignment of stimulus position with current response. Currents recorded in response to centrifugal and centripetal stimulation (A and B respectively. Black trace shows average responses from 18 cells and gray shaded area indicates standard deviation. Solid and dotted lines above traces indicate

position of leading edge and trailing edge, respectively, on the y-axis against time.

In contrast to the activation of inputs by the leading edge of the stimulus, the inactivation of inputs caused by the trailing edge of the stimulus, is relatively symmetrical between centrifugal and centripetal directions. The 10% to 90% rise time of the rebound does occur faster for centripetal motion (150±52 ms for centripetal versus 182±37 ms for centrifugal, $p=0.005$, $n=30$). Though the difference in rise time between centrifugal and centripetal motion reached significance, the AI for this metric was small and variable (AI=0.100±0.167). When compared to the AI for amplitude, rise time, and integral of the leading edge response the AI for trailing edge rise time and was significantly smaller than all three ($p<0.001$, $n=30$).

Thus, we propose that the critical directional non-linearity in the SBACs is generated by the suppression of proximal excitatory inputs by more distal inputs. This model is similar to that proposed by Lee and Zhou, (2006) where inhibitory inputs activated outside the dendritic extent of the cell subtract from excitation activated over the cell center. However, this model relied on a GABAergic chloride conductance to mediate surround-activated inhibition. In our recordings the chloride reversal potential is -69mV so that GABAergic inhibition should have little effect on the current amplitude at a -60mV holding potential; however, it is possible that a large chloride conductance could be contributing to the inward

current we record at -60mV or that inhibition is acting “silently” to shunt the excitatory conductance and make the inward current appear asymmetrical.

Excitatory inputs to the SBAC are directional

To test for such a mechanism, we performed whole-cell voltage clamp recordings and measured the excitatory and inhibitory synaptic conductance during centrifugal and centripetal stimuli (Fig. 3 and see methods). Current voltage relations plotted near the peak of the response (dotted lines Fig. 3a & b) were linear for both centrifugal and centripetal stimulation (Fig. 3c, see (Taylor and Wässle, 1995b)). Comparing the slopes of the I-V relations indicates that the total light evoked synaptic conductance was larger during centrifugal stimulation (Figure 3d). We calculated the excitatory and inhibitory components of the synaptic conductance based on a reversal potential of 0mV for excitation and -69mV for inhibition (Fig. 3e & f, see Methods), and it is clear that direct inhibitory synaptic input does not contribute significantly, if at all, to the response.

Figure 3

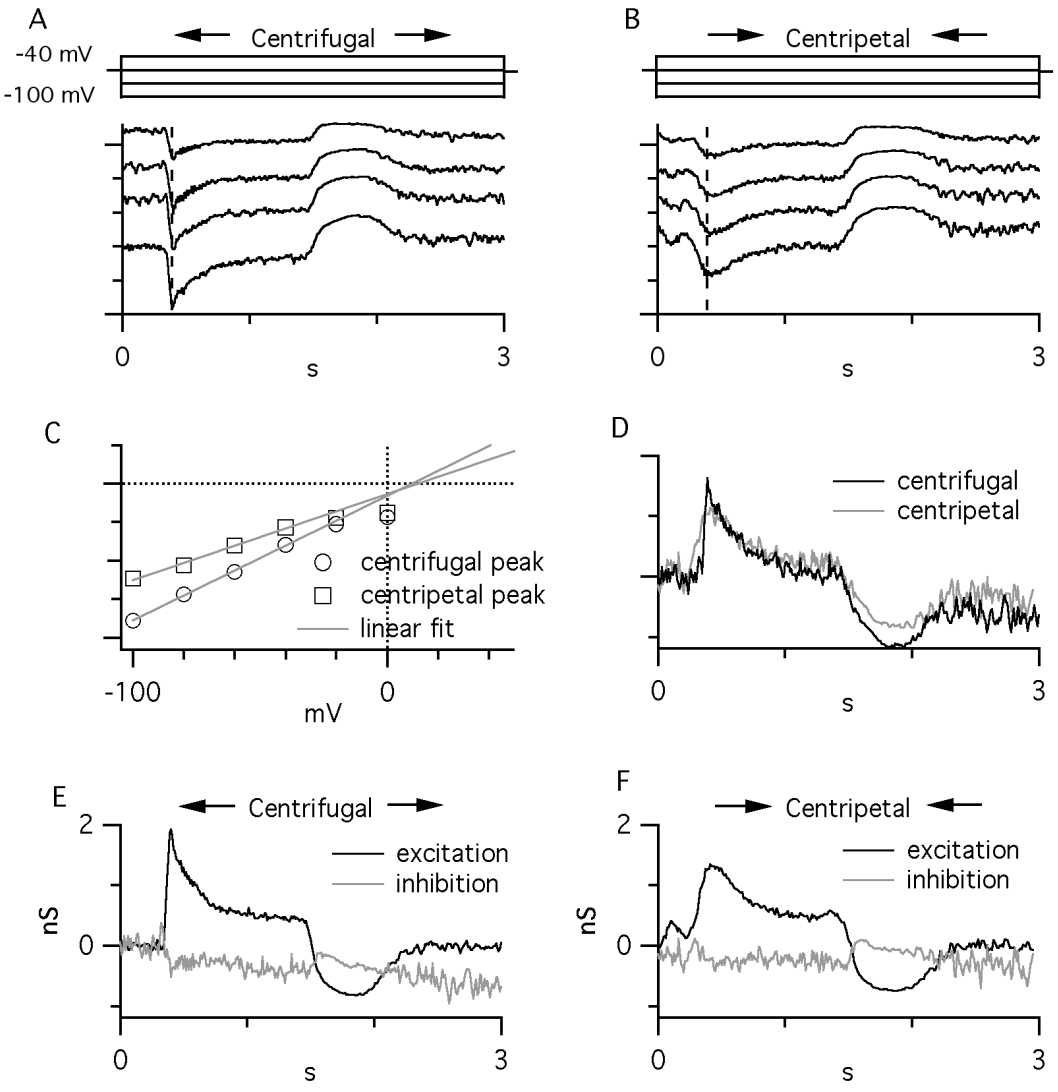

Figure 3.3:

Conductance measurements of SBAC synaptic inputs. A and B show the currents recorded during centrifugal and centripetal stimulation, respectively, during command potentials ranging from -100 mV to -40 mV. Solid lines above show command voltage. Vertical dashed lines indicate time point where sample IVs shown in C were measured. C shows plots of IV at the

peak responses as indicated by the dashed line in figure A and B for centrifugal (circles symbols) and centripetal (square symbols) motion. The solid line indicates the linear fit between -100 mV and -40 mV. D shows the total conductance measured every 10 ms for centrifugal and centripetal traces, in black and gray, respectively. E and F show the separated excitatory (black traces) and inhibitory conductances (gray traces) for centrifugal and centripetal motion, respectively.

A possible objection to our results is that larger voltage-clamp errors at positive potentials do not allow us to adequately resolve inhibitory inputs. Two lines of evidence discount this possibility. Blocking GABAergic transmission did not alter the amplitude, integral or rise time of the responses or change the directionality for any of these metrics (n=5; Fig. 4). Moreover, some cells displayed sparse, spontaneous synaptic inhibitory currents that had a reversal potential near -65mV suggesting that voltage control was adequate (Fig. 4e).

Even in the absence of GABAergic input to the SBAC it is clear that centrifugal and centripetal responses remain directional (Fig. 4c). Hausselt et al (2007) observed similar results, and proposed that a voltage-gradient in the SBAC dendrite was an integral part of the mechanism generating the directional excitatory responses in the SBACs, and that this voltage gradient was generated by the tonic excitatory input to the SBAC dendrites (Peters and Masland, 1996a; Taylor and Wässle, 1995b). Previous groups reported that quinoxaline AMPA/kainate antagonists blocked this tonic input (Peters and Masland, 1996b,

Hausselt, 2007; Taylor and Wässle, 1995b), and that these antagonists eliminated directional responses in DSGCS by revealing spikes during null-direction motion (Cohen and Miller, 1995).

Figure 4

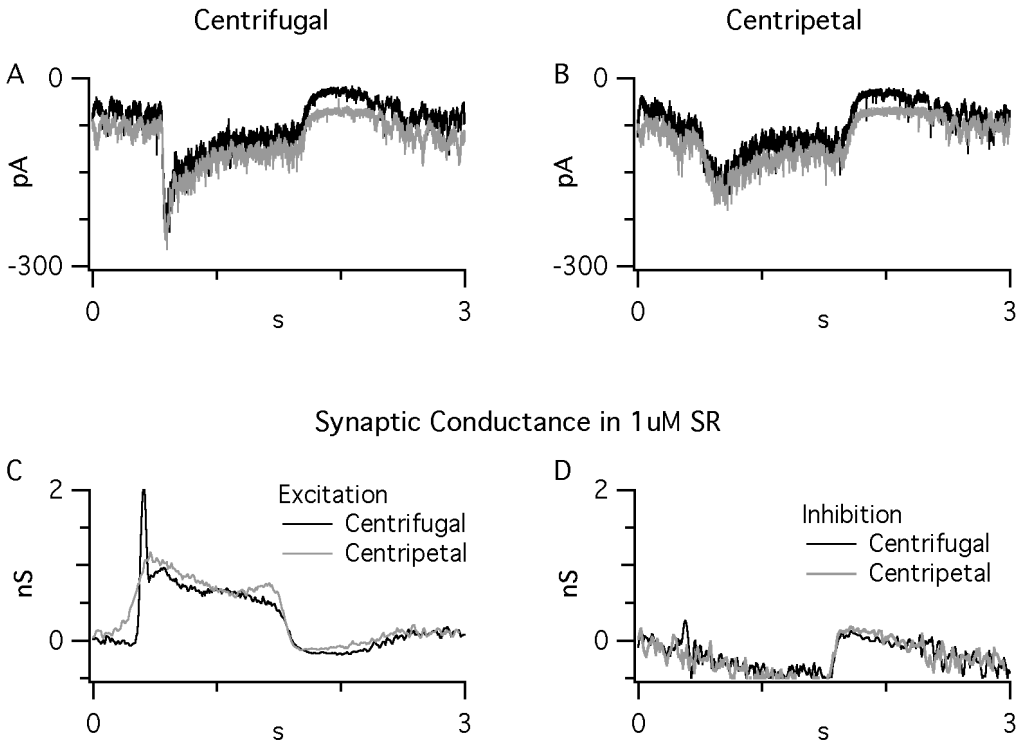

Figure 3.4:

GABAergic inhibition does not contribute to responses to moving stimuli. A and B show control currents (Black traces) and currents recorded in the presence of 2 μM SR-95531 (gray traces), in response to centrifugal (A) and centripetal stimuli (B). C and D show excitatory (C) and inhibitory (D) conductances for centrifugal (black traces) and centripetal (gray traces) stimuli in the presence of SR-95531

NBQX blocks noise, but not directional inputs to SBAC

In a series of preliminary experiments we determined that directional spiking responses in DSGCs could be blocked by as little as 750nM of the quinoxalone derivative NBQX, a potent AMPA/kainate antagonist (see Results below). In SBACs 750nM NBQX blocked a net inward current of 13.9±8.9 pA and decreased the membrane current variance from 1.15e-22±6.2e-23 to 6.19e-24±7.1e-24 (Significance $p<0.005$, $n=8$). Despite this block of the sustained synaptic input, NBQX did not significantly reduce the peak amplitude of the responses during either centrifugal or centripetal motion. In 8 cells, the peak responses were only modestly reduced by 12.9±30.7 and 17.5±29.2 pA, or 9.4% and 18.3% respectively, but these effects were variable and failed to reach significance ($p=0.231$ and 0.096 respectively. Fig. 5a and b). Similarity, the small decrease (5.0±6.5 ms) in the 10-90% rise time for the centrifugal response was not significant ($p=0.095$). The integral of the centrifugal response was significantly reduced by 32.7% ($p=0.009$, $n=8$). This reduction was probably due to NBQXs blockate of the tonic component of the light response. The integral for centripetal motion was not changed. As expected the AI for these parameters were also not significantly affected, though the trend was towards an increase in AI. For amplitude the AI increased from 0.16±0.06 to 0.20±0.07 in the presence of NBQX and for rise time the AI increased from 0.60±0.15 to 0.69±0.07 ($p=0.21$ and 0.08, respectively). These results indicate that a tonic NBQX sensitive current in the SBAC does not play any role in generating directional responses in the SBAC.

Because NBQX blocks the tonic noisy input current and also blocked the sustained component of the light response, we were better able to reveal the time course of the synaptic input to the leading edge of the stimulus in the presence of NBQX. The time course of the responses in NBQX remains quantitatively similar to control conditions. Taken together the data is consistent with the idea that during centripetal motion when the stimulus is traversing the dendritic field it activates fewer or smaller synaptic inputs over a greater time span.

Surprisingly, during application of 750nM NBQX, we observed a light evoked inhibitory conductance that was not present under control conditions (Fig. 5d); however, this inhibition had a slow onset, reaching a peak between 250 to 500ms after the peak of the excitatory conductance, when the leading edge of the stimulus had completely traversed the dendritic extent. Furthermore, the inhibitory input was symmetrical in both amplitude and time-course, providing no additional directional signal (Fig. 5d). This also provides further evidence that our conductance measurements are able to detect the presence of inhibitory inputs to the SBAC. In summary, neither the tonic inward current that is characteristic of SBACs, nor $GABA_a$ receptor activity are required to generate directional inputs to these cells. How do these low concentrations of NBQX block directional spiking in DSGCs?

Figure 5

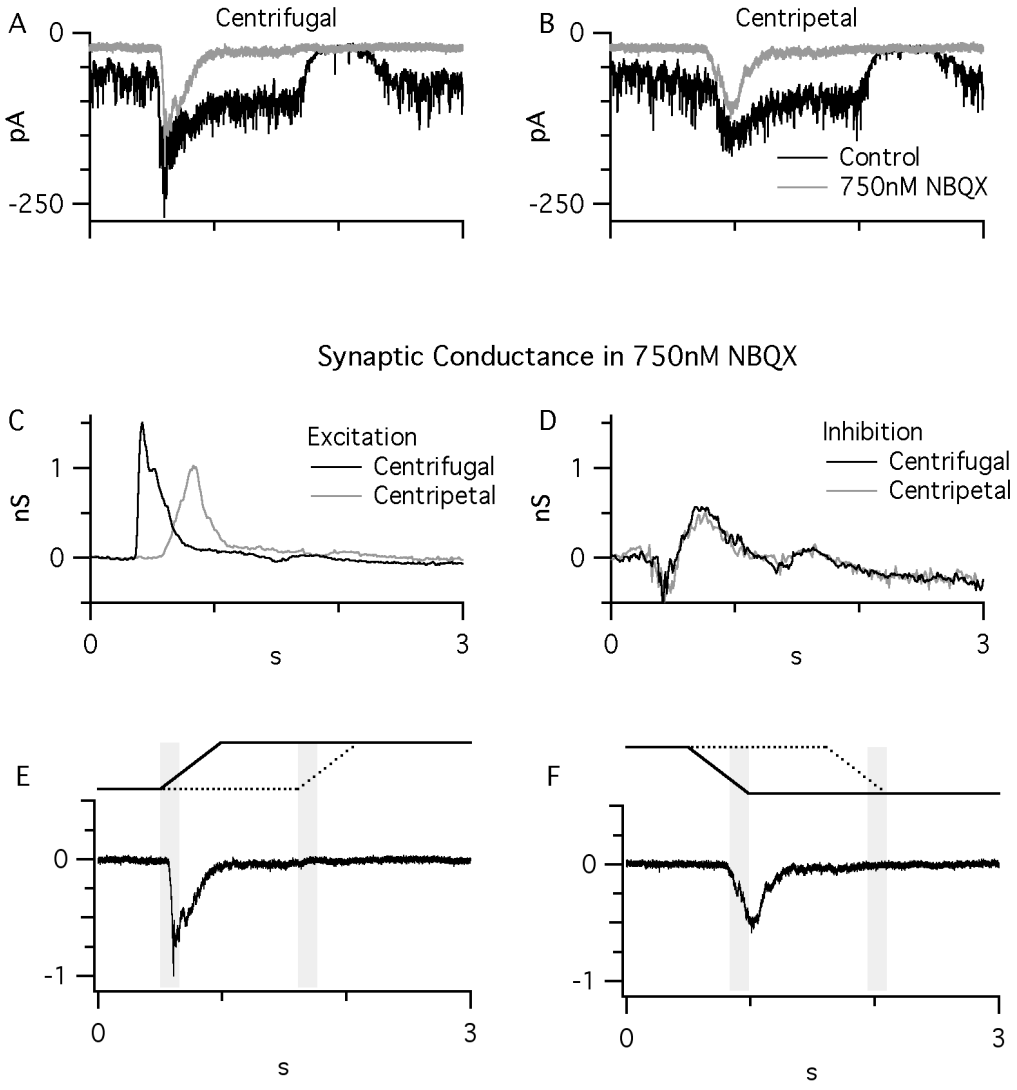

Figure 3.5:

NBQX does not alter directionality of SBAC currents. A and B show control currents (Black traces) and currents recorded in the presence of 750 nM NBQX (gray traces), in response to centrifugal (A) and centripetal stimuli (B). C and D show excitatory (C) and inhibitory (D) conductances for centrifugal (black traces) and centripetal (gray traces) stimuli in the presence of NBQX. E

and F show centrifugal (E) and centripetal (F) responses in the presence of NBQX aligned with the stimulus position, indicated by the solid and dotted lines, indicating position of leading and trailing edges of stimuli, respectively, relative to the cell some.

NBQX blocks inhibitory synaptic inputs to the DSGC

In their original report, Cohen and Miller (1995) hypothesized that NBQX blocked directionality by blocking the excitatory drive to the SBACs, thereby eliminating the critical directional GABAergic input to the DSGC. Our finding that SBACs still receive significant excitatory input in the presence of concentrations of NBQX sufficient to block direction selectivity in the DSGCS, is inconsistent with this hypothesis, but we wanted to test Cohen & Miller's idea by directly recording inhibitory inputs to DSGCs. First we confirmed that NBQX eliminates directional responses in DSGCs (Fig. 6). The strength of the directional tuning was quantified by calculating a directional selectivity index DSI (see Methods). In close agreement with previous estimates in rabbit (Taylor et al., 2000; Taylor and Vaney, 2002), DSI measured from extracellular spikes in loose-patch recordings averaged 0.52±0.12 for the ON response and 0.55±0.15 for the OFF response (Figure 6a, N=6). Application of 750 nM NBQX increased the number of null direction spikes and decreased the number of preferred direction spikes, so that the number of spikes was independent of stimulus direction, similar to previous results (Cohen and Miller, 1995). The average DSI measured in the presence of 750 nM NBQX was reduced to 0.07±0.02 for the ON response and 0.06±0.28 for

the OFF response (Figure 6b, N=6). The effect of NBQX was reversible and repeatable (Figure 6c). Given that synaptic transmission in the OPL is mediated by mGluR6 and AMPA/Kainiate receptors for the ON and OFF responses respectively, it was surprising to see that NBQX decreased preferred direction spiking in the ON response more that the OFF (Figure 6d); However, these results are consistant with a previous report on the network actions of quinoxalines in the retina (Cohen and Miller, 1999) . Concentrations of NBQX higher that 750nm did not have any additional effect on direction selectivity (data not shown).

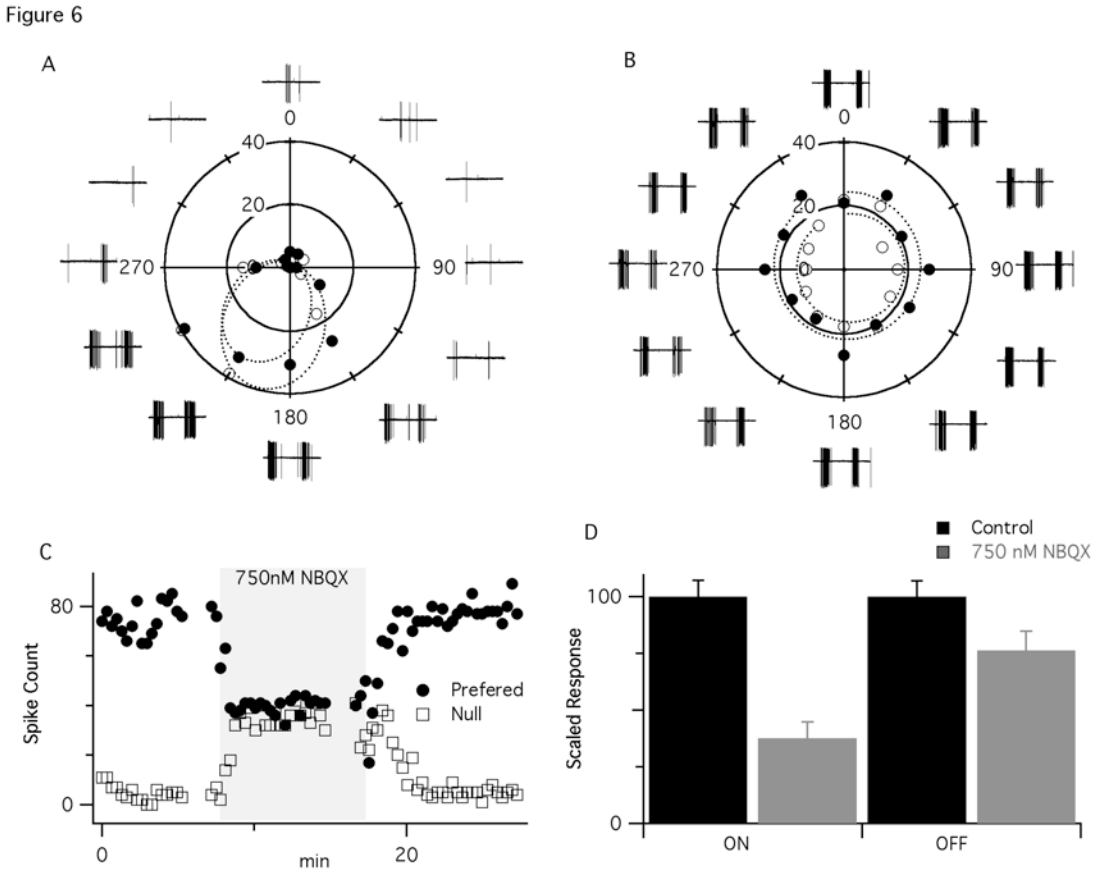

Figure 3.6:

NBQX blocks direction selectivity in DSGCs. A. Extracellular spike responses to sweeping bar stimuli in each of 12 directions are shown adjacent to the

stimulus angle. Each point on the polar plot shows the total number of spikes for the ON (open symbols) and OFF (closed symbols). The solid lines indicate the best-fit von Mises distribution for the ON and OFF responses. Asymmetry in polar plot indicates directional selectivity of response. B. Same as A, but in the presence of 750 nM NBQX. Polar plot becomes symmetric in NBQX. C. Spike-counts during repeated preferred (filled circles) and null (open squares) direction stimuli plotted against time. Gray box indicates duration of NBQX application. Effect is rapid and reversible. D. Relative reduction of preferred direction spiking. Black bars indicate control spikes scaled to maximal spike response for ON and OFF responses. Gray bars indicate preferred direction spiking responses scaled to the maximal response in control. Error bars equal standard deviation.

In agreement with Cohen and Miller's original suggestion, measurements of the synaptic conductance revealed that 750nM NBQX nearly completely blocked the inhibitory conductance during preferred and null direction stimulation for both the ON and OFF responses (fig. 7). During null-direction stimulation, the integral of the inhibitory conductance was reduced by 96±8% & 97±5% for ON and OFF responses respectively (N=9). The corresponding reductions for preferred direction stimulation were 96±13% & 95±14 for ON and OFF responses respectively. The larger error for preferred direction measurements was due to the smaller absolute magnitude of the preferred direction inhibition. Thus our results confirm to some extent Cohen and Millers original hypothesis that NBQX

abolishes directionality by blocking the inhibitory input to the DSGC; however, this was not simply due to a suppression of the excitatory inputs to the SBACs, since the peak amplitude of the SBAC light response is not significantly reduced by 750nM NBQX (fig. 5).

Figure 7

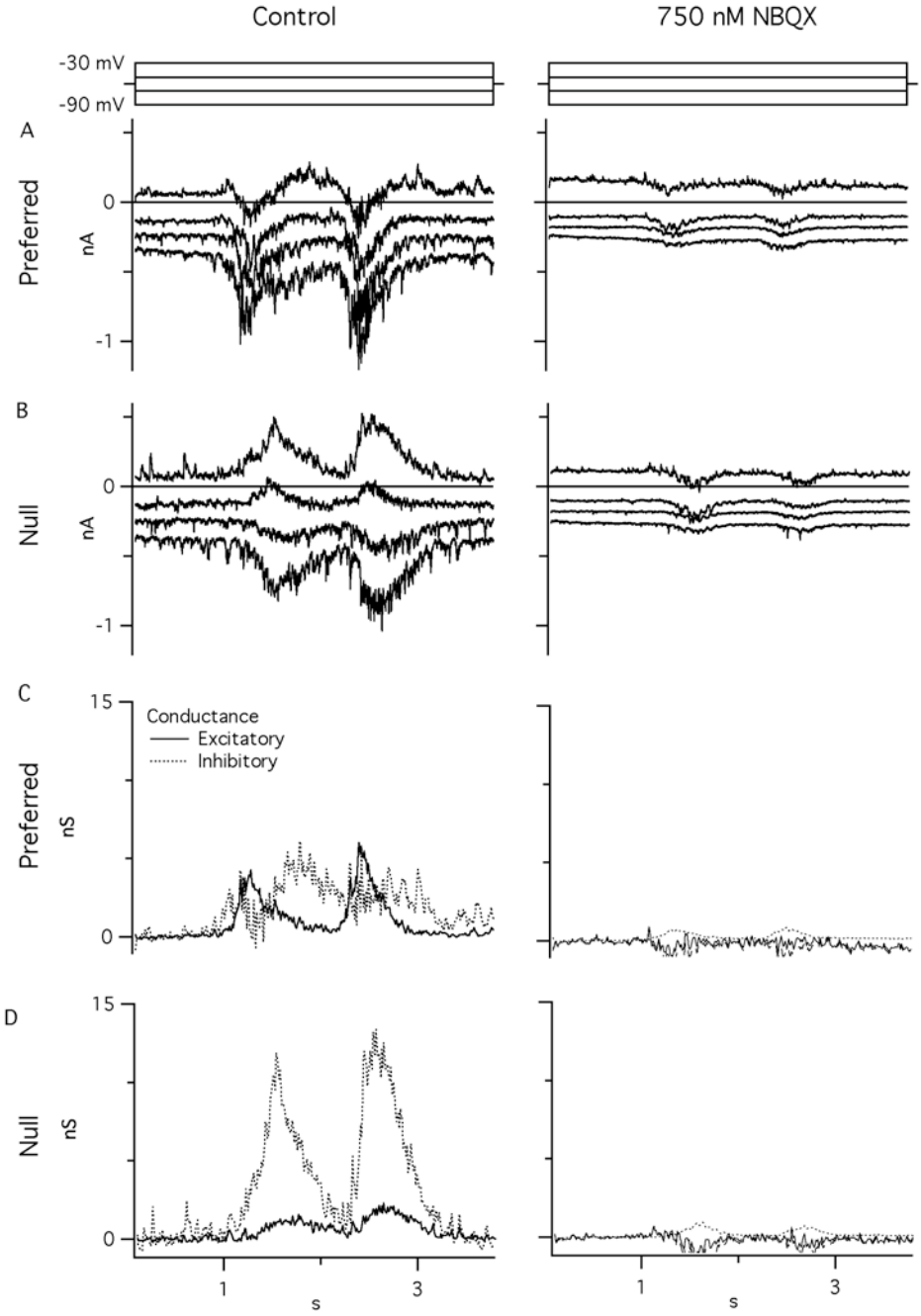

Figure 3.7:

NBQX blocks inhibitory and most excitatory input to the DSGC. A. Current recordings during preferred direction stimulation at a series of command potentials between -90 and -30 mVs, in control (left traces) and in the presence of 750 nM NBQX (right traces). Traces in B are displayed the same as A, but for null direction stimulation. C. Excitatory (solid line) and inhibitory (broken line) are conductance of the preferred direction evoked synaptic inputs are plotted against time under control conditions (left) and in the presence of NBQX (right). D. Same as C, but for null direction evoked excitatory conductances.

GABA release onto the DSGC is mediated by voltage-gated calcium channels

Thus, the effects of NBQX on the DS circuitry appear more complex than expected. We considered the possibility that GABA release from SBACs, might be mediated at least in part by direct calcium influx through calcium permeable AMPA receptors, which lack the GluR2 subunit (Bowie and Mayer, 1995; Geiger et al., 1995); for review see Isaac, 2007). This mechanism was recently demonstrated to mediate fast synaptic GABA release from another type of retinal amacrine cell, the A17 (Chávez et al., 2006). We activated the glutamate receptors on the amacrine cells by puffing glutamate onto inner plexiform layer on the null-side of the DSGC dendrites. The puffs of glutamate evoked both excitatory and inhibitory currents (figure 3.8) in the DSGC. The inhibitory inputs were presumably generated by depolarization of the SBACs, because inhibitory currents were not evoked by puffs on the preferred side of the DSGC, consistent with pre-

vious descriptions of SBAC mediated inhibitory currents in the DSGC (Fried et al., 2002a)). The calcium permeable AMPA receptor antagonist IEM-1460 completely blocked the inhibitory current in three out of seven cells; however, the inhibitory input was also blocked by 200µM cadmium in all three cells. Since cadmium blocks calcium influx through voltage-gated calcium channels and not through the calcium-permeable AMPA receptors, the results are consistent with conventional release of GABA via voltage-dependent calcium channels in the presynaptic neurons.

Figure 8

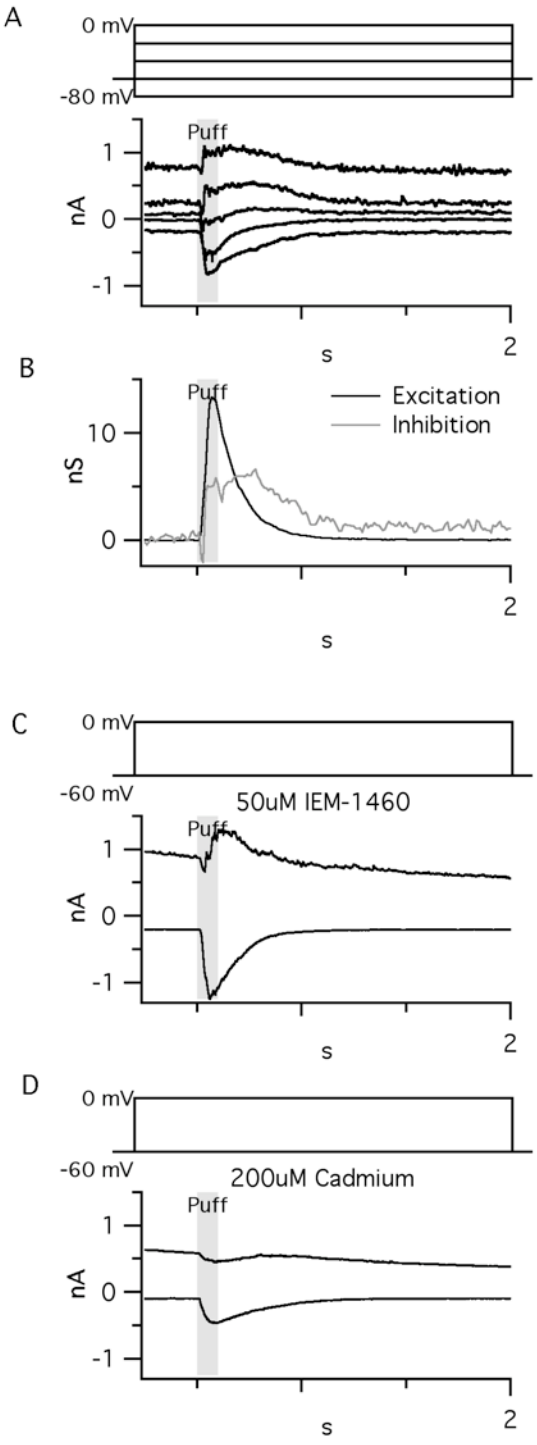

Figure 3.8:

Glutamate evoked inhibition in the DSGC. A. Example recordings of currents

evoked by a brief (50 ms) application of 200 μM glutamate in Ames into the IPL of the DSGC at a series of command potentials. Puffing pipette was located ~100 μm from the DSGC soma on the null side of the receptive field. Schematic above traces denotes series of command voltages. B. Excitatory (black trace) and inhibitory (gray trace) conductance of puff evoked responses. Both excitatory and inhibitory conductances are evoked from glutamate application. C. Puff evoked responses recorded at -60 and 0 mV command potentials in the presence of the calcium-permeable AMPA receptor channel blocker IEM-1460. D. Puff evoked responses recorded at -60 and 0 mV command potentials in the presence 200 μM cadmium.

TTX-resistant sodium channels boost directional synaptic input to the SBAC

Two previous reports have suggested that directional responses in SBACs might be enhanced by voltage-gated ion channels in the SBAC dendrites (Hausselt et al., 2007; Tukker et al., 2004). There are reports of both voltage-gated calcium and sodium currents in SBACs; however, the existence of tetrodotoxin-sensitive channels in SBACs has been disputed (Bloomfield, 1992a; Bloomfield, 1992c; Cohen, 2001; Hausselt et al., 2007; Jensen, 1995a; Ozaita et al., 2004; Peters and Masland, 1996b; Taylor and Wässle, 1995b; Zhou and Fain, 1996). More recently, a systematic study of the voltage-gated currents in mouse SBACs found evidence for N, P and Q type calcium currents, but did not find evidence for TTX sensitive sodium currents (Kaneda et al., 2007) however, they did not rule out the possibility of tetrodotoxin-resistant voltage-gated sodium

channels (TTX-R VGSC). A recent anatomical study demonstrated immuno-reactivity using a TTX-resistant sodium channel (Na_V 1.8) antibody is consistent with expression in the SBACs (O'Brien et al., 2008). In light of these previous studies, we examined the effect of ambroxol hydrochloride, a selective TTX-R VGSC blocker, on the SBAC light responses to determine whether TTX-resistant sodium currents contributed to the directional asymmetry.

We applied a series of depolarizing voltage steps and measured the current amplitude 1.2ms after the voltage step. The linear component of the membrane current was subtracted (see Methods). Under control conditions a negative slope conductance can be observed between -40 and 0 mV consistent with the activation of an inward voltage-gated current (Fig. 9a). During application of 200-500µM ambroxol the negative slope of the IV between -40 and 0 mV decreased, indicating that SBACs express a TTX-R VGSC conductance that is sensitive to ambroxol hydrochloride. Ambroxol significantly changed the slope of the best-fit line to the IV between -40 and 0 mV from -3.51±0.70 to -1.74±0.37 nS (P=0.015, N=3).

Ambroxol decreased the peak amplitude of currents elicited by centrifugal stimulation by 54.6±12.4 pA or 47.9% (p=0.002, n=6), but had no effect on the sustained component of the light response. The peak amplitude of the centripetal response was reduced by 25.7±15.5 pA or 37.3%. Despite the smaller magnitude of reduction for the centripetal peak response, the reduction in centripetal amplitude was still significantly different than control (p=0.008, n=6). This selectively larger reduction in centrifugal peak amplitude significantly reduced the directional

difference between centrifugal and centripetal peak amplitudes from 42.7±15.3 pA in control to 14.7±4.3 pA in ambroxol a reduction of 64.2% (p=0.002, n=6). In addition, the AI for amplitude was significantly decreased from 0.26±0.07 to 0.19±0.08 (p=0.008), n=6). Despite the significant reduction in the asymmetry, the centrifugal and centripetal amplitudes were still significantly different from each other (p=0.001). Ambroxol had no significant effect on the time course of the centrifugal response, but for centripetal responses a variable increase was observed and on average the centripetal rise times was increased by 56±68 ms in the presence of ambroxol. Given the variability of the effect, the difference failed to reach significance (p=0.098, n=6).

Despite the overall reduction in SBAC AI, we could not detect any effect of ambroxol on the currents measured in DSGCs. Since ambroxol also blocks spiking in the DSGCs, it is not possible to determine whether the ambroxol had reduced directional spiking responses in the DSGCs, and therefore the results of these experiments, were inconclusive.

There have been conflicting reports about the presence of TTX sensitive currents in SBACs, and the presence of a negative conductance that was insensitive to ambroxol (Fig. 9a), prompted us to determine whether TTX sensitive VGSCs also contribute to the directional asymmetry in SBACs. To this end we tested the effects of 500nM TTX on the SBAC responses. TTX slightly decreased the negative slope in the IV from -8.7±2.6 to -7.1±2.9 nS, but the difference was not significant (n=6). In contrast to ambroxol, TTX increased the peak amplitude of the SBAC responses by 12.6±8.2 pA for centrifugal and 17.4±10.9 pA for cen-

tripetal, a change of 14.9% and 29.3% respectively (p=0.027 and 0.023, respectively, n=5). However, because both centrifugal and centripetal response amplitudes were changed by a similar amount, TTX had no significant effect on the directional differences or the AI. TTX also had no discernable affect on the centripetal rise time, but similar to ambroxol, it did slow the centrifugal rise time by 9.0±6.0 ms (p=0.037, n=5). The most parsimonious explanation for the increase of the SBAC response amplitude by TTX is that TTX suppresses the activity of spiking amacrine cells which make inhibitory contacts with bipolar cell terminals, as has been shown for other cells (refs). These data are consistent with the conclusion that the reduction in SBAC asymmetry caused by ambroxol is mediated through TTX-R VGSC blockade and not by TTX-sensitive sodium channel blockade (figure 9b).

It is clear from previous work, that there are voltage-gated calcium channels (VGCCs) present in SBACs (Kaneda et al., 2007; Zheng et al., 2004b) and there have been suggestions that they too may contribute to the directional asymmetry in the SBAC currents (Hausselt et al., 2007; Tukker et al., 2004). To test this idea we tested the effects of 25-30μM cadmium on the SBAC responses. We did not see any change in the negative slope of the IV relation in cadmium, nor could we resolve any differences in response amplitudes, rise times, or the AI (Fig. 9c). These observations argue that VGCCs do not play a role in generating the directional asymmetry.

Taken together our results suggest that the observation of directional excitatory inputs to the SBAC cannot be explained by postsynaptic non-linearities. It

is clear that TTX-R sodium channels boost the directional difference in excitatory inputs; however, as observed in the presence of ambroxol hydrochloride TTX-R sodium channels cannot account for the entire asymmetry observed between centrifugal and centripetal motion.

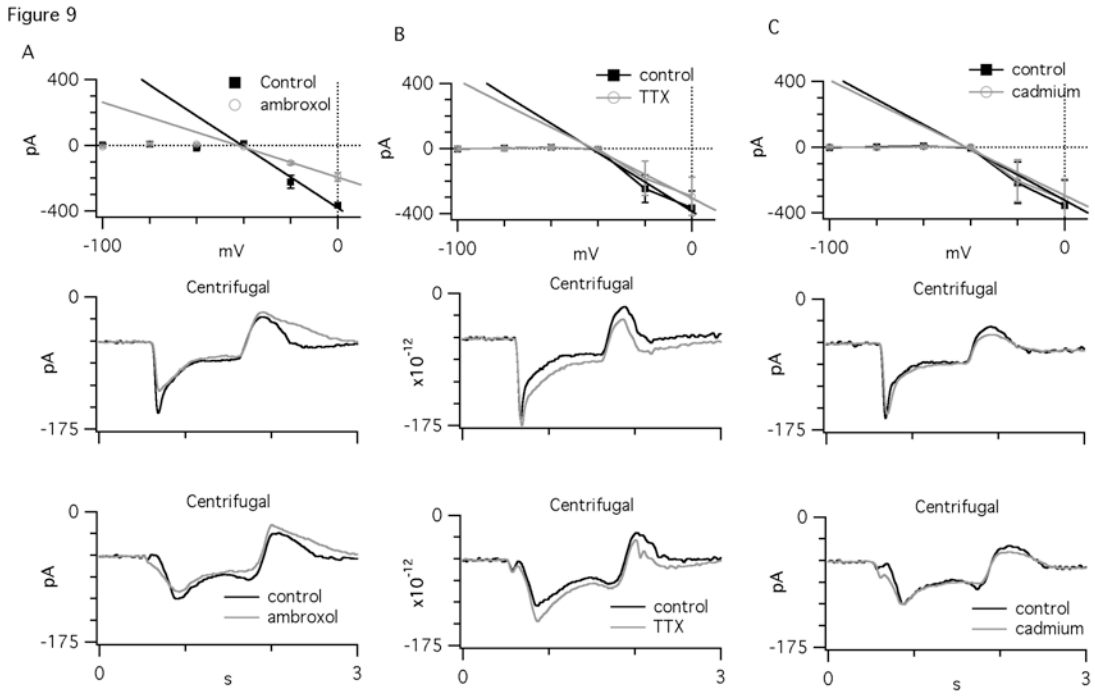

Figure 3.9:

Ambroxol blocks reduces SBAC AI, but not TTX or cadmium. Top row shows shows the average IV relation measured 1.2 ms after the command step to voltages between -100 and 0 mV, under control conditions (closed squares) and drug (open circles). Error bars show standard error. The linear portion of the IV has been subtracted leaving the negative slope portion of the IV (see Methods). The solid lines indicate the best-fit line between -40 and 0 mV. A shows 300 μM ambroxol hydrochloride (n=3), B shows 500 nM TTX (n=6), and C shows 25 μM cadmium (n=5). The second and third rows show the

average filtered (25 Hz cutoff Gaussian) current traces in response to centrifugal and centripetal stimulation, respectively. Control traces are in black and drug traces are in gray. A shows 300 μM ambroxol hydrochloride (n=3), B shows 500 nM TTX (n=5), and C shows 25 μM cadmium (n=6)

Discussion

While it is well understood that the directional GABA release on the DSGC is important for computing the direction of motion in the retina, the mechanisms that generate the directional GABA signal are not well understood. It has been suggested from previous work that the SBAC dendrites first compute the directional signal in the retina (for review see (Demb, 2007); however, our work suggest that the directional signal arises prior to the SBAC dendrites. We conclude from this study that directional selectivity in the retina is first formed at the level of transmitter release from bipolar cell terminals, which generate directional excitatory inputs to the SBAC, and that the directional difference in the excitatory currents is enhanced by TTX-resistant voltage-gated sodium channels.

Evidence for Directional Inputs

The conclusion that the excitatory synaptic inputs to the SBAC are themselves directional come from the primary observations that isolated excitatory currents measured in the SBAC are directional, with centrifugal motion evoking an excitatory postsynaptic current (EPSC) that has a larger peak current amplitude and integral over the time than the leading edge traverses the stimulus field, and is also faster to rise to peak. This implies that during centrifugal motion either

more or larger inputs are activated for centrifugal stimulation, and the onset of activation is more synchronous than during centripetal motion. There are two important factors that could make excitatory symmetrical inputs appear to be asymmetrical. First, large inhibitory inputs for centripetal motion could shunt excitatory inputs. Second, poorly voltage-clamped voltage-gated ion channels could introduce non-linearities that selectively boost excitatory input in one direction, but not the other. The idea that inhibition could account for the SBAC DS has received recent experimental support from Lee et al (2006), who demonstrated that SBACs make reciprocal GABAergic contacts with their neighbors. Furthermore, they demonstrated that inhibition from neighboring SBACs contributed asymmetrically to the SBAC response.

This lead us to ask whether inhibition could account for the directional signals we observed in the SBAC by measuring excitatory and inhibitory synaptic conductance and by using pharmacological blockers of GABA receptors. Under control conditions we did not observe any evidence of a significant inhibitory input. One explanation might be that we did not have significant voltage control over the cell to modulate the driving force at GABAergic inputs. We do not believe that this is true because in some cells we did observe a low frequency of spontaneous inhibitory inputs that were outward at holding potentials above the synaptic reversal potential for chloride. Furthermore, when we applied the $GABA_a$ receptor antagonist SR-95531, we were unable to observe any change in the light evoked EPSC to the SBAC in the presence of SR, or any change in the directional asymmetry. We did observe light -evoked inhibitory postsynaptic poten-

tial in the SBAC when we applied the AMPA/kainate antagonist NBQX to the preparation; however, the NBQX induced inhibition was non-directional, and blocking this current with SR-95531, did not change the asymmetry of the remaining excitatory input. Based on these observations, inhibitory inputs cannot account for the asymmetry in the SBAC excitatory inputs.

The second alternative hypothesis that could explain the observed asymmetry in the SBAC is that, poorly voltage-clamped voltage gated ion channels could introduce non-linearities that boost excitatory input in one direction. Many hypothesis to explain SBAC DS have focused on non-linearities in the SBAC dendrites, and it seems reasonable that voltage control in the SBAC dendrites could be poor enough to allow for unclamped voltage-gated channels to be activated (Hausselt et al., 2007; Kaneda et al., 2007; Miller and Bloomfield, 1983; Ozaita et al., 2004; Taylor and Wässle, 1995a; Velte and Miller, 1997). Recently, Hausselt et al (2007), also demonstrated that GABAergic inhibition could not account for SBAC DS in their preparation, in accordance with our results with GABA antagonists; however, they found that SBAC DS was modulated by SBAC membrane potential, suggesting a role for a voltage-dependant non-linearity. Based on their observations and compartmental modeling they proposed that directional discrimination relies on an interaction between VGCCs and a dendritic voltage gradient created by tonic glutamatergic input.

To assess the role that a dendritic voltage gradient and voltage-gated channels might play in generating the observed asymmetry in the SBAC inputs we used pharmacological blockers of voltage-gated ion channels and NBQX to

block the tonic glutamatergic input proposed to be responsible for generating the dendritic voltage gradient. Jensen (1995) provided evidence suggesting direction selectivity in the DSGC may be mediated by P or Q type voltage-gated calcium channels (VGCCs). This suggestion was based on the observation that low concentrations of cadmium and some VGCC selective conotoxins blocked directional spiking in the DSGC. Hausselt et al. found that cadmium reduced SBAC DS; yet, they found that conotoxins could not account for any of the SBAC directional asymmetry short of blocking all light-evoked synaptic input to the cell. Hausselt et al had found that low concentrations of cadmium (10µM), reduced the directional signal in the SBAC, when we applied low concentrations of cadmium (15-30µM cadmium to our preparation we did not observe any change in the size of the SBAC currents and the directional asymmetry remained unchanged. Previous results using cadmium and calcium channel blockers have produced variable and unpredictable results. Jensen (1995) had found that higher concentrations of cadmium (73-100µM) blocked direction selectivity in DSGCs; however, Hausselt et al (2007) found that those concentrations completely blocked the light response in SBACs; furthermore, neither Hausselt et al. nor we were able to find more selective VGCC blockers which could block SBAC DS without blocking the entire light response. Our own data indicates that concentrations of cadmium could abolish direction selectivity in the DSGC at concentrations ranging from 50 to 100 µM; however, if the concentration was sufficient to block directional selectivity in the DSGC, the ON response was also irreversible abolished. (data not shown). The observation that cadmium can block TTX-resistant VGSCs (Leffler

et al., 2005; Satin et al., 1992; Sunami et al., 2000) may confound the results of the cadmium experiments limiting the usefulness of cadmium as a selective blocker of calcium channels; however, it does raise the possibility that TTX-R VGSCs may be playing a role in SBAC DS. This idea gains further support form the recent report showing a distribution of Na_V 1.8 immuno-reactivity that is consistent with expression by SBACs. To examine if TTX-R VGSCs may be contributing to the SBAC non-linearity, we used the selective TTX-R VGSC blocker ambroxol hydrochloride to block these channels (Weiser and Wilson, 2002). We demonstrated that ambroxol did reduce the directional asymmetry in the SBAC response; however, the signals remained significantly directional, so it appears that TTX-R VGSCs are boosting an already directional signal. The observation that ambroxol had no effect on the directional responses of the DSGC calls into question the importance of the increase in asymmetry that ambroxol creates; however, it is important to note, that the directional responses of DSGCs were only tested for one set of stimulus conditions. It is clear that ambroxol cannot account for the entire directional asymmetry in the SBAC and it is possible that TTX-R channels may function to make the directional asymmetry more robust over a range of stimulus conditions.

Finally, to address the question of how a dendritic voltage gradient might give rise to non-linear input summation in the SBAC dendrite and contribute to the apparent directionality of inputs to the SBAC we applied NBQX to block the tonic input to the SBAC, which should consequently block the dendritic voltage gradient as proposed by Hausselt et al. (2007). Others before us have reported

that NBQX blocks a large tonic input to the SBAC (Hausselt et al., 2007; Peters and Masland, 1996b; Taylor and Wässle, 1995b). Despite blocking the tonic input to the SBAC, we could not detect any significant decrease in the SBAC asymmetry, though small NBQX induced changes tended to increase the SBAC AI, these differences did not reach statistical significance.

It is interesting to note that low concentrations of NBQX (750 µM) did not block the light evoked excitatory input. Currently the only known significant source of excitatory inputs to the SBAC are mediated through AMPA receptors (Zheng et al., 2004b; Zhou and Fain, 1995). Others have demonstrated that higher concentrations of quinoxolines do block all synaptic input (Linn et al., 1991; Peters and Masland, 1996b; Petit-Jacques and Bloomfield, 2008; Petit-Jacques et al., 2005; Taylor and Wässle, 1995b). This suggests that low concentrations of NBQX, must have some subunit specificity, consequently indicating that light evoked synaptic currents are mediated through different AMPA receptor subtypes than the tonic AMPAergic synaptic current.

Our experiments rule out both the possibility for inhibitory inputs accounting for the observed directional difference in inputs to the SBAC, as well as the possibility of various non-linear processes in the SBAC that might account for the observed directional difference in inputs. While we did find evidence that TTX-resistant sodium channels boost the directional difference in SBAC inputs, which represents a previously unknown mechanism for enhancing directional selectivity in the SBAC, TTX-R sodium channels could not account for the entire directional difference in SBAC input. Based on this evidence we conclude that excitatory

neurotransmitter release onto the SBAC must itself be directional. This represents the first experimental evidence that the directional signal in the retina may arise as early as the bipolar cell terminal.

Source of directional excitation in the SBAC

By demonstrating that SBACs receive directional excitatory inputs, even in the absence of feedback from GABAa receptors, we raise the question of the source of directional inputs to the DSGC. The most parsimonious explanation for the source of the excitatory inputs to the SBAC are ionotropic glutamate receptor mediated bipolar cell input; however, we currently do not have an understanding of how bipolar cell terminals could directionally release glutamate onto the SBAC dendrite. One likely explanation is that inhibitory synapses onto bipolar cell terminals could modulate synaptic output. There is significant evidence for this type of interaction in the retina (Kolb, 1977; Tachibana, 1999; Tachibana and Kaneko, 1987; Vaughn et al., 1981; Wu et al., 1981) and our TTX results match well with others observations that spiking amacrine cells could mediate this interaction (Shields and Lukasiewicz, 2003); however, the neurotransmitter responsible for this interaction remains unknowns, as we did not observe any change in the excitatory inputs, when we applied the GABAa antagonist SR-95531, thus ruling out GABAa receptors. It is worth noting that others have proposed that directional transmitter release from bipolar cell terminals could account for the directional excitation observed in the DSGC (Brown and Masland, 1999a; Famiglietti, 2002; Kim and Rieke, 2003).

Because the SBAC also releases acetylcholine and have a high degree of overlap one could postulate that the source of directional excitation is a cholinergic input; however, Zheng et al (2004) reported that while developing SBACs make nicotinic cholinergic synapses onto their neighbors, in the mature SBAC these synapses are lost and there is no evidence of a cholinergic input. If cholinergic receptors were responsible for generating directional input to the SBAC, we would expect that cholinergic antagonists should abolish directional inhibition in the DSGC and consequently abolish direction selectivity, yet despite an extensive search for a definitive role for cholinergic receptors in direction selectivity. DSGCs remain robustly directional in the presence of cholinergic antagonists (Ariel and Daw, 1982a; Chiao and Masland, 2002a; He and Masland, 1997; Kittila and Massey, 1997b), as do the inhibitory inputs (Fried et al., 2005a). Furthermore, while a low dose of 750 nM NBQX does not completely block all of the inputs to the DSGC, our results (data not shown) and others have demonstrated that higher concentrations (5-10μM) NBQX do abolish the entire fast transient component of the light response, which is the directional component of the light response Linn, 1991; Taylor, 1995; Peters, 1996; Petit-Jacques, 2008; Petit-Jacques, 2005). These arguments rule out the possibility that the directional excitatory inputs are mediated by cholinergic receptors on the SBAC.

The only remaining source for the directional excitation is the bipolar cell, as there are no other known glutamatergic neurons that could make contact with the SBAC. While we do not have a complete understanding of the mechanism

that shapes excitatory input to the SBAC at the bipolar cell, it is likely that the mechanism involves feedback at the bipolar cell terminal.

Implications for Direction Selectivity

Prior to our report, it had been assumed that the SBAC was the first point where direction selectivity arose in the retinal direction selective circuit. Regardless of how the directional signal is first generated it is clear that the SBAC responds directionally to light stimulation (Euler et al., 2002b; Hausselt et al., 2007; Lee and Zhou, 2006) and its role as the source of directional GABA input to the DSGC is crucial to retinal direction selectivity (Amthor et al., 2002; Fried et al., 2002a; Yoshida et al., 2001). Our work provides another description of the directional signals in the SBAC and provides insight into how the SBAC integrates and processes the directional input it receives. From this work it is clear that not only is the amplitude of the SBAC response is directional, but also the time course of the response. For centripetal motion the 10% to 90% rise time in response to centripetal motion was over 200 ms slower than for centrifugal motion which had an average rise time of ~ 40 ms. This directional difference in rise time could have important implications for SBAC functionality. In particular, we describe evidence suggesting that the SBAC expresses TTX-R sodium currents and demonstrate that TTX-R sodium currents boost the directional asymmetry in the SBAC, this implies that these channels must be able to discriminate between directions based on one of these asymmetries.

Our observation that ambroxol hydrochloride, a TTX-R selective sodium channel blocker (Weiser and Wilson, 2002) blocks an inward depolarization activated current suggests that one or more TTX-R sodium channel must be expressed in the SBAC and contributing to the SBAC response. Recent work from Obrien et al (2008) showed that some retinal amacrine and ganglion cells have show staining to the tetrodotoxin-resistant sodium channel type Na_V 1.8 antibody. Interestingly some sub-populations of Na_V 1.8 reactive amacrine cell colocalize with both GABA and Ach reactivity, indicating that this population of amacrine cells is likely the SBAC. Na_V 1.8 is an unusual sodium channel, both in its pharmacological profile as well as its activation and inactivation kinetics. While it is largely insensitive to the classical sodium channel blocker TTX and also to QX-314, it is blocked by ambroxol hydrochloride with a sensitivity three times greater than TTX sensitive channels. Na_V 1.8 channels are kinetically distinct from TTX-sensitive sodium channels as they have slower activation and inactivation kinetics, a more depolarized activation threshold, and a more depolarized steady state activation and inactivation curves. The time course of inactivation for Na_V 1.8 is approximately 5 ms, compared to a 0.5 ms inactivation at 0mV for a typical fast TTX sensitive current. Na_V 1.8 also has a more depolarized half maximal activation value of approximately -15 mV compared to -27.6 to -40 mV for TTX-sensitive currents (Cummins and Waxman, 1997; Elliott and Elliott, 1993; Ogata and Tatebayashi, 1993). The unique kinetics may make Na_V 1.8 well suited to take advantage of the directional differences in peak amplitude and rise time between centrifugally centripetally evoked synaptic inputs. The involvement of TTX-

resistant sodium channels in sharpening the directional response of the SBAC light response represents a previously undescribed mechanism involved in the direction selective circuit. In addition, this work describes a new physiological role for TTX-resistant sodium channels in information processing in the nervous system.

Multiple mechanism shape SBAC directional signaling

Our conclusion that synaptic input into SBAC is itself directional and that TTX-R sodium channels boost these directional inputs do not exclude the results of recent reports from Lee et al, (2006), Haussult et al, (2007), or Gavrikov et al (2006), which all proposed different mechanisms within the SBAC or SBAC-SBAC network to account for the directional signals in the retina. While there are key differences between our data and the results from these other groups, there is nothing in their data that would exclude the possibility of a directional excitatory input from bipolar cells. It is entirely plausible that there are multiple mechanisms at work in the SBAC which contribute to and sharpen the directional output of the cell. The mechanism of direction selectivity in the retina has been repeatedly shown to be robust over a broad range of stimulus conditions as well as a broad range of pharmacological manipulations, so it is not surprising that multiple mechanisms would contribute to the mediation of the directional GABA signal by the SBAC, which is a crucial step in the extraction of directional information in the direction selective circuit. While we did not find evidence for all of the proposed mechanism contributing to the directional responses that have ben previously

proposed, it is possible that there are differences in our preparations that do not emphasize all possible mechanisms contributing to SBAC DS. Nevertheless, our results clearly demonstrate two novel mechanisms that shape the directional responses of the SBAC.

Methods

Tissue Preparation and Maintenance

Experiments were conducted in accordance with protocols approved by the Institutional Animal Care and Use Committee at OHSU and NIH guidelines. Dark-adapted, out-bread pigmented rabbits were surgically anesthetized and the right eye removed under dim-red illumination. The animal was then killed by anesthetic overdose. All subsequent manipulations were performed under infrared illumination (>900nm). The anterior portion of the eye was removed, the eyecup transected just above the visual streak, and the dorsal piece discarded. The retina was dissected from the sclera, and a 5 by 5 mm section of central retina was adhered, photoreceptor-side down, to a glass cover-slip coated with poly-L-lysine (Sigma) or Cell-Tak (Becton Dickinson GmbH, Germany). The preparation was placed in a recording chamber (~0.5 ml volume) and continually perfused (~4 ml/min) with oxygenated bicarbonate-buffered Ames medium (Ames and Nesbett, 1981), pH 7.4 maintained at 34–36 ºC. The major electrolytes in Ames medium are (mM): 120 NaCl, 23 $NaHCO_3$, 3.1 KCl, 1.15 $CaCl_2$ and 1.24 $MgCl_2$. Pharmacological agent were dissolved in oxygenated Ames media and perfused through the recording chamber identically to the control Ames solution.

Electrophysiology and Light Stimulation

Patch electrodes were pulled from borosilicate glass to have a final resistance of 4–8 MΩ. For extracellular recording, the electrodes were filled with Ames medium. For intracellular recording, the electrodes were filled with the following electrolytes: 110 mM Cs-methylsulfonate, 10 mM NaCl, 5 mM Na-HEPES, 1 mM K-EGTA, 1 mM Na-ATP, 0.1 mM Na-GTP. Retinal neurons were visualized using differential infrared differential interference contrast microscopy. ON starburst amacrine cells SBACs were targeted based on their location in the ganglion cell layer and their comparatively small round somas. Prior to patching onto the SBAC we made a small hole in the inner limiting membrane near the cell soma, through which the patch electrode applied to the cell. The SBACs identity was confirmed by its physiological response characteristics, which included a high variance noise consisting of large fast inward currents a biphasic light response with a fast transient component, a sustained component, and a characteristic decrease in noise at light termination was also a identifying characteristic. For ganglion cells we targeted cells with a medium soma diameter and a crescent-shaped nucleus (Vaney, 1994b). The extracellular electrode was applied to the soma under visual control through a small hole in the overlying inner limiting membrane, and a loose patch recording was formed. After establishing that the ganglion cell was a DSGC and determining its preferred direction (see below), the extracellular recording electrode was removed and an intracellular patch-electrode applied to the same cell. During whole cell recordings current signals

were filtered at 4kHz through the 4-pole Bessel filter of the EPC10 dual amplifier (HEKA Elektronics, Canada), and digitized at 10-50kHz.

Light stimuli, generated on a mini-CRT computer monitor (MicroBright-Field, Inc, refresh rate, 60 Hz), were focused onto the photoreceptor outer segments through a 20x (NA 0.95) Olympus water-immersion objective. The percent stimulus contrast was defined as $C=100 \times (L-L_{mean})/L_{mean}$, where L is the stimulus intensity and L_{mean} is the background intensity. For SBAC stimulation the standard moving stimulus consisted of two 150 x 900µm bars moving along their long axis in opposite directions at 900µm/s. Each bar covered an opposing half of the SBAC dendritic field. For centrifugal motion, the rectangle moved along its long axis from behind a mask into the SBAC receptive field so that its leading edge first appeared 75 µm from the center of the soma, until its trailing edge had traversed 450 µm from the center of the soma. For centripetal motion the bar entered the field 450 µm from the cell soma and drifted along the long axis until it has passed completely behind the mask beginning 20µm from the cell soma. The contrast of the bar was set to 100%. For DSGCs the standard moving stimulus comprised a light or dark bar, moving along its long axis at 800–1200 µm/s on the retina, and traversed the entire width of the stimulation field. The bar's width was 250µm, and its length was set to achieve a 1-2 second separation of the leading- and trailing-edge responses. All light stimuli were centered with respect to the tip of the recording electrode, and thus also with the soma of the target cell. The stimulus area was limited by the size of the CRT monitor, and covered a circular region 0.7 mm in diameter. Since the dendritic extents of SBAC and

DSGCs receptive fields range from 200µm t0 300µm for SBACs (Peters and Masland, 1996a; Taylor and Wässle, 1995b) to 400 µm for DSGCS (Vaney, 1994b), they were fully contained within the stimulus area.

Analysis

For SBACs the magnitude of the directional asymmetry was calculated using an asymmetry index which ranged from 0 to 1, with values closer to one indicating a stronger asymmetry. For voltage and current measurements we defined AI = (CF-CP)/(CF+CP), so that a positive index means that centrifugal motion is preferred. For rise time the AI was defined as AI = (CP-CF)/(CF+CP), so that a positive index indicates that centrifugal motion is faster. For DSGCs, the preferred direction of the cells and the strength of the directional tuning were calculated from responses to stimuli in each of 12 stimulus directions evenly spanning 360 degrees. Responses were represented as vectors with the angle representing the direction of stimulus motion, and length equal to the number of action potentials or the peak amplitude of PSPs. The preferred direction was obtained from the angle of the resultant vector, which was the the vector sum of all 12 responses. The directional tuning index (DSI) was calculated as the normalized length of the resultant vector. DSI can range from 0, when the magnitude of the response is the same in all stimulus directions, to 1, for perfect tuning when a response is produced only for a single stimulus direction (Taylor and Vaney, 2002). The directional tuning data in figures 5a and b is well described by a von Mises distribution, which is the circular analogue to the Gaussian distribution. The re-

sponse R, as a function of stimulus direction is given as, $R=R_{max}\ e^{(\kappa\ cos((x-\mu)\pi/180))}/e^{\kappa}$, where R_{max} is the maximum response, μ becomes the preferred direction in degrees, and κ is the concentration parameter, which accounts for the width of the directional tuning.

Conductance was calculated using methods previously described by Borg-Graham (2001) and Taylor and Vaney (2002). Briefly light evoked synaptic currents were assumed to arise from either excitatory synaptic inputs, being mediated by a non-selective cation current with a reversal potential, V_e = 0 mV, or through inhibitory synaptic currents being mediated by chloride reversal potential with a reversal potential, V_i = -69 mV based on our internal and external recordings solutions. The currents resulting from these currents obey Ohm's law so that $I_e = g_e(t)(V - V_e)$, and $I_i = g_i(t)(V - V_i)$, where the inhibitory, $g_i(t)$ and excitatory, $g_e(t)$ conductances are functions of time. If we assume that the cell is isopotential so that synaptic currents sum linearly, the totally light evoked synaptic current is, $I_T = g_T(t)(V - V_t(t))$. Therefore, the observed reversal potential $V_r(t)$ is the sum of V_e and V_i so, $V_r(t) = (g_e(t\ ) / g_T(t))V_e + (g_i(t) / g_T(t))V_i$. By rearrangement excitatory and inhibitory synaptic conductances can be separated out according to the equations: $g_e(t) = (g_T(t)(V_r(t) - V_i)) / (V_e - V_i)$ and $g_i(t) = (g_T(t)(V_r(t) - V_e)) / (V_e - V_e)$. To collect the data necessary to calculate the synaptic conductance we presented centrifugal or centripetal (or preferred or null) stimuli while holding the cell at command voltages ranging between -100 mV and 0 mV by increments of 20 mV. We then calculated IV relations for points every 10 ms and baseline leak conductance to isolate the light evoked changes in current. Each IV was fit with a

line between -100 mV and -40 mV where the IV relation was most linear. The slope g_T and intercept V_r were determined from the fit equation, thus producing a discrete measurement for g_T and V_r at every point.

Analysis was performed using custom procedures in IgorPro (Wavemetrics, USA). To obtain average values for peak amplitudes and rise times, individual traces were filtered using a gaussian filter with a 20 Hz cutoff to eliminate the high variance noise associated with the SBAC. Unless otherwise noted, the mean ± standard deviation is quoted throughout the paper. Significance values for comparing pharmacological manipulations to control were generated using the paired t-test, significance was considered to be $p<0.05$.

CHAPTER 4: DISCUSSION

I conclude from the results of the experiments presented in Chapter Two of this thesis, that the direction selective ganglion cell initiates action potentials at multiple spike initiation zones in its dendrites and that these dendritic spikes propagate to the soma to signal local directional synaptic input in its dendrites. Dendritic spikes initiate somatic spikes and the directional information is passed to the brain via the DSGC axon. Dendritic spikes enhance the directional tuning of the DSGC particularly for weak stimuli and movements that cover only portions of the DSGC receptive field, and they provide a substrate for local computations to take place in the dendrites.

From the second study presented in this thesis, I conclude that the directionally asymmetric responses of SBACs are the result of directional excitatory synaptic inputs indicating that directional selectivity is generated presynaptically to the SBAC itself. From these data, I also conclude that the SBAC does play a role in enhancing the directional differences in the synaptic input it receives, by using tetrodotoxin-resistant voltage-gated sodium channels to threshold the difference between synaptic input and selectively boost the response for centrifugal direction over centripetal motion. Furthermore, I conclude that the source of the directional difference in inputs, must be in a non-linearity of transmitter release from bipolar cell terminals during centrifugal motion.

These conclusions represent significant advancements in our understanding of the direction selective circuit of the retina and fill two important gaps in our knowledge about the mechanism of retinal direction selectivity. The first gap in knowledge regards our understanding about how synaptic inputs are integrated in the DSGC and signal motion to the brain via the cells spiking mechanism. The second gap in our understanding regards our understanding of the specific mechanism that generates directional inhibitory input, which has been shown to be crucial to obtaining directional responses in the DSGC. In the next sections I will individually outline the key disparities in our understanding of the retinal direction selective mechanism and explain how the work presented in this thesis fills in our knowledge regarding these previously unresolved questions.

Directional subunits in the DSGC

The first deficiency in our understanding of the direction selective mechanism, stems from the observation that the DSGC receptive field is composed of directionally selective subunits that can be independently activated, and contain all the necessary circuitry components to make them fully directionally selective (Barlow and Levick, 1965a). This indicates that the functional unit of direction selectivity in the DSGC is smaller than the receptive field. By most estimates it is approximately 5 to 10% of the size of the receptive field, although one account suggests that it is much smaller than that (Grzywacz et al., 1994). This work has also revealed that these directional subunits are repeated over the entire receptive field, with one exception, the non-DS zone of the DSGC receptive field (Barlow and Levick, 1965a; Grzywacz et al., 1994; He et al., 1999a). As de-

scribed in Chapter One, the non-DS zone is located on the preferred side of the receptive field and encompasses approximately 20-25% of the receptive field area. Aside from this non-DS region, it appears that directional subunits are evenly distributed throughout the remainder of the DSGC receptive field. The most parsimonious explanation for the existence of these directional subunits is that the directional computation takes place in the DSGC dendrite over a small portion of the cells receptive field. Numerous mechanisms that could account for local and repeatable directional subunits of direction selectivity computed in the dendrite of the DSGC have been proposed, and most of these models favores an interaction between excitation and shunting inhibition (Barlow and Levick, 1965a; Koch et al., 1982; Koch et al., 1983; Torre and Poggio, 1978). This post-synaptic model to explain direction selectivity was widely favored, until analysis of the light-evoked synaptic conductances during preferred and null direction motion indicated that the synaptic inputs to the DSGC were already directional (Borg-Graham, 2001a; Taylor and Vaney, 2002).

Presynaptic models of direction selectivity provided an attractive alternative to post-synaptic models based on shunting inhibition, because in the shunting inhibition models the effectiveness of inhibition to discriminate motion direction was highly dependent on stimulus conditions and often could not reproduce robust directional selectivity over a wide range stimulus conditions (Grzywacz and Koch, 1987; Koch et al., 1983; Torre and Poggio, 1978). In addition, the experimental evidence that directional signals arise in the retinal circuitry prior to the DSGC is now considerable (Borg-Graham, 2001a; Fried et al., 2002b; Fried

et al., 2005b; Taylor and Vaney, 2002). Since the initial demonstration of the involvement of a pre-synaptic mechanisms for directional selectivity, much less consideration has been given to synaptic integration of inputs in the DSGC. In presynaptic models of direction selectivity the role of the DSGC is relegated to implementing a typical thesholding non-linearity. Though much less theoretical modeling has been done on a strictly presynaptic mechanism for direction selectivity, it should be obvious that this simple presynaptic model coupled with a point neuron integrator cannot account for the observed behavior of the neuron.

The limitation of the point neuron model for direction selectivity lies in the limited dynamic range that a single spike threshold is capable of encoding. Inputs causing a PSP up to a certain value should increase the directionality of the signal; however, saturation at the spiking mechanism will then decrease the directional output for larger inputs, and limit the dynamic range that the neuron is capable of encoding. Given the limited range over which a single spike threshold can operate it is difficult to image how a point neuron model could account for robust direction selectivity over an extremely wide range of stimulus intensities and conditions. Its is well established that direction selectivity is robust within discrete directional subunits in the DSGC receptive field (Barlow and Levick, 1965a; Grzywacz et al., 1994; He et al., 1999a). A single spike generating mechanism would have to effectively discriminate preferred null differences in synaptic inputs under conditions when only 5 to 10% of the inputs are activated and under conditions when 100% of the synaptic inputs are activated. According to Gryzwacz et al, (1994), discrimination may occur with as little as 0.25 to 0.5% of the synaptic

inputs. The demands placed on the spike generating mechanism in the DSGC by the requirement to discriminate synaptic differences over such a broad range of input conditions raises suggest a more complicated model of action potential thersholding than has currently been considered.

In this thesis, I present data that shows that the axo-somatic spike generating mechanism of the DSGC operates over a narrower range than light evoked spiking appears to be encoded. This axo-somatic spike threshold is not sufficient to account for the robust light evoked directional spiking observed in the DSGC. Furthermore, the spike axo-somatic spike threshold we measured at the soma with experimental current injection did not accurately match the distribution of spike thresholds that we observed in response to light evoked synaptic input, with the threshold distribution being narrower and more depolarized than we measured for spikes evoked by the light activated synaptic circuitry. We discovered that this discrepancy could be accounted for by the existence of dendritically initiated action potentials that propagate to the soma and initiate the axo-somatic spike threshold, and we concluded that the dendritic spike spike generating mechanism represents the critical threshold that signal light evoked synaptic information in the cell. In addition, we provided evidence that these dendritic spike were sodium based action potentials and were dependent on voltage-gated sodium channels located in the dendrites.

The primary evidence for the existence of dendritic action potentials comes from the observation that small spikelets are observed when the axo-somatic spiking mechanism is attenuated or blocked by the local application of

TTX. There are a few alternative explanations for the identity of these spikelets that have been discussed in depth in the discussion in Chapter 2. Briefly, spikelets could represent attenuated axo-somatic spikes. We do not believe this to be the case, because under some conditions both full spikes and spikelets could be observed and their amplitudes, clearly had a bimodal distribution, indicating that two distinct populations of spikes exist. Furthermore, this distribution of spike amplitudes was observed in response to both local application of TTX to the soma, as well as during hyperpolarizing current injection, which should have the similar effect of blocking the axo-somatic spike generating mechanism, but through a different mechanism. A second alternative explanation for dendritic spikes is that they represent full action potentials in neighboring DSGCs that are electrically coupled to the DSGC (Vaney, 1994a). We do not believe this to be the case because only one-quarter of DSGCs are coupled to each other, yet we observed spikelets in every DSGC we examined. Furthermore, the population of coupled DSGCs is thought to correspond to one of the four directions of DSGC, and we observed spikelets in all four populations of DSGCs.

It is worth noting that another report has observed spikelets in DSGCs. Jensen and DeVoe (Jensen and De Voe, 1983), described multiple spike amplitudes during sharp electrode recording from the DSGC; however, they attributed the reduced amplitude spikelets to action potetials initiated in the initial segment of the DSGCs that failed to invade the soma and trigger a somatic action potential. It seems likely that their work and ours describes the same phenomena, as we observed that under some current-clamp recording conditions we observed

spikelets, even in the absence of TTX application. We attributed this phenomena to the current-clamp recording depressing the resting membrane potential below its natural value, or to some other reduction in the axo-somatic spike generating mechanism caused by whole-cell current clamp recording. It seems likely that under sharp electrode recording conditions Jensen and DeVoe could be experiencing a similar phenomenon. Furthermore, though they did not quantitate the distribution of sizes of spikes, it appears from the traces presented in their report that the amplitudes would show a similar bimodal distribution to what we reported. Given the similarity between their basic observation and ours, it is reasonable to ask if their explanation of spikelets could account for our observations as well. We do not believe this to be the case, because when we apply TTX to the soma to locally block somatic spikes we cannot precisely control the extent of TTX diffusion. The axonal hillock of the DSGC is located well within the region that we presume to experience a blocking concentration of TTX (a maximum of 30-50μm) (Boiko et al., 2001; Van Wart et al., 2007). Therefore, it is not likely that TTX could have a differential affect on the initial segment and the axon spike generators. Therefore, the extent of spread of TTX during conditions that selectively reveal spikelets argues against Jensen and DeVoes hypothesis that DSGC spikelets are axonal spikes observed in the absence of a somatic spike. In fact, we believe we cannot distinguish between blocking axonal and somatic spikes we have taken to refereeing to large spikes blocked by local TTX application to the soma as axo-somatic spikes.

The discovery of dendritic spiking in DSGCs has important implications for understanding the mechanism of directional signaling in the retina. Prior to our investigations it was not clear how a presynaptic model of direction selectivity could be reconciled with the well-founded observations of directional subunits (Barlow and Levick, 1965b; Grzywacz et al., 1994; He et al., 1999b) and still encode robust directional tuning over a wide range of stimulus characteristics (Barlow and Levick, 1965a; Grzywacz et al., 1994; He et al., 1999a). Prior to our description of dendritic action potentials to signal directional light information in the DSGC, this discrepancy had not been given serious consideration.

While our observations published in Oesch et at, 2005, provides an attractive resolution to the discrepancy in the integrative properties of the DSGC, it left open two alternative means that dendritic action potentials could signal directional information in the retina. One possibility is that thresholding takes place at the local spike initiation zone and the dendritic spike is the result of the non-linear discrimination between preferred and null direction synaptic inputs, by the spike generating mechanism. In this model, spikes are only initiation in the preferred direction based on the difference in synaptic input between the two directions. An alternative hypothesis makes use of the properties of shunting inhibition described by (Koch et al., 1982; Koch et al., 1983), which suggested that inhibition could effectively shunt a propagating action potential if it was sufficiently large and located “on the path”. In this model, excitatory input would evoke dendritic spikes for all directions of motion, and asymmetric inhibition would cause spike failure when the inhibition fell between the spike initiation zone and the soma, the

result being that spikes initiated during null direction movement would fail to reach the soma and initiate a somatic spike, thus accounting for the observation of directional spiking in the DSGC. The simplest way to test between these two possibilities would be to record from the dendrite at the sight of action potential generation in the DSGC and determine if dendritic action potentials are initiated only for preferred directions, or for all directions. Because the dendrites of the DSGC branch quickly to very fine diameters, electrical recording from the DSGC dendrites is not possible. Therefore, to discriminate between these two possibilities, we created a biophysical compartmental model of the DSGC in collaboration with the lab of Dr. Robert Smith and the University of Pennsylvania. To generate the model, I recorded DSGC morphologies using multi-photon microscopy from dye filled physiologically identified DSGCs. These morphologies were entered into a computational model of the DSGC by Mike Schacter in Dr. Smiths laboratory using NeuronC, a computational modeling program of the retina developed by Dr. Smith (Smith, 1992). As described in the results of Chapter 2, the model indicated that dendritic action potentials are initiated only during preferred direction stimuli. Furthermore, we demonstrated that under no physiological conditions of inhibition could dendritic spikes be attenuated so that they were not visible at the soma, on the path inhibition that was artificially larger (50 to 80 nS). These data taken together strongly argue against the dendritic spike failure model of directionally selective dendritic action potentials. It is interesting to note the discrepancy between the results from our physiologically calibrated model and other modeling results from Koch et al (1983). A major difference between our model

and theirs is that in their model the dendrites were endowed with strictly passive properties, though they did suggest that their rule would hold true for an actively propagated action potential. Another key difference is the level of complexity in compartmental morphology of the two models. Our model consisted of a significantly more complex morphology with many more biophysical compartments. Furthermore, we calibrated the spiking behavior of the cell for each specific morphology. This suggests that the complement between morphology and spiking behavior may function to make action potential propagation significantly more robust than in a generic model.

Directional Signaling by the SBAC

The second major shortcoming in our understanding of the direction selective mechanism of the retina regards the mechanism that generates directional responses in the SBAC. As previously described, directional signals are computed in the retinal circuitry prior to the DSGC, and the SBAC represents the most likely presynaptic inhibitory parter to the DSGC. The SBAC responds to directionally to motion along its radial axis and multiple mechanisms have been proposed to explain the ability, yet, to date experimental evidence is contradicory and incomplete (Gavrikov et al., 2006; Hausselt et al., 2007; Lee and Zhou, 2006), see Chapter 1).

There are several discrepancies in the literature, but they can be divided into a few key contentious issues. First, is the mechanism of direction selectivity self contained within the SBAC dendrite (Gavrikov et al., 2006; Hausselt et al., 2007; Tukker et al., 2004) or is it generated through synaptic interaction with

other cells (Borg-Graham and Grzywacz, 1992; Lee and Zhou, 2006). A second disagreement in the literature regards the involvement of GABAa inhibition in generating the directional signal. Gavrikov et al, (2003; 2005) suggest that GABAa inputs are key, though the asymmetry lies in the choliride reversal potential in the dendrites and not in the GABA inputs themselves. Lee and Zhou, (2006) also provide evidence that GABA is involved in shaping directional SBAC responses; however, in contrast to Gavrikov et al, they suggest that GABA input is itself asymmetric at distal locations in the dendrite. In contrast, Tukker et al (2004), suggested a theoretical construct that did not depend on inhibition to generate asymmetric responses in the SBACs distal dendritic tips and more importantly Hausselt et al (2007) presented data showing that SBAC asymmetry persisted in the presence of GABA blockade and was independent of GABAergic transmission. This is in direct contradiction to Lee and Zhou, who reported the opposite observation, that the asymmetry was reduced or abolished in the presence of GABA blockade. Given wide disparity of results, it is difficult to conclude anything about the mechanism generating SBAC DS other than to observation that the SBAC responds differentially between centrifugal and centripetal motion. It is important to note that the conclusion that the SBAC actually generates direction selectivity itself does not follow from the observation that it responds directionally to different stimuli. There is a possibility that the SBAC does not generate directional responses, but instead receives directional inputs and its responses merely reflect these directional inputs, or perhaps sharpens the directional responses, as is the case for the DSGC (Oesch et al., 2005b).

In Chapter Three of this thesis, I present data demonstrating that the inputs to the SBAC are themselves directional, and that the SBAC employs TTX-R VGSCs to enhance the directional difference in its inputs. Furthermore, the data demonstrates that the directional signals recorded in the SBAC remain directional in the presence of GABAa antagonists. From these data I conclude that the SBAC is not the primary source of directional signaling in the retinal direction selective circuit, but simply enhances a directional synaptic input. In regards to the controversy of a dendrite autonomous mechanism for direction selectivity, my data points to a mechanism located within the dendrite of the SBAC that sharpens directional responses to directional input, as opposed to a mechanism based on GABAergic connections with other neurons, though it is important to note that this differs significantly from the suggestion that DS itself arises within the dendrite. Furthermore, it is important to note that the dendritic mechanism that I conclude to sharpen direction selectivity in the SBAC differs significantly from the mechanism Hausselt et al (2007) proposed generated the directional signals. These differences are described in detail in Chapter Three, but briefly, Hausselt et al proposed that a synergistic interaction between a dendritic voltage gradient generated by a tonic AMPAegic input and a voltage-gated calcium channel in the dendrite generated directional signals in SBAC. In contrast, I found the directional asymmetry was not dependent on the tonic AMPAergic leak, postulated to generate the voltage-gradient in the Hausselt et al model. Furthermore, the directional differences were not dependent on low doses of cadmium ions, which have

previously been proposed to selectively block some of the high-voltage activated VGCCs in the SBAC (Hausselt et al., 2007; Jensen, 1995b)

While I conclude that the directional signal in the retina is not generated in the SBAC, I cannot draw any conclusions from the data about the mechanism for generating the direction selective inputs, other than to suggest that it must arise in the bipolar cell terminals. While the idea of directional output of bipolar cells has been viewed with skepticism by some, it has long been postulated to explain directional excitatory input to the DSGC (Barlow and Levick, 1965a). The idea gains support from the observation that excitatory input to the DSGC is directional. For a majority of the history of the retina DS circuit, it was assumed that directional excitation came from nicotinic inputs to the DSGC; however, more recently the role of Ach as an excitatory neurotransmitter has been called into question, based on the observation that blockade of nicotinic receptors has a limited effect on excitatory synaptic inputs (Fried et al., 2005b). Furthermore work presented in this thesis suggests that all of the excitatory inputs to the DSGC are mediated by glutamatergic input. Therefore, it follows that transmitter release from bipolar cells must be made directional by some means, and it seems likely that the mechanism could be conserved between bipolar cell terminals synapsing onto SBACs and DSGCs. Many ultrasructural studies of synapses onto the DSGC reveal evidence to suggest a mechanism that could modulate the output of bipolar cell synapses onto DSGCs. This includes amacrine cell processes making synapses onto bipolar cell terminals that are presynaptic to both DSGCs and SBACs. it is clear that non-SBAC amacrine cells are involved in this ar-

rangement there is some controversy as to whether SBAC terminals synapse onto bipolar cell terminals (Brandon, 1987a; Famiglietti, 1991). More detailed ultra-structural examination of the synaptic inputs to DSGCs that had their preferred direction physiologically identified, revealed synaptic structures involving complex serial synapses terminating on bipolar cell dendrites or DSGC dendrites, and complexes of reciprocal synapses between amacrine and bipolar cell terminals. The authors of the paper concluded that these complicated structures showed an asymmetry along the preferred and null axis of the DSGC and comprised a putative mechanism for shaping directional synaptic inputs to the DSGC (Dacheux et al., 2003)

Though SBACs have been shown to receive synaptic input over the entire range of their dendrites, our recordings from SBACs during stimulation with a moving stimulus showed that the synaptic input to the SBAC is concentrated within a duration of time that corresponds to movement of the stimulus over only a portion of the dendritic field. In fact, the rise time of the currents were only slightly longer than for a full field static stimuli in which all the inputs should be activated simultaneously. This violates the default expectation that inputs will be activated sequentially over the entire time course that the stimulus traverses the cells receptive field. In contrast, during centripetal stimulation inputs appeared to be activated sequentially as the stimulus moved across the receptive field, though during centripetal motion the cell did appear to integrate inputs over a distance larger than expected based on the average receptive field of the SBAC. This suggests that inputs in the centrigual direction may be somehow synchro-

nized to release at a coordinated time point, instead of being sequentially activate. Though it is unclear how this mechanism might operate, future investigation should focus on systems that satisfy this requirement.

As discussed in Chapter 3 there is strong evidence to suggest that a significant portion of the ambroxol sensitive effect in reducing SBAC directionality is mediated by the tetrodotoxin-resistant sodium channel NaV 1.8, which has unique kinetic properties compared to most common VGSCs that are typically involved in action potential initiation and propagation (for review see, (McCleskey and Gold, 1999, 1999; Waxman et al., 1999). As one key difference in the responses evoked between centrifugal and centripetal motion is the time to peak of the rising phase of the response. Having substantially slower activation and inactivation kinetics (Elliott and Elliott, 1993; Kostyuk et al., 1981), as well as a significant slow inactivation component (Fazan et al., 2001; Ogata and Tatebayashi, 1993; Rush et al., 1998), I postulate that the unique kinetics of Nav 1.8 may be well suited to take advantage of this difference in rise time. It is well known that the action potential threshold is dependent on the slope of the depolarizing potential (Calvin, 1974; Schlue et al., 1974; Stafstrom et al., 1984; VALLBO, 1964), due to the gating kinetics of sodium and potassium channels (HODGKIN and HUXLEY, 1952a; HODGKIN and HUXLEY, 1952b; Noble and Stein, 1966; Regehr et al., 1992) and that this dynamic regulation of action potential threshold can have physiologically relevant consequences for information coding and neural computation in the brain (Azouz and Gray, 2000; Azouz and Gray, 2003; de Polavieja et al., 2005; Henze and Buzsáki, 2001; McGinley and Oertel, 2006).

Given the role of sodium channel kinetics in regulating sodium current in response to voltage it seems reasonable to postulate that the ambroxol sensitive sodium current in the SBAC may be differentially activated based on the difference in rise time between centrifugal and centripetal stimulation; however, more careful theoretical studies should be carried out to determine if the kinetics of the TTX-R sodium channels could read out this difference.

Future Directions

The results of this thesis point to several key questions worth examining in further detail. The observation of dendritic action potentials in the DSGC, raises the need for further investigation of the properties and patterns of initiation of dendritic spikes by direct observation through direct dendritic recording or optical voltage recording. The observation that the synaptic inputs to the SBAC are already directional, raises the question of the mechanism that shapes directional excitatory input to the SBAC as well as the DSGC. Finally, the observation that TTX-resistant sodium channels boost the directional differences in SBAC inputs raises the question of how the kinetics of the TTX-resistant sodium channels could selectively boost directional differences in synaptic input

REFERENCES:

Ames, A. I., and Nesbett, F. B. (1981). In vitro retina as an experimental model of the central nervous system. Journal of Neurochemistry *37*, 867-877.

Amthor, F., and Grzywacz, N. (1991). Nonlinearity of the inhibition underlying retinal directional selectivity. Vis Neurosci *6*, 197-206.

Amthor, F. R., and Grzywacz, N. M. (1993). Inhibition in ON-OFF directionally selective ganglion cells of the rabbit retina. J Neurophysiol *69*, 2174-2187.

Amthor, F. R., Keyser, K. T., and Dmitrieva, N. A. (2002). Effects of the destruction of starburst-cholinergic amacrine cells by the toxin AF64A on rabbit retinal directional selectivity. Vis Neurosci *19*, 495-509.

Amthor, F. R., and Oyster, C. W. (1995). Spatial organization of retinal information about the direction of image motion. Proc Natl Acad Sci U S A *92*, 4002-4005.

Amthor, F. R., Oyster, C. W., and Takahashi, E. S. (1984). Morphology of on-off direction-selective ganglion cells in the rabbit retina. Brain Research *298*, 187-190.

Amthor, F. R., Takahashi, E. S., and Oyster, C. W. (1989). Morphologies of rabbit retinal ganglion cells with complex receptive fields. J Comp Neurol *280*, 97-121.

Ariel, M., and Daw, N. W. (1982a). Effects of cholinergic drugs on receptive field properties of rabbit retinal ganglion cells. Journal of Physiology *324*, 135-160.

Ariel, M., and Daw, N. W. (1982b). Pharmacological analysis of directionally sensitive rabbit retinal ganglion cells. Journal of Physiology *324*, 161-185.

Azouz, R., and Gray, C. M. (2000). Dynamic spike threshold reveals a mechanism for synaptic coincidence detection in cortical neurons in vivo. Proc Natl Acad Sci USA *97*, 8110-8115.

Azouz, R., and Gray, C. M. (2003). Adaptive coincidence detection and dynamic gain control in visual cortical neurons in vivo. Neuron *37*, 513-523.

Barlow, H., Hill, R., and Levick, W. (1964). Rabbit retinal ganglion cells responding selectively to direction and speed of image motion in the rabbit. Journal of Physiology *173*, 377-407.

Barlow, H., and Levick, W. (1965a). The mechanism of directionally selective units in rabbit's retina. Journal of Physiology *178*, 477-504.

BARLOW, H. B. (1953). Action potentials from the frog's retina. J Physiol (Lond) *119*, 58-68.

Barlow, H. B., and Hill, R. M. (1963a). Evidence for a Physiological Explanation of the Waterfall Phenomenon and Figural after-Effects. Nature *200*, 1345-1347.

Barlow, H. B., and Hill, R. M. (1963b). Selective sensitivity to direction of movement in ganglion cells of the rabbit retina. Science *139*, 412-414.

BARLOW, H. B., and HILL, R. M. (1963). Selective sensitivity to direction of movement in ganglion cells of the rabbit retina. Science *139*, 412-414.

Barlow, H. B., and Levick, W. R. (1965b). The mechanism of directionally selective units in rabbit's retina. J Physiol (Lond) *178*, 477-504.

Bennett, M. V., and Zukin, R. S. (2004). Electrical coupling and neuronal synchronization in the Mammalian brain. Neuron *41*, 495-511.

Berger, T., Senn, W., and Luscher, H. R. (2003). Hyperpolarization-activated current Ih disconnects somatic and dendritic spike initiation zones in layer V pyramidal neurons. J Neurophysiol *90*, 2428-2437.

Berridge, M. J. (1998). Neuronal calcium signaling. Neuron *21*, 13-26.

Bloomfield, S. A. (1992a). Effects of tetrodotoxin on receptive fields of amacrine and ganglion cells in the rabbit retina. Ophthalmology and Visual Science *33*, 2407a.

Bloomfield, S. A. (1992b). Relationship between receptive and dendritic field size of amacrine cells in the rabbit retina. J Neurophysiol *68*, 711-725.

Bloomfield, S. A. (1992c). Relationship between receptive field and dendritic field size of amacrine cells in the rabbit retina. Journal of Neurophysiology *68*, 711-725.

Boiko, T., Rasband, M. N., Levinson, S. R., Caldwell, J. H., Mandel, G., Trimmer, J. S., and Matthews, G. (2001). Compact myelin dictates the differential targeting of two sodium channel isoforms in the same axon. Neuron *30*, 91-104.

Borg-Graham, L. (2001a). The computation of directional selectivity in the retina occurs presynaptic to the ganglion cell. Nature Neuroscience *4*, 176.

Borg-Graham, L. J. (2001b). The computation of directional selectivity in the retina occurs presynaptic to the ganglion cell. Nat Neurosci *4*, 176-183.

Borg-Graham, L. J., and Grzywacz, N. M. (1992). A model of the directional selectivity circuit in retina: Transformations by neurons singly and in concert. In Single Neuron Computation (Boston, Academic Press), pp. 347-375.

Borst, A., and Egelhaaf, M. (1989). Principles of visual motion detection. Trends in Neurosciences *12*, 297-306.

Bowie, D., and Mayer, M. L. (1995). Inward rectification of both AMPA and kainate subtype glutamate receptors generated by polyamine-mediated ion channel block. Neuron *15*, 453-462.

Brandon, C. (1987a). Cholinergic neurons in the rabbit retina: dendritic branching and ultrastructural connectivity. Brain Res *426*, 119-130.

Brandon, C. (1987b). Cholinergic neurons in the rabbit retina: immunocytochemical localization, and relationship to GABAergic and cholinesterase-containing neurons. Brain Res *401*, 385-391.

Brivanlou, I. H., Warland, D. K., and Meister, M. (1998). Mechanisms of concerted firing among retinal ganglion cells. Neuron *20*, 527-539.

Brown, S. P., and Masland, R. H. (1999a). Costratification of a population of bipolar cells with the direction-selective circuitry of the rabbit retina. J Comp Neurol *408*, 97-106.

Brown, S. P., and Masland, R. H. (1999b). Costratification of a population of bipolar cells with the direction-selective circuitry of the rabbit retina. J Comp Neurol *408*, 97-106.

Buchner, E. (1984). Photoreception and Vision in Invertebrates, Plenum Press).

Caldwell, J., and Daw, N. (1978). Effects of picrotoxin and strychnine on rabbit retinal ganglion cells: changes in centre surround receptive fields. Journal of Physiology *276*, 299-310.

Caldwell, J., Daw, N., and Wyatt, H. (1978). Effects of picrotoxin and strychnine on rabbit retinal ganglion cells: lateral interactions for cells with more complex receptive fields. Journal of Physiology *276*, 277-298.

Calvin, W. H. (1974). Three modes of repetitive firing and the role of threshold time course between spikes. Brain Res *69*, 341-346.

Chávez, A. E., Singer, J. H., and Diamond, J. S. (2006). Fast neurotransmitter release triggered by Ca influx through AMPA-type glutamate receptors. Nature *443*, 705-708.

Chen, W. R., Midtgaard, J., and Shepherd, G. M. (1997). Forward and backward propagation of dendritic impulses and their synaptic control in mitral cells. Science *278*, 463-467.

Chen, Y. C., and Chiao, C. C. (2008). Symmetric synaptic patterns between starburst amacrine cells and direction selective ganglion cells in the rabbit retina. J Comp Neurol *508*, 175-183.

Chiao, C. C., and Masland, R. H. (2002a). Starburst cells nondirectionally facilitate the responses of direction-selective retinal ganglion cells. J Neurosci *22*, 10509-10513.

Chiao, C. C., and Masland, R. H. (2002b). Starburst cells nondirectionally facilitate the responses of direction-selective retinal ganglion cells. J Neurosci *22*, 10509-10513.

Cohen, E., and Miller, R. (1994). The role of NMDA and non-NMDA excitatory amino acid receptors in the functional organization of primate retinal ganglion cells. In Vis. Neurosci., pp. 317-332.

Cohen, E. D. (2001). Voltage-gated calcium and sodium currents of starburst amacrine cells in the rabbit retina. Vis Neurosci *18*, 799-809.

Cohen, E. D., and Miller, R. F. (1995). Quinoxalines block the mechanism of directional selectivity in ganglion cells of the rabbit retina. Proceedings of the National Academy of Sciences of the United States of America *92*, 1127-1131.

Cohen, E. D., and Miller, R. F. (1999). The network-selective actions of quinoxalines on the neurocircuitry operations of the rabbit retina. Brain Res *831*, 206-228.

Cummins, T. R., and Waxman, S. G. (1997). Downregulation of tetrodotoxin-resistant sodium currents and upregulation of a rapidly repriming tetrodotoxin-sensitive sodium current in small spinal sensory neurons after nerve injury. J Neurosci *17*, 3503-3514.

Dacheux, R. F., Chimento, M. F., and Amthor, F. R. (2003). Synaptic input to the on-off directionally selective ganglion cell in the rabbit retina. J Comp Neurol *456*, 267-278.

de Polavieja, G. G., Harsch, A., Kleppe, I., Robinson, H. P., and Juusola, M. (2005). Stimulus history reliably shapes action potential waveforms of cortical neurons. J Neurosci *25*, 5657-5665.

Demb, J. B. (2007). Cellular mechanisms for direction selectivity in the retina. Neuron *55*, 179-186.

Denk, W., and Detwiler, P. B. (1999). Optical recording of light-evoked calcium signals in the functionally intact retina. Proc Natl Acad Sci U S A *96*, 7035-7040.

Djurisic, M., Antic, S., Chen, W. R., and Zecevic, D. (2004). Voltage Imaging from Dendrites of Mitral Cells: EPSP Attenuation and Spike Trigger Zones. Journal of Neuroscience *24*, 6703-6714.

Dong, C. J., and Hare, W. A. (2002). GABAc feedback pathway modulates the amplitude and kinetics of ERG b-wave in a mammalian retina in vivo. Vision Res *42*, 1081-1087.

Elliott, A. A., and Elliott, J. R. (1993). Characterization of TTX-sensitive and TTX-resistant sodium currents in small cells from adult rat dorsal root ganglia. J Physiol *463*, 39-56.

Euler, T., Detwiler, P. B., and Denk, W. (2002a). Directionally selective calcium signals in dendrites of starburst amacrine cells. Nature *418*, 845-852.

Euler, T., Detwiler, P. B., and Denk, W. (2002b). Directionally selective calcium signals in dendrites of starburst amacrine cells. Nature *418*, 845-852.

Famiglietti, E. V. (1983a). On and off pathways through amacrine cells in mammalian retina: the synaptic connections of "starburst" amacrine cells. Vision Research *23*, 1265-1279.

Famiglietti, E. V. (1983b). 'Starburst' amacrine cells and cholinergic neurons: mirror-symmetric on and off amacrine cells of rabbit retina. Brain Res *261*, 138-144.

Famiglietti, E. V. (1987). Starburst amacrine cells in cat retina are associated with bistratified, presumed directionally selective, ganglion cells. Brain Research *413*, 404-408.

Famiglietti, E. V. (1991). Synaptic organization of starburst amacrine cells in rabbit retina: Analysis of serial thin sections by electron microscopy and graphic reconstruction. Journal of Comparative Neurology *309*, 40-70.

Famiglietti, E. V. (1992). Dendritic co-stratification of ON and ON-OFF directionally selective ganglion cells with starburst amacrine cells in rabbit retina. Journal of Comparative Neurology *324*, 322-335.

Famiglietti, E. V. (2002). A structural basis for omnidirectional connections between starburst amacrine cells and directionally selective ganglion cells in rabbit retina, with associated bipolar cells. Vis Neurosci *19*, 145-162.

Famiglietti, E. V. (2005a). Synaptic organization of complex ganglion cells in rabbit retina: Type and arrangement of inputs to directionally selective and local-edge-detector cells. J Comp Neurol *484*, 357-391.

Famiglietti, E. V. (2005b). Synaptic organization of complex ganglion cells in rabbit retina: type and arrangement of inputs to directionally selective and local-edge-detector cells. J Comp Neurol *484*, 357-391.

Famiglietti, E. V. J. (1983c). 'Starburst' amacrine cells and cholinergic neurons: mirror-symmetric on and off amacrine cells of rabbit retina. Brain Research *261*, 138-144.

Fatt, P., and Katz, B. (1953). The effect of inhibitory nerve impulses on a crustacean muscle fibre. J Physiol *121*, 374-389.

Fazan, R., Jr., Whiteis, C. A., Chapleau, M. W., Abboud, F. M., and Bielefeldt, K. (2001). Slow inactivation of sodium currents in the rat nodose neurons. Auton Neurosci *87*, 209-216.

Fohlmeister, J. F., and Miller, R. F. (1997). Mechanisms by which cell geometry controls repetitive impulse firing in retinal ganglion cells. J Neurophysiol *78*, 1948-1964.

Fried, S. I., Munch, T. A., and Werblin, F. S. (2002a). Mechanisms and circuitry underlying directional selectivity in the retina. Nature *420*, 411-414.

Fried, S. I., Munch, T. A., and Werblin, F. S. (2005a). Directional selectivity is formed at multiple levels by laterally offset inhibition in the rabbit retina. Neuron *46*, 117-127.

Fried, S. I., Münch, T. A., and Werblin, F. S. (2002b). Mechanisms and circuitry underlying directional selectivity in the retina. Nature *420*, 411-414.

Fried, S. I., Münch, T. A., and Werblin, F. S. (2005b). Directional selectivity is formed at multiple levels by laterally offset inhibition in the rabbit retina. Neuron *46*, 117-127.

Fujita, Y. (1968). Activity of dendrites of single Purkinje cells and its relationship to so-called inactivation response in rabbit cerebellum. J Neurophysiol *31*, 131-141.

Gavrikov, K. E., Dmitriev, A. V., Keyser, K. T., and Mangel, S. C. (2003). Cation--chloride cotransporters mediate neural computation in the retina. Proc Natl Acad Sci U S A *100*, 16047-16052.

Gavrikov, K. E., Nilson, J. E., Dmitriev, A. V., Zucker, C. L., and Mangel, S. C. (2006). Dendritic compartmentalization of chloride cotransporters underlies directional responses of starburst amacrine cells in retina. Proc Natl Acad Sci USA *103*, 18793-18798.

Geiger, J. R., Melcher, T., Koh, D. S., Sakmann, B., Seeburg, P. H., Jonas, P., and Monyer, H. (1995). Relative abundance of subunit mRNAs determines gating and Ca2+ permeability of AMPA receptors in principal neurons and interneurons in rat CNS. Neuron *15*, 193-204.

Goldberg, J. H., Tamas, G., and Yuste, R. (2003). Ca2+ imaging of mouse neocortical interneurone dendrites: Ia-type K+ channels control action potential backpropagation. J Physiol *551*, 49-65.

Golding, N. L., and Spruston, N. (1998). Dendritic sodium spikes are variable triggers of axonal action potentials in hippocampal CA1 pyramidal neurons. Neuron *21*, 1189-1200.

Grzywacz, N. M., Amthor, F. R., and Merwine, D. K. (1994). Directional hyperacuity in ganglion cells of the rabbit retina. Visual Neuroscience *11*, 1019-1025.

Grzywacz, N. M., Amthor, F. R., and Mistler, L. A. (1990). Applicability of quadratic and threshold models to motion discrimination in the rabbit retina. Biological Cybernetics *64*, 41-49.

Grzywacz, N. M., and Koch, C. (1987). Functional properties of models for direction selectivity in the retina. Synapse *1*, 417-434.

Gulledge, A. T., Kampa, B. M., and Stuart, G. J. (2005). Synaptic integration in dendritic trees. J Neurobiol *64*, 75-90.

Hassenstein, B., and Reichardt, W. (1951). Funktionsanalyse der Bewegungsperzeption eines Käfers. Naturwissenschaften.

Hausselt, S. E., Euler, T., Detwiler, P. B., and Denk, W. (2007). A Dendrite-Autonomous Mechanism for Direction Selectivity in Retinal Starburst Amacrine Cells. PLoS Biology *5*, e185.

Hausser, M., Spruston, N., and Stuart, G. J. (2000). Diversity and dynamics of dendritic signaling. Science *290*, 739-744.

Hausser, M. L. a. M. (2005). DENDRITIC COMPUTATION.

Hayden, S. A., Mills, J. W., and Masland, R. M. (1980). Acetylcholine synthesis by displaced amacrine cells. Science *210*, 435-437.

He, S., Jin, Z. F., and Masland, R. H. (1999a). The nondiscriminating zone of directionally selective retinal ganglion cells: comparison with dendritic structure and implications for mechanism. Journal Of Neuroscience *19*, 8049-8056.

He, S., Jin, Z. F., and Masland, R. H. (1999b). The nondiscriminating zone of directionally selective retinal ganglion cells: comparison with dendritic structure and implications for mechanism. J Neurosci *19*, 8049-8056.

He, S., and Masland, R. H. (1997). Retinal direction selectivity after targeted laser ablation of starburst amacrine cells. Nature *389*, 378-382.

Henze, D. A., and Buzsáki, G. (2001). Action potential threshold of hippocampal pyramidal cells in vivo is increased by recent spiking activity. Neuroscience *105*, 121-130.

Hidaka, S., Akahori, Y., and Kurosawa, Y. (2004). Dendrodendritic electrical synapses between mammalian retinal ganglion cells. Journal of Neuroscience *24*, 10553-10567.

HODGKIN, A. L., and HUXLEY, A. F. (1952a). A quantitative description of membrane current and its application to conduction and excitation in nerve. J Physiol (Lond) *117*, 500-544.

HODGKIN, A. L., and HUXLEY, A. F. (1952b). Currents carried by sodium and potassium ions through the membrane of the giant axon of Loligo. J Physiol (Lond) *116*, 449-472.

Hoffman, D. A., Magee, J. C., Colbert, C. M., and Johnston, D. (1997). K+ channel regulation of signal propagation in dendrites of hippocampal pyramidal neurons. Nature *387*, 869-875.

Hu, E. H., and Bloomfield, S. A. (2003). Gap Junctional Coupling Underlies the Short-Latency Spike Synchrony of Retinal {alpha} Ganglion Cells. J Neurosci *23*, 6768-6777.

Huguenard, J., Hamill, O., and Prince, D. (1989a). Sodium channels in dendrites of rat cortical pyramidal neurons. Proc Natl Acad Sci U S A *86*, 2473-2477.

Huguenard, J. R., Hamill, O. P., and Prince, D. A. (1989b). Sodium channels in dendrites of rat cortical pyramidal neurons. Proc Natl Acad Sci USA *86*, 2473-2477.

Jack, J. N., D Tsien, RY (1975). Electic Current Flow in Excitable Cells (Oxford, UK, Oxford University Press).

Jensen, R. (1995a). Receptive-field properties of displaced starburst amacrine cells change following axotomy-induced degeneration of ganglion cells. Vis Neurosci *12*, 177-184.

Jensen, R. J. (1995b). Effects of Ca2+ channel blockers on directional selectivity of rabbit retinal ganglion cells. J Neurophysiol *74*, 12-23.

Jensen, R. J. (1999). Responses of directionally selective retinal ganglion cells to activation of AMPA glutamate receptors. Vis Neurosci *16*, 205-219.

Jensen, R. J., and De Voe, R. D. (1983). Comparisons of direction-selective with other ganglion cells of the turtle retina: intracellular recording and staining. J Comp Neurol *217*, 271-287.

Jeon, C. J., Kong, J. H., Strettoi, E., Rockhill, R., Stasheff, S. F., and Masland, R. H. (2002a). Pattern of synaptic excitation and inhibition upon direction-selective retinal ganglion cells. J Comp Neurol *449*, 195-205.

Jeon, C. J., Kong, J. H., Strettoi, E., Rockhill, R., Stasheff, S. F., and Masland, R. H. (2002b). Pattern of synaptic excitation and inhibition upon direction-selective retinal ganglion cells. J Comp Neurol *449*, 195-205.

Jeong, S. A., Kwon, O. J., Lee, J. Y., Kim, T. J., and Jeon, C. J. (2006). Synaptic pattern of AMPA receptor subtypes upon direction-selective retinal ganglion cells. Neurosci Res *56*, 427-434.

Kaneda, M., Ito, K., Morishima, Y., Shigematsu, Y., and Shimoda, Y. (2007). Characterization of voltage-gated ionic channels in cholinergic amacrine cells in the mouse retina. J Neurophysiol *97*, 4225-4234.

Kasuga, A., Enoki, R., Hashimoto, Y., Akiyama, H., Kawamura, Y., Inoue, M., Kudo, Y., and Miyakawa, H. (1993). Optical detection of dendritic spike initiation in hippocampal CA1 pyramidal neurons. Neuroscience *118*, 899-907.

Kasuga, A., Enoki, R., Hashimoto, Y., Akiyama, H., Kawamura, Y., Inoue, M., Kudo, Y., and Miyakawa, H. (2003). Optical detection of dendritic spike initiation in hippocampal CA1 pyramidal neurons. Neuroscience *118*, 899-907.

Kier, C. K., Buchsbaum, G., and Sterling, P. (1995). How retinal microcircuits scale for ganglion cells of different size. J Neurosci *15*, 7673-7683.

Kim, H. G., Beierlein, M., and Connors, B. W. (1995). Inhibitory control of excitable dendrites in neocortex. J Neurophysiol *74*, 1810-1814.

Kim, K. J., and Rieke, F. (2003). Slow Na+ inactivation and variance adaptation in salamander retinal ganglion cells. J Neurosci *23*, 1506-1516.

Kittila, C., and Massey, S. (1997a). Pharmacology of directionally selective ganglion cells in the rabbit retina. J Neurophysiol *77*, 675-689.

Kittila, C. A., and Massey, S. C. (1995). Effect Of On Pathway Blockade On Directional Selectivity In The Rabbit Retina. Journal of Neurophysiology *73*, 703-712.

Kittila, C. A., and Massey, S. C. (1997b). Pharmacology of directionally selective ganglion cells in the rabbit retina. J Neurophysiol *77*, 675-689.

Koch, C., Poggio, T., and Torre, V. (1982). Retinal ganglion cells: A functional interpretation of dendritic morphology. Philosophical Transactions of the Royal Society London Series B *298*, 227-264.

Koch, C., Poggio, T., and Torre, V. (1983). Nonlinear interactions in a dendritic tree: localization, timing, and role in information processing. Proceedings of the National Academy of Sciences USA *80*, 2799-2802.

Koch, C., Poggio, T., and Torre, V. (1986). Computations in the vertebrate retina: gain enhancement, differentiation and motion discrimination. Trends in Neurosciences *9*, 204-211.

Kolb, H. (1977). The organization of the outer plexiform layer in the retina of the cat: electron microscopic observations. Journal of Neurocytology *6*, 131-153.

Kostyuk, P. G., Veselovsky, N. S., and Tsyndrenko, A. Y. (1981). Ionic currents in the somatic membrane of rat dorsal root ganglion neurons-I. Sodium currents. Neuroscience *6*, 2423-2430.

Kwon, O. J., Kim, M. S., Kim, T. J., and Jeon, C. J. (2007). Identification of synaptic pattern of kainate glutamate receptor subtypes on direction-selective retinal ganglion cells. Neurosci Res *58*, 255-264.

Larkum, M. E., Zhu, J. J., and Sakmann, B. (2001). Dendritic mechanisms underlying the coupling of the dendritic with the axonal action potential initiation zone of adult rat layer 5 pyramidal neurons. J Physiol *533*, 447-466.

Lee, S., and Zhou, Z. J. (2006). The synaptic mechanism of direction selectivity in distal processes of starburst amacrine cells. Neuron *51*, 787-799.

Leffler, A., Herzog, R. I., Dib-Hajj, S. D., Waxman, S. G., and Cummins, T. R. (2005). Pharmacological properties of neuronal TTX-resistant sodium channels and the role of a critical serine pore residue. Pflugers Arch *451*, 454-463.

Linden, D. J. (1999). The return of the spike: postsynaptic action potentials and the induction of LTP and LTD. Neuron *22*, 661-666.

Linn, D. M., Blazynski, C., Redburn, D. A., and Massey, S. C. (1991). Acetylcholine release from the rabbit retina mediated by kainate receptors. Journal of Neuroscience *11*, 111-122.

Lipowsky, R., Gillessen, T., and Alzheimer, C. (1996). Dendritic Na+ channels amplify EPSPs in hippocampal CA1 pyramidal cells. J Neurophysiol *76*, 2181-2191.

Liu, G. (2004). Local structural balance and functional interaction of excitatory and inhibitory synapses in hippocampal dendrites. Nat Neurosci *7*, 373-379.

Llinas, R., and Hess, R. (1976). Tetrodotoxin-resistant dendritic spikes in avian Purkinje cells. Proc Natl Acad Sci U S A *73*, 2520-2523.

Llinas, R., and Nicholson, C. (1971). Electrophysiological properties of dendrites and somata in alligator Purkinje cells. J Neurophysiol *34*, 532-551.

Llinas, R., Nicholson, C., Freeman, J. A., and Hillman, D. E. (1968). Dendritic spikes and their inhibition in alligator Purkinje cells. Science *160*, 1132-1135.

Llinas, R., and Sugimori, M. (1980). Electrophysiological properties of in vitro Purkinje cell dendrites in mammalian cerebellar slices. J Physiol *305*, 197-213.

London, M., Meunier, C., and Segev, I. (1999). Signal transfer in passive dendrites with nonuniform membrane conductance. J Neurosci *19*, 8219-8233.

Lowe, G. (2002). Inhibition of backpropagating action potentials in mitral cell secondary dendrites. J Neurophysiol *88*, 64-85.

MacVicar, B. A., and Dudek, F. E. (1982). Electrotonic coupling between granule cells of rat dentate gyrus: physiological and anatomical evidence. Journal of Neurophysiology *47*, 579-592.

Magee, J. C. (1998). Dendritic hyperpolarization-activated currents modify the integrative properties of hippocampal CA1 pyramidal neurons. J Neurosci *18*, 7613-7624.

Magee, J. C. (1999). Dendritic Ih normalizes temporal summation in hippocampal CA1 neurons. Nat Neurosci *2*, 508-514.

Magee, J. C., and Carruth, M. (1999). Dendritic voltage-gated ion channels regulate the action potential firing mode of hippocampal CA1 pyramidal neurons. J Neurophysiol *82*, 1895-1901.

Magee, J. C., and Johnston, D. (1997). A synaptically controlled, associative signal for Hebbian plasticity in hippocampal neurons. Science *275*, 209-213.

Marr, D., and Ullman, S. (1981). Directional selectivity and its use in early visual processing. Proc R Soc Lond B Biol Sci *211*, 151-180.

Martina, M., Vida, I., and Jonas, P. (2000). Distal initiation and active propagation of action potentials in interneuron dendrites. Science *287*, 295-300.

Masland, R. H., and Ames, A. (1976). Responses to acetylcholine of ganglion cells in an isolated mammalian retina. Journal of Neurophysiology *39*, 1220-1235.

Masland, R. H., and Mills, J. W. (1979). Autoradiographic identification of acetylcholine in the rabbit retina. Journal of Cell Biology *83*, 159-178.

Massey, S. C., Linn, D. M., Kittila, C. A., and Mirza, W. (1997). Contributions of GABAA receptors and GABAC receptors to acetylcholine release and directional selectivity in the rabbit retina. Visual Neuroscience *14*, 939-948.

Mastronarde, D. N. (1983). Correlated firing of cat retinal ganglion cells. I. Spontaneously active inputs to X- and Y-cells. Journal Of Neurophysiology *49*, 303-324.

Maturana, H., and Frenk, S. (1963). Directional movement and horizontal edge detectors in the pigeon retina. Science *142*, 977-979.

McCleskey, E. W., and Gold, M. S. (1999). Ion channels of nociception. Annu Rev Physiol *61*, 835-856.

McGinley, M. J., and Oertel, D. (2006). Rate thresholds determine the precision of temporal integration in principal cells of the ventral cochlear nucleus. Hear Res *216-217*, 52-63.

Mel, B. W. (1993). Synaptic integration in an excitable dendritic tree. J Neurophysiol *70*, 1086-1101.

Miller, R. F., and Bloomfield, S. A. (1983). Electroanatomy of a unique amacrine cell in the rabbit retina. Proc Natl Acad Sci U S A *80*, 3069-3073.

Noble, D., and Stein, R. B. (1966). The threshold conditions for initiation of action potentials by excitable cells. J Physiol *187*, 129-162.

O'Brien, B. J., Caldwell, J. H., Ehring, G. R., Bumsted O'Brien, K. M., Luo, S., and Levinson, S. R. (2008). Tetrodotoxin-resistant voltage-gated sodium channels Na(v)1.8 and Na(v)1.9 are expressed in the retina. J Comp Neurol *508*, 940-951.

O'Malley, D. M., and Masland, R. H. (1989). Co-release of acetylcholine and gamma-aminobutyric acid by a retinal neuron. Proc Natl Acad Sci USA *86*, 3414-3418.

Oesch, N., Euler, T., and Taylor, W. R. (2005a). Direction-selective dendritic action potentials in rabbit retina. Neuron *47*, 739-750.

Oesch, N., Euler, T., and Taylor, W. R. (2005b). Direction-selective dendritic action potentials in rabbit retina. Neuron *47*, 739-750.

Ogata, N., and Tatebayashi, H. (1993). Kinetic analysis of two types of Na+ channels in rat dorsal root ganglia. J Physiol (Lond) *466*, 9-37.

Oviedo, H., and Reyes, A. D. (2002). Boosting of neuronal firing evoked with asynchronous and synchronous inputs to the dendrite. Nat Neurosci *5*, 261-266.

Oyster, C., Amthor, F., and Takahashi, E. (1993). Dendritic architecture of ON-OFF direction-selective ganglion cells in the rabbit retina. Vision Research *33*, 579-608.

Oyster, C. W. (1968). The analysis of image motion by the rabbit retina. Journal Of Physiology *199*, 613-635.

Oyster, C. W., and BARLOW, H. B. (1967). Direction-selective units in rabbit retina: distribution of preferred directions. Science *155*, 841-842.

Oyster, C. W., Takahashi, E., and Collewijn, H. (1972). Direction-selective retinal ganglion cells and control of optokinetic nystagmus in the rabbit. Vision Res *12*, 183-193.

Ozaita, A., Petit-Jacques, J., Völgyi, B., Ho, C. S., Joho, R. H., Bloomfield, S. A., and Rudy, B. (2004). A unique role for Kv3 voltage-gated potassium channels in starburst amacrine cell signaling in mouse retina. J Neurosci *24*, 7335-7343.

Panico, J., and Sterling, P. (1995). Retinal neurons and vessels are not fractal but space-filling. J Comp Neurol *361*, 479-490.

Peters, B., and Masland, R. (1996a). Responses to light of starburst amacrine cells. J Neurophysiol *75*, 469-480.

Peters, B. N., and Masland, R. H. (1996b). Responses to light of starburst amacrine cells. J Neurophysiol *75*, 469-480.

Petit-Jacques, J., and Bloomfield, S. A. (2008). Synaptic regulation of the light-dependent oscillatory currents in starburst amacrine cells of the mouse retina. J Neurophysiol.

Petit-Jacques, J., Völgyi, B., Rudy, B., and Bloomfield, S. (2005). Spontaneous oscillatory activity of starburst amacrine cells in the mouse retina. J Neurophysiol *94*, 1770-1780.

Pinato, G., and Midtgaard, J. (2005). Dendritic sodium spikelets and low-threshold calcium spikes in turtle olfactory bulb granule cells. J Neurophysiol *93*, 1285-1294.

Poggio, T., and Reichardt, W. (1973). Considerations on models of movement detection. Kybernetik *13*, 223-227.

Poirazi, P., Brannon, T., and Mel, B. W. (2003). Pyramidal neuron as two-layer neural network. Neuron *37*, 989-999.

Poirazi, P., and Mel, B. W. (2001). Impact of active dendrites and structural plasticity on the memory capacity of neural tissue. Neuron *29*, 779-796.

Rall, W. (1964). Theoretical significance of dendritic trees for neuronal input-output relations. In Neural Theory and Modeling, R. Reiss, ed. (Stanford, Stanford University Press), pp. 73-97.

Regehr, W., Kehoe, J., Ascher, P., and Armstrong, C. (1993). Synaptically triggered action potentials in dendrites. Neuron *11*, 145-151.

Regehr, W. G., Konnerth, A., and Armstrong, C. M. (1992). Sodium action potentials in the dendrites of cerebellar Purkinje cells. Proc Natl Acad Sci USA *89*, 5492-5496.

Reichardt, W. (1961). Sensory Communication (New York, Wiley).

Reichardt, W. (1987). Evaluation of optical motion information by movement detectors. J Comp Physiol [A] *161*, 533-547.

Rush, A. M., Bräu, M. E., Elliott, A. A., and Elliott, J. R. (1998). Electrophysiological properties of sodium current subtypes in small cells from adult rat dorsal root ganglia. J Physiol (Lond) *511 (Pt 3)*, 771-789.

Satin, J., Kyle, J. W., Chen, M., Bell, P., Cribbs, L. L., Fozzard, H. A., and Rogart, R. B. (1992). A mutant of TTX-resistant cardiac sodium channels with TTX-sensitive properties. Science *256*, 1202-1205.

Schiller, J., Major, G., Koester, H. J., and Schiller, Y. (2000). NMDA spikes in basal dendrites of cortical pyramidal neurons. Nature *404*, 285-289.

Schiller, J., and Schiller, Y. (2001). NMDA receptor-mediated dendritic spikes and coincident signal amplification. Curr Opin Neurobiol *11*, 343-348.

Schlue, W. R., Richter, D. W., Mauritz, K. H., and Nacimiento, A. C. (1974). Responses of cat spinal motoneuron somata and axons to linearly rising currents. J Neurophysiol *37*, 303-309.

Schwindt, P. C., and Crill, W. E. (1995). Amplification of synaptic current by persistent sodium conductance in apical dendrite of neocortical neurons. J Neurophysiol *74*, 2220-2224.

Schwindt, P. C., and Crill, W. E. (1997). Local and propagated dendritic action potentials evoked by glutamate iontophoresis on rat neocortical pyramidal neurons. J Neurophysiol *77*, 2466-2483.

Segev, I., and Parnas, I. (1983). Synaptic integration mechanisms. Theoretical and experimental investigation of temporal postsynaptic interactions between excitatory and inhibitory inputs. Biophys J *41*, 41-50.

Shields, C. R., and Lukasiewicz, P. D. (2003). Spike-dependent GABA inputs to bipolar cell axon terminals contribute to lateral inhibition of retinal ganglion cells. J Neurophysiol *89*, 2449-2458.

Smith, R. G. (1992). NeuronC: a computational language for investigating functional architecture of neural circuits. Journal of Neuroscience Methods *43*, 83-108.

Soodak, R. E., and Simpson, J. I. (1988). The accessory optic system of rabbit. I. Basic visual response properties. Journal of Neurophysiology *60*, 2037-2054.

Spencer, W. A., and Kandel, E. R. (1961). Electrophysiologyt of hippocampal neurons: IV Fast prepotentials. J Neurophysiol *24*, 272-285.

Spruston, N., Schiller, Y., Stuart, G., and Sakmann, B. (1995). Activity-dependent action potential invasion and calcium influx into hippocampal CA1 dendrites. Science *268*, 297-300.

Stafstrom, C. E., Schwindt, P. C., Flatman, J. A., and Crill, W. E. (1984). Properties of subthreshold response and action potential recorded in layer V neurons from cat sensorimotor cortex in vitro. J Neurophysiol *52*, 244-263.

Stone, J., and Fabian, M. (1966). Specialized receptive fields of the cat's retina. Science *152*, 1277-1279.

Stuart, G., Schiller, J., and Sakmann, B. (1997a). Action potential initiation and propagation in rat neocortical pyramidal neurons. J Physiol *505 (Pt 3)*, 617-632.

Stuart, G., Spruston, N., Sakmann, B., and Hausser, M. (1997b). Action potential initiation and backpropagation in neurons of the mammalian CNS. Trends Neurosci *20*, 125-131.

Stuart, G. J., and Sakmann, B. (1994). Active propagation of somatic action potentials into neocortical pyramidal cell dendrites. Nature *367*, 69-72.

Sunami, A., Glaaser, I. W., and Fozzard, H. A. (2000). A critical residue for isoform difference in tetrodotoxin affinity is a molecular determinant of the external access path for local anesthetics in the cardiac sodium channel. Proc Natl Acad Sci USA *97*, 2326-2331.

Tachibana, M. (1999). Regulation of transmitter release from retinal bipolar cells. progress in biophysics and molecular biology *72*, 109-133.

Tachibana, M., and Kaneko, A. (1987). gamma-Aminobutyric acid exerts a local inhibitory action on the axon terminal of bipolar cells: evidence for negative feedback from amacrine cells. proceedings of the national academy of sciences of the united states of america *84*, 3501-3505.

Tauchi, M., and Masland, R. H. (1984). The shape and arrangement of cholinergic neurons in the rabbit retina. Proceedings of the Royal Society of London Series B: Biological Sciences *223*, 101-119.

Taylor, W. R., He, S., Levick, W. R., and Vaney, D. I. (2000). Dendritic computation of direction selectivity by retinal ganglion cells. Science *289*, 2347-2350.

Taylor, W. R., and Vaney, D. I. (2002). Diverse Synaptic Mechanisms Generate Direction Selectivity in the Rabbit Retina. J Neurosci *22*, 7712-7720.

Taylor, W. R., and Vaney, D. I. (2003). New directions in retinal research. Trends Neurosci *26*, 379-385.

Taylor, W. R., and Wässle, H. (1995a). Receptive field properties of starburst cholinergic amacrine cells in the rabbit retina. Eur J Neurosci *7*, 2308-2321.

Taylor, W. R., and Wässle, H. (1995b). Receptive field properties of starburst cholinergic amacrine cells in the rabbit retina. European Journal of Neuroscience *7*, 2308-2321.

Torre, V., and Poggio, T. (1978). A synaptic mechanism possibly underlying directional selectivity to motion. Proceedings of the Royal Society of London Series B: Biological Sciences *202*, 409-416.

Tsubokawa, H., and Ross, W. N. (1996). IPSPs modulate spike backpropagation and associated [Ca2+]i changes in the dendrites of hippocampal CA1 pyramidal neurons. J Neurophysiol *76*, 2896-2906.

Tukker, J. J., Taylor, W. R., and Smith, R. G. (2004). Direction selectivity in a model of the starburst amacrine cell. Vis Neurosci *21*, 611-625.

Turner, R. W., Meyers, D. E., and Barker, J. L. (1989). Localization of tetrodotoxin-sensitive field potentials of CA1 pyramidal cells in the rat hippocampus. J Neurophysiol *62*, 1375-1387.

Turner, R. W., Meyers, D. E., Richardson, T. L., and Barker, J. L. (1991). The site for initiation of action potential discharge over the somatodendritic axis of rat hippocampal CA1 pyramidal neurons. J Neurosci *11*, 2270-2280.

Ullman, S. (1983). The measurement of visual motion Computational considerations and some neurophysiological implications. Trends Neurosci *6*, 177-179.

Valiante, T. A., Perez Velazquez, J. L., Jahromi, S. S., and Carlen, P. L. (1995). Coupling potentials in CA1 neurons during calcium-free-induced field burst activity. Journal of Neuroscience *15*, 6946-6956.

VALLBO, A. B. (1964). ACCOMMODATION RELATED TO INACTIVATION OF THE SODIUM PERMEABILITY IN SINGLE MYELINATED NERVE FIBRES FROM XENOPUS LAEVIS. Acta Physiol Scand *61*, 429-444.

van Doorn, A. J., and Koenderink, J. J. (1982). Visibility of movement gradients. Biol Cybern *44*, 167-175.

Van Wart, A., Trimmer, J. S., and Matthews, G. (2007). Polarized distribution of ion channels within microdomains of the axon initial segment. J Comp Neurol *500*, 339-352.

Vaney, D. I. (1994a). Patterns of neuronal coupling in the retina. Progress in Retinal and Eye Research *13*, 301-355.

Vaney, D. I. (1994b). Territorial organization of direction-selective ganglion cells in rabbit retina. Journal of Neuroscience *14*, 6301-6316.

Vaney, D. I. (1994c). Territorial organization of direction-selective ganglion cells in rabbit retina. J Neurosci *14*, 6301-6316.

Vaney, D. I., Collin, S. P., and Young, H. M. (1989). Dendritic relationships between cholinergic amacrine cells and direction-selective ganglion cells. In Neurobiology of the inner retina, R. Weiler, and N. N. Osborne, eds. (Berlin, Springer), pp. 157-168.

Vaney, D. I., He, S., Taylor, W. R., and Levick, W. R. (2001). Direction-Selective Ganglion Cells in the Retina. From: Motion Vision - Computational, Neural, and Ecological Constraints, 44.

Vaney, D. I., and Pow, D. V. (2000). The dendritic architecture of the cholinergic plexus in the rabbit retina: selective labeling by glycine accumulation in the presence of sarcosine. Journal of Comparative Neurology *421*, 1-13.

Vaney, D. I., and Taylor, W. R. (2002). Direction selectivity in the retina. Current Opinions in Neurobiology *12*, 405-410.

Vaney, D. I., and Young, H. M. (1988). GABA-like immunoreactivity in cholinergic amacrine cells of the rabbit retina. Brain Research *438*, 369-373.

Vaughn, J. E., Famiglietti, E. V. J., Barber, R. P., Saito, K., Roberts, E., and Ribak, C. E. (1981). GABAergic amacrine cells in rat retina: immunocytochemical identification and synaptic connectivity. Journal Of Comparative Neurology *197*, 113-127.

Velte, T. J., and Masland, R. H. (1999a). Action potentials in the dendrites of retinal ganglion cells. Journal of Neurophysiology *81*, 1412-1417.

Velte, T. J., and Masland, R. H. (1999b). Action potentials in the dendrites of retinal ganglion cells. J Neurophysiol *81*, 1412-1417.

Velte, T. J., and Miller, R. F. (1997). Spiking and nonspiking models of starburst amacrine cells in the rabbit retina. Vis Neurosci *14*, 1073-1088.

Wässle, H., and Riemann, H. J. (1978). The mosaic of nerve cells in the mammalian retina. Proc R Soc Lond, B, Biol Sci *200*, 441-461.

Waxman, S. G., Dib-Hajj, S., Cummins, T. R., and Black, J. A. (1999). Sodium channels and pain. Proc Natl Acad Sci USA *96*, 7635-7639.

Weiser, T., and Wilson, N. (2002). Inhibition of tetrodotoxin (TTX)-resistant and TTX-sensitive neuronal Na(+) channels by the secretolytic ambroxol. Mol Pharmacol *62*, 433-438.

Werblin, F. (1970). Responses of retinal cells to moving spots: Intracellular recording in Necturus maculosus. J Neurophys *33*, 342-350.

Williams, S. R. (2004). Spatial compartmentalization and functional impact of conductance in pyramidal neurons. Nat Neurosci *7*, 961-967. Epub 2004 Aug 2022.

Williams, S. R., and Stuart, G. J. (1999). Mechanisms and consequences of action potential burst firing in rat neocortical pyramidal neurons. J Physiol *521 Pt 2*, 467-482.

Wong, R. K., and Prince, D. A. (1978). Participation of calcium spikes during intrinsic burst firing in hippocampal neurons. Brain Res *159*, 385-390.

Wong, R. K., Prince, D. A., and Basbaum, A. I. (1979). Intradendritic recordings from hippocampal neurons. Proc Natl Acad Sci U S A *76*, 986-990.

Wu, J. Y., Brandon, C., Su, Y. Y., and Lam, D. M. (1981). Immunocytochemical and autoradiographic localization of GABA system in the vertebrate retina. Mol Cell Biochem *39*, 229-238.

Wyatt, H. J., and Daw, N. D. (1975). Directionally sensitive ganglion cells in the rabbit retina: Specificity for stimulus direction, size and speed. Journal of Neurophysiology *38*, 613-626.

Wyatt, H. J., and Daw, N. D. (1976). Specific effects of neurotransmitter antagonists on ganglion cells in rabbit retina. Science *191*, 204-205.

Wyatt, H. J., and Day, N. W. (1976). Specific effects of neurotransmitter antagonists on ganglion cells in rabbit retina. Science *191*, 204-205.

Xiong, W., and Chen, W. R. (2002). Dynamic gating of spike propagation in the mitral cell lateral dendrites. Neuron *34*, 115-126.

Yang, G., and Masland, R. H. (1992). Direct visualization of the dendritic and receptive fields of directionally selective retinal ganglion cells. Science *258*, 1949-1952.

Yang, G., and Masland, R. H. (1994a). Receptive fields and dendritic structure of directionally selective retinal ganglion cells. Journal of Neuroscience *14*, 5267-5280.

Yang, G., and Masland, R. H. (1994b). Receptive fields and dendritic structure of directionally selective retinal ganglion cells. J Neurosci *14*, 5267-5280.

Yoshida, K., Watanabe, D., Ishikane, H., Tachibana, M., Pastan, I., and Nakanishi, S. (2001). A key role of starburst amacrine cells in originating retinal directional selectivity and optokinetic eye movement. Neuron *30*, 771-780.

Zheng, J. J., Lee, S., and Zhou, Z. J. (2004a). A developmental switch in the excitability and function of the starburst network in the mammalian retina. Neuron *44*, 851-864.

Zheng, J. J., Lee, S., and Zhou, Z. J. (2004b). A developmental switch in the excitability and function of the starburst network in the mammalian retina. Neuron *44*, 851-864.

Zhou, Z., and Fain, G. (1995). Neurotransmitter receptors of starburst amacrine cells in rabbit retinal slices. J Neurosci *15*, 5334-5345.

Zhou, Z., and Fain, G. (1996). Starburst amacrine cells change from spiking to nonspiking neurons during retinal development. Proc Natl Acad Sci U S A *93*, 8057-8062.

Zucker, R. (1999). Calcium- and activity-dependent synaptic plasticity. Curr Opin Neurobiol *9*, 305-313.